Regulatory Signaling Networks Governing Budding Yeast Filamentous Growth

by

Christian A. Shively

A dissertation submitted in partial fulfillment
of the requirements for the degree of
Doctor of Philosophy
(Cellular and Molecular Biology)
in the University of Michigan
2014

Doctoral Committee:

> Associate Professor Anuj Kumar, Chair
> Professor Philip C. Andrews
> Professor Robert S. Fuller
> Professor Daniel J. Klionsky
> Associate Professor Eric Krukonis, University of Detroit Mercy
> Associate Professor Alexey Nesvizhskii

# TABLE OF CONTENTS

# LIST OF FIGURES

# LIST OF TABLES

# Chapter 1. Introduction

1.1 Budding yeast *Saccharomyces cerevisiae* as a Model Eukaryote

Used in baking and brewing for millennia, the budding yeast *Saccharomyces cerevisiae* has become widely used as a model organism in cell and molecular biology research beginning in the middle of the twentieth century due to several inherent qualities: The organism is eukaryotic, with cellular organization and many cellular pathways and processes conserved in "higher" eukaryotes and metazoans, including humans. In fact, nearly 1,000 budding yeast genes have substantial homology with genes known to cause disease in humans (Botstein & Fink, 2011). Also, the fungus is unicellular with a fast generation time, enabling many clones of an individual cell to be obtained relatively quickly. Moreover, *S. cerevisiae* is easily grown and propagated in the laboratory setting, with defined minimal nutrition requirements, allowing early studies of metabolism. The number of Nobel Prize recipients who have used *S. cerevisiae* as their choice model organism exemplifies the utility of budding yeast as a relevant model organism for the study of cell biology and genetics.

The genetic power of *S. cerevisiae* has been a particular advantage to studies of cell and molecular biology. *S. cerevisiae* can exist as either haploid or diploid, and the sexual cycle can be exploited for genetic mapping. Gene deletion and modification of chromosomal genes can be easily accomplished by lithium acetate transformation and PCR-mediated gene disruption (Hinnen, Hicks, & Fink, 1978; Wach, Brachat, Pohlmann, & Philippsen, 1994). Another advance in the utility of *S. cerevisiae* as a model organism was the engineering of "shuttle" vectors, which could be propagated in either *S. cerevisiae* or *E. coli* (Beggs, 1978; Sikorski & Hieter, 1989). In addition, the complete sequencing of the *S. cerevisiae* genome and development of the yeastgenome.org database has greatly facilitated reverse genetic approaches (Cherry et al., 2012; Goffeau et al., 1996).

1.2 High-throughput Technologies for Systems Biology Research in Yeast

As opposed to highly focused investigations of one particular gene or cellular pathway in a reductionist view, systems biology approaches attempt to determine the complex connectivity and dynamics of cell systems on a global scale, which can then be used to generate and inform new hypotheses for more focused inquiry.  Systems biology platforms aim to characterize the global changes occurring during a perturbed cell state or condition, including the dynamics of these changes and the relationships of these changes to one another.  To this end, systems biology methods are often high-throughput and large-scale in nature.

Due to the genetic tractability and ease of manipulation of budding yeast, a number of systems biology methodologies have been pioneered in *Saccharomyces cerevisiae*.  These studies include "omics" work, studies on the genome, transcriptome, proteome, or metabolome in their entirety, which are often infeasible in more complex organisms. Genomic work has attempted to define all of the ORFs of budding yeast and the functions of their gene products.  These efforts have been greatly facilitated by the sequencing of the *S. cerevisiae* genome, and, since the completion of the sequencing project in 1996, the fraction of protein-coding genes for which some biological function has been annotated has risen from ~30% to ~85% (Botstein & Fink, 2011).  Proteomic studies have characterized the subcellular localization of proteins, protein complexes, and protein abundances in different experimental contexts.  For example, in 2003, Weissman, O'Shea, and colleagues analyzed subcellular localization of 4,156 budding yeast proteins by systematic GFP-tagging and microscopic analysis in a high-throughput format, providing a localization map of much of the yeast proteome (Huh et al., 2003).  Physical interaction maps of the yeast proteome include large-scale two-hybrid screens and systematic identification of protein complexes by mass spectrometry (Y. Ho et al., 2002; Uetz et al., 2000).

1.2.1 Genome-wide Gene Deletion Collection

Many classical studies in budding yeast have employed mutagenesis screening to identify genes contributing to phenotypes of interest.  In 1999, an initial collection of 2,026 barcoded deletion mutants in *S. cerevisiae* was completed in reference strain S288c.  PCR-mediated gene disruption was employed, in which ~50base pairs (bp) of sequence

upstream of a gene's start codon and downstream of the stop codon flank a selectable marker, which then replaces the gene through homologous recombination. In addition, two molecular barcodes (20mer DNA sequences) were designed into the knockout cassette to allow ease of identification of each strain when multiple knockout strains are grown in parallel (Winzeler et al., 1999). Through pooling of multiple knockout strains for parallel assays of fitness, thousands of novel phenotypes for genes were uncovered (Giaever et al., 2002). The yeast knockout collections in diploid and both haploid mating types have since been used for far-reaching analysis of genes affecting growth under varying physiological conditions, as well as for screens affecting specific cellular processes (Scherens & Goffeau, 2004).

1.2.2 Genome-wide Gene Overexpression Studies

Conversely, systematic overexpression of genes has been used as a complimentary approach to deletion or transposon mutagenesis disruption mutant collections to reveal novel phenotypes, as well as phenotypes for essential genes. Induction of gene overexpression often results in augmented or gain-of-function phenotypes due to misregulation, and rarely does gene overexpression mimic corresponding gene deletion (Sopko et al., 2006). Several systems have been developed to induce the overexpression of genes in budding yeast: A galactose-inducible N-terminally GST-tagged plasmid-born ORF collection and subsequent yeast strain collection transformed with this vector library have been used in the development of proteome chips and gene interaction discovery, respectively (Sopko et al., 2006; Zhu et al., 2001). In addition, a plasmid library termed the moveable ORF (mORF) collection features a large fraction of budding yeast ORFs C-terminally tagged with HA and Protein A under galactose overexpression control (Gelperin et al., 2005).

1.2.3 Mass Spectrometry-Based Proteomic Studies and Kinase Signaling Networks

Phosphorylation of proteins is one of the best-studied post-translational modifications and is predicted to be a regulatory mechanism for roughly 30% of budding yeast proteins. Consequently, considerable effort has been invested into surveying the complete phosphoproteome of budding yeast to identify phosphorylation events and, when

possible, the protein kinases and phosphatases that regulate them, as well as to map the physical interactions of protein kinases and phosphatases to identify substrates and regulatory factors.

Advances in large-scale analysis of proteins using mass spectrometry methodology have been instrumental in global analyses of signaling networks of phosphorylation. A seminal work in the field of phosphorylation networks in budding yeast was an investigation into the physical kinase and phosphatase interaction (KPI) network by immuno-affinity purification of kinases, phosphatases, and their associated regulators, and mass spectrometry analysis of protein complexes. Through analysis of 276 immune complexes, 1,844 interactions were identified between 887 protein partners at a high confidence level, with many novel interactions between kinases and phosphatases identified and new functions and regulatory modules assigned. The KPI network firmly established a concept of connectivity and communication among kinases and phosphatases, with signaling and regulation *in vivo* likely occurring via complex networks rather than in isolation (Breitkreutz et al., 2010).

Another recent work analyzed perturbations of the budding yeast phosphorylation network by deletion or pharmacological inhibition of 124 kinases and phosphatases followed by mass spectrometry phosphoproteomic analysis, in which phosphopeptides across the phosphoproteome were surveyed and their relative abundance in perturbed strains versus wild type were measured. By this methodology, while deletion/inhibition of a small number of kinases and phosphatases only changed abundance of fewer than 10 phosphopeptides, deletion/inhibition of a much larger number of kinases and phosphatases examined had a considerable impact on the phosphoproteome on the whole, either directly or indirectly. Interestingly, while deletion of a kinase would be expected to reveal phosphopeptides mostly decreasing in abundance, this directionality bias of differential phosphopeptide abundance was largely not observed, with decreased phosphopeptides observed roughly as often as increases (Bodenmiller et al., 2010).

Two major obstacles have continued to plague the emerging field of phosphoproteomics. First, phosphorylation events are extremely dynamic and reversible by design in response to environmental and cellular state, making complete mapping of phosphorylation events of the phosphoproteome extremely difficult. Second, while the

sheer number of budding yeast phosphorylation sites continues to grow, assigning a functional effect or consequence of these phosphorylation events to protein activity or even broader cell phenotype remains a low-throughput endeavor.

1.3 Filamentous Growth in Budding Yeast *Saccharomyces cerevisiae*

When specific strain backgrounds of the budding yeast *Saccharomyces cerevisiae* are stressed by lack of nitrogen, they undergo a striking change in growth form termed filamentous or pseudohyphal growth, in which cells adopt an elongated shape and remain connected together following cytokinesis. Filamentous growth is considered to be an entirely different growth form from the simple budding cell division occurring during nutrient replete conditions. Substantial alteration of numerous cellular processes is coordinated during the transition to filamentous growth during stress conditions: a unipolar budding pattern is adopted by diploids; the cell cycle is delayed at G2/M; cytoskeletal rearrangements effect a polarized growth morphology; and unique transcriptional and translational signatures are observed (Ahn, Acurio, & Kron, 1999; Gimeno, Ljungdahl, Styles, & Fink, 1992; J. Ho & Bretscher, 2001; Ma, Jin, Dobry, Lawson, & Kumar, 2007).

Filamentous growth in *Saccharomyces cerevisiae* has been a subject of scientific scrutiny for over two decades. Because filamentation is easily assayed and many tools for genetic manipulation are available in the budding yeast *Saccharomyces cerevisiae*, filamentous growth can be used as a model stress response to investigate how eukaryotes detect stress and enact the appropriate response. Also, much of the molecular signal transduction machinery governing the filamentous growth transition has been characterized and found to bear homology to regulatory mechanisms conserved in higher eukaryotes and metazoans. This protein machinery includes conserved protein kinases and small GTPases, such as RAS. Lastly, pseudohyphal growth in *Saccharomyces cerevisiae* strongly parallels the hyphal growth form of a number of pathogenic fungi infecting humans, such as *Candida albicans,* the most common human fungal pathogen. In fact, filamentous growth of both *Candida albicans* and *Saccharomyces cerevisiae* are regulated by homologous protein kinase signaling cascades (Gow, van de Veerdonk, Brown, & Netea, 2011). *Candida albicans* strains lacking the ability to undergo hyphal growth have been

found to be avirulent in mouse models of infection (H. J. Lo et al., 1997). In addition, hyphal growth is observed in a number of plant fungal pathogens important in agriculture, such as *Ustilago maydis* and *Magnaporthe grisea* (Madhani & Fink, 1998).

1.4 Laboratory Assays of Filamentation: Diploid Surface-Spread Filamentation (Pseudohyphal Growth) vs. Haploid Invasive Growth

 A number of different methods for assaying filamentous growth in budding yeast are commonly used. In diploids, the most common assay is for surface-spread filamentation (pseudohyphal growth) of strains growing on nitrogen-limited agar media. A mimimal media consisting only of yeast nitrogen base without ammonium sulfate (6.7g/liter), 2% glucose as carbon source, 50μ$M$ ammonium sulfate, and supplemental amino acids for auxotrophies is used to induce filamentation. The colonies of diploid strains incubated on this nitrogen deprivation media for approximately 3 days display a striking array of peripheral filaments emanating outward from the colony, which can be observed by light microscopy (Gimeno et al., 1992). In haploid strains, an invasive growth assay is often performed. Invasive growth describes the ability of a filamentous strain growing on a rich media agar plate to adhere to and embed itself within the agar substrate. In this assay, the strain is spot-plated onto the surface of the agar plate and incubated for 3-4 days. Following incubation, the surface of the plate is gently rinsed with water to remove surface cells, with only cells adhering to the plate remaining (Madhani, Styles, & Fink, 1997). Haploids grown in liquid media culture can be induced to undergo filamentation by addition of 1% butanol to the media. Butanol treatment is thought to mimic a nitrogen deprivation stress. Much of the same signal transduction machinery governs surface-spread filamentation, invasive growth, and butanol-induced filamentation (Lorenz, Cutler, & Heitman, 2000).

1.5 Regulatory Kinase Signaling Pathways of Yeast Filamentous Growth

Filamentous growth of budding yeast is regulated by protein kinase signaling pathways largely conserved in metazoans. The best studied and established of these protein kinase signaling pathways of filamentation are the MAPK pathway, the RAS-cAMP-PKA pathway, and the AMPK Snf1p pathways (Kuchin, Vyas, & Carlson, 2002; H. Liu, Styles, & Fink, 1993; Pan & Heitman, 1999). All three kinase signaling pathways are thought to function by detecting stress through cell-membrane sensor proteins and relaying that information via phosphorylation of substrate proteins to the nucleus to signal transcription of surprisingly few effector target genes, with the most critical being a cell-surface flocculin called Muc1p. Filamentation is abrogated in the *muc1Δ* mutant; and, in fact, MUC1 has one of the largest promoter regions of any budding yeast gene, presumably to allow the convergence of numerous transcription factors to create a combinatorial regulatory system (Rupp, Summers, Lo, Madhani, & Fink, 1999a). This canonical view of simple linear kinase signaling to regulate filamentation has persisted in the literature of the field, despite the growing appreciation for complex networks of kinase signaling informed by advances in proteomic mass spectrometry methodologies. Moreover, the number of protein kinases regulating filamentous growth is growing to include the Hog1p MAPK, Fus3p MAPK, Yak1p, Ksp1p, Npr1p, Sks1p, and a signaling pathway of Elm1p-Hsl1p-Swe1p-Cdc28p (Bharucha et al., 2008; Blacketer, Koehler, Coats, Myers, & Madaule, 1993; Edgington, Blacketer, Bierwagen, & Myers, 1999a; Lorenz & Heitman, 1998; Madhani et al., 1997; Malcher, Schladebeck, & Mosch, 2011; O'Rourke & Herskowitz, 1998).

1.5.1 Filamentation MAPK Pathway

Filamentous growth is regulated by a number of conserved protein kinase signaling pathways. A mitogen-activated protein kinase (MAPK) pathway dedicated to the regulation of filamentous growth consists of the p21-activated kinase Ste20p acting as a MAPKKKK, resulting in the sequential phosphorylation and activation of downstream MAPKs Ste11p (MAPKKK), Ste7p (MAPKK), and Kss1p (MAPK). The activated MAPK Kss1p then releases inhibition of the Ste12p and Tec1p transcription factors, enabling the transcription of target genes. The roles of the MAPK Kss1p in haploid invasive growth and diploid surface-spread filamentation initially appeared contradictory, given that the

7

haploid *kss1Δ* mutant is defective in invasion, yet the diploid *kss1Δ/Δ* mutant has no altered surface-spread filamentation phenotype. The role of Kss1p as the filamentation-specific MAPK in both haploids and diploids was subsequently elegantly characterized by Thorner, Fink, and colleagues, who demonstrated both inhibition and activation functions of Kss1p (Cook, Bardwell, & Thorner, 1997; Madhani et al., 1997). Upon activation, the transcription factors Ste12p and Tec1p together bind a consensus DNA motif termed the filamentous response element (FRE) to initiate transcription of specific effector genes (Madhani & Fink, 1997). The filamentous growth MAPK pathway also requires components upstream of the p21-activated kinase Ste20p: the signaling mucin-like protein Msb2p, and the small G proteins Cdc42p and Ras2p (Cullen et al., 2004; Mosch, Roberts, & Fink, 1996). Remarkably, Ste20p, Ste11p, Ste7p, and Kss1p are shared by both the filamentous growth MAPK pathway and the mating MAPK pathway (H. Liu et al., 1993). How such signaling pathways with shared components detect different environmental cues (nitrogen stress vs. pheromone) yet maintain specificity to direct the appropriate cellular response has been a subject of ongoing research (Chou, Huang, & Liu, 2004; Shock, Thompson, Yates, & Madhani, 2009).

1.5.2 RAS-cAMP-PKA Pathway

The small GTPase Ras2p is thought to act upstream of both Ste20p, as well as the cAMP protein kinase A (PKA) pathway regulating filamentation. Ras2p signaling activates production of cAMP by the adenylyl cyclase Cyr1p. Consequently, cAMP activates the paralogous PKAs Tpk1p, Tpk2p, and Tpk3p, of which Tpk2p plays a positive role in the regulation of filamentous growth by acting upstream of the transcription factor Flo8p to govern transcription of target genes (Pan & Heitman, 1999). The primary genetic determinant enabling invasive growth and surface-spread filamentation in filamentous *Saccharomyces cerevisiae* backgrounds is thought to be a functional allele of the *FLO8* transcription factor, since the non-filamentous reference *S. cerevisiae* strain S288c contains a missense mutation in *FLO8* (H. Liu, Styles, & Fink, 1996). cAMP production can also be triggered by a second upstream branch of this pathway consisting of the receptor Gpr1p, the Gα protein Gpa2p, and the ammonium permease Mep2p at the cell membrane (Lorenz & Heitman, 1997; Lorenz & Heitman, 1998; Lorenz et al., 2000; Pan & Heitman, 1999).

Interestingly, the three paralogues of PKA in budding yeast have different roles in the regulation of filamentous growth, with Tpk2p positively regulating filamentation and Tpk1p and Tpk3p negatively regulating filamentation (Pan & Heitman, 1999).

1.5.3 AMPK Snf1p Pathway

Lastly, the Snf1p kinase, the homolog of AMP-activated protein kinase (AMPK) in budding yeast, governs the filamentous growth transition by relieving the activity of two transcriptional repressors Nrg1p and Nrg2p (Kuchin et al., 2002). Deletion of *SNF1* in diploids ablates surface-spread filamentation, and defective invasive growth in the *snf1Δ* haploid is observed on rich YPD or glucose-depleted agar media (Cullen & Sprague, 2000; Kuchin et al., 2002). The upstream signaling machinery of the Snf1p kinase signaling pathway in the context of filamentation remains poorly elucidated; however, of the three upstream Snf1p-activating kinases, the Sak1p kinase may be the primary orchestrator of Snf1p signaling in response to nitrogen deprivation (Orlova, Ozcetin, Barrett, & Kuchin, 2010). Of the MAPK, RAS-cAMP-PKA, and Snf1p AMPK pathways, Snf1p is the sole kinase pathway not yet implicated in the hyphal growth of the opportunistic pathogen, likely because the orthologue of *SNF1* in *Candida* appears to be essential (Petter, Chang, & Kwon-Chung, 1997). However, the orthologue of the transcription repressor *NRG1* in *C. albicans* has a similar function repressing filamentation, suggesting that *SNF1* may have similar function in *Candida albicans* (Braun, Kadosh, & Johnson, 2001).

1.5.4 Other Kinases Regulating Filamentous Growth

The Elm1p kinase is one of the three protein kinases that can phosphorylate and activate the Snf1p kinase, which, as described above, is essential for filamentous growth. Somewhat counterintuitively, deletion of *ELM1* leads to constitutive surface-spread filamentation in diploids and elongated cell shape, altered budding pattern, and invasive growth in haploids, despite being a positive regulator of Snf1p. Alternative to its role in Snf1p signaling, the Elm1p kinase may regulate filamentation through an axis of signaling comprised of the Hsl1p kinase, the Swe1p kinase, and the cyclin-dependent kinase Cdc28p. In support of this hypothesis, replacement of *CDC28* with *CDC28*$^{Y19F}$, in which the tyrosine phosphorylated by Swe1p was mutated to phenylalanine, effectively blocks the cell

9

elongation and hyper-invasion phenotypes of *HSL1* or *ELM1* deletion (Edgington, Blacketer, Bierwagen, & Myers, 1999b).

Numerous other protein kinases have also been implicated in the control of the filamentous growth transition. Yak1p kinase regulates *MUC1* transcription and invasive growth in haploids through the transcription factors Sok2p and Phd1p (Malcher et al., 2011). The Hog1p MAPK negatively regulates the filamentous growth MAPK pathway by an incompletely understood mechanism. Hog1p activation results in phosphorylation of both the MAPKK Ste7p and MAPK Kss1p, yet the downstream transcription factor Tec1p is somehow prevented from binding upstream of *MUC1* to activate transcription (Shock et al., 2009).

1.6 Other Cellular Processes and Pathways Playing Roles in Filamentous Growth

In addition to signal transduction pathways, an exhaustive list of other cellular processes has been compiled in the ongoing study of filamentous growth over the past two decades, and five such processes are noteworthy here. (1) As expected during a nutrient responsive stress condition, metabolic changes resulting from altered nitrogen and carbon source acquisition are hallmarks of filamentous growth (Cutler, Pan, Heitman, & Cardenas, 2001; Lorenz et al., 2000; Orlova, Kanter, Krakovich, & Kuchin, 2006). (2) The exaggerated polarized growth during filamentation requires the cell polarity regulatory machinery Cdc42p and Ras2p, as well as proper arrangement by the actin cytoskeleton and delivery of material to the site of polarized growth via the secretory pathway (J. Ho & Bretscher, 2001). (3) Bud-site selection proteins Rsr1p, Bud8p, and Bud9p function in the switch from axial to unipolar budding pattern during filamentous growth (Cullen & Sprague, 2002). (4) A cell cycle delay at G2/M occurs during filamentous growth, and loss of function of cyclins *CLB1/2* or the cyclin-dependent kinase *CDC28* enhances filamentous growth (Edgington et al., 1999b; Rua, Tobe, & Kron, 2001). (5) Posttranslational modifications including glycosylation, urmylation, and sumoylation of specific filamentous growth regulatory proteins have also been described (Goehring, Rivers, & Sprague, 2003; Wang, Abu Irqeba, Ayalew, & Suntay, 2009; Yang, Tatebayashi, Yamamoto, & Saito, 2009).

1.7 Systems Biology Approaches to the Study of Filamentous Growth

Due to the broad scope of cellular processes and pathways thought to play roles in the filamentous growth transition, a systems biology approach to the study of filamentation is warranted. The principle obstacle impeding systems biology investigation of the filamentous growth transition is the necessity of conducting studies in a filamentous genetic background; high-throughput reagents and libraries in budding yeast have nearly exclusively been created in the non-filamentous reference strain S288c. Despite this disadvantage, a limited number of studies have been conducted in the filamentous Σ1278b background. Comprehensive systematic gene disruption by transposon mutagenesis and complementary overexpression analysis undertaken previously by Kumar and colleagues identified 487 genes conferring altered filamentous growth phenotype upon disruption or overexpression (Jin, Dobry, McCown, & Kumar, 2008). The subcellular localization of the kinome, or complement of protein kinases, of budding yeast has also been analyzed during the filamentous transition, with five protein kinases and one kinase regulatory subunit found to transit from the cytoplasm to the nucleus upon butanol induction of filamentation (Bharucha et al., 2008). A haploid and diploid gene deletion collection in the filamentous Σ1278b background has been recently completed and screened for differential haploid invasive growth and diploid surface-spread filamentous growth phenotypes. Although core regulatory pathways were found to be important for both invasive growth and surface-spread filamentous growth, the gene set contributing to each program was not identical. In total, 577, 700, and 688 genes were identified contributors to haploid invasive growth, diploid pseudohyphal growth, and biofilm development, respectively (Ryan et al., 2012). Fascinatingly, the essential gene set for the filamentous Σ1278b background is different than that of reference strain S288c, with some genes essential only in a specific genetic context, even though these are both strains of the same species and can be mated together (Dowell et al., 2010). The assembly of a gene deletion collection in a filamentous genetic background will hopefully aid large-scale study of filamentous growth; however, the deletion collection in the filamentous Σ1278b background has not been made commercially available.

1.8 Critical Gaps in Understanding: (1) The Genomic Complement Contributing to Filamentous Growth and (2) the Kinase Signaling Networks Underlying Filamentous Growth

(1) While the genomic contribution to filamentous growth has now been explored through the gene disruption and systematic knockout collections described above, the genomic complement contributing to filamentous growth upon overexpression has not been completely uncovered, given that the overexpression constructs used by Kumar and colleagues in 2008 only covered roughly a third of predicted ORFs in budding yeast. Also, the affect of gene overexpression was assayed by examination of filamentation of haploids under butanol induction of filamentous growth, yet the genetic complement of filamentous growth is almost certain to be ploidy dependent (Jin et al., 2008). Thus, more thorough systematic study is required to undercover the full scope of genes contributing to filamentation upon overexpression.

(2) Although kinase signaling is now understood to occur through complex networks of kinase-phosphatase connectivity and regulated phosphorylation across the phosphoproteome, the kinase signaling networks regulating filamentous growth remain unexplored. This lack of understanding becomes most obvious when the "primary" role of these pathways, regulation of *MUC1* expression, is considered. While the MAPK, RAS-cAMP-PKA, and AMPK kinase signaling pathways described above all converge on the large promoter of *MUC1* to regulate transcription of this critical effector, these kinases must play additional regulatory roles during this stress response, since deletion of *MUC1* does not entirely abrogate the changes to all cellular processes during filamentous growth (Ahn et al., 1999). For example, a *muc1Δ* strain displays defective invasive growth; however, deletion of *MUC1* causes a specific cell-cell adhesion defect, while not affecting cell elongation or the unipolar-distal budding pattern characteristic of haploid invasive growth. In contrast, the *ste20Δ* is defective in cell-cell adhesion, cell elongation, and unipolar budding (Cullen & Sprague, 2002) implying that the MAPKKKK Ste20p does not solely govern filamentation through *MUC1*. Likewise, while the AMPK Snf1p protein kinase is thought to regulate *MUC1* expression by inhibiting the function of the transcriptional

repressors Nrg1p and Nrg2p, the triple *nrg1/2Δ/Δ snf1Δ/Δ* strain displays a wild-type level of surface-spread filamentation, suggesting that Snf1p contribution to filamentous growth is not solely inhibition of NRG1/2p (Kuchin et al., 2002).  These observations among others suggest that the signal transduction cascades critical for filamentous growth are not completely understood.  The master regulatory kinase signaling networks governing filamentous growth represent a second critical gap in our understanding of this stress response.

## Chapter 2. Genetic Networks Inducing Invasive Growth in *Saccharomyces cerevisiae* Identified through Systematic Genome-wide Overexpression

2.1 Introduction

The budding yeast *Saccharomyces cerevisiae* is dimorphic, exhibiting both a unicellular growth form and a multicellular filamentous state generated presumably as a foraging mechanism under conditions of nutritional stress (Cook, Bardwell, Kron, & Thorner, 1996; Gimeno et al., 1992; H. Liu et al., 1993; R. L. Roberts & Fink, 1994). In *S. cerevisiae*, nitrogen stress (Gimeno et al., 1992), growth in the presence of short-chain alcohols (Dickinson, 1996; Lorenz et al., 2000), and glucose stress (Cullen & Sprague, 2000) can induce the transition to a filamentous form characterized morphologically as follows. Yeast cells undergoing filamentous growth are elongated in shape, due to delayed G2/M progression and prolonged apical growth (Ahn et al., 1999; Gimeno et al., 1992; Kron, Styles, & Fink, 1994; Miled, Mann, & Faye, 2001). Some reports indicate that these cells bud in a preferentially unipolar fashion (Gimeno et al., 1992; Kron et al., 1994), and, most distinctively during filamentous growth, daughter cells bud from mother cells but remain physically connected after septum formation (Gimeno et al., 1992). As a result, the interconnected cells form filaments that are termed pseudohyphae since they superficially resemble hyphae but lack the structure of a true hyphal tube with parallel-sided walls (Berman & Sudbery, 2002). Depending on the induction condition and strain ploidy, pseudohyphal filaments can spread outward from a yeast colony over an agar surface and can also invade the agar (Gancedo, 2001). This pseudohyphal growth response is not unique to *S. cerevisiae*; the related pathogenic fungus *Candida albicans* also exhibits pseudohyphal and hyphal morphologies, and the ability to switch between yeast, pseudohyphal, and hyphal growth forms is generally considered to be necessary for

virulence in *C. albicans* (Braun & Johnson, 1997; Jayatilake, Samaranayake, Cheung, & Samaranayake, 2006; H. J. Lo et al., 1997).

Pseudohyphal growth in *S. cerevisiae* is mediated by at least three well-studied signaling pathways encompassing the mitogen-activated protein kinase (MAPK) Kss1p, the AMP-activated kinase family member Snf1p, and cyclic AMP-dependent protein kinase A (PKA). The filamentous growth MAPK cascade consists of Ste11p, Ste7p, and Kss1p (Cook et al., 1997; H. Liu et al., 1993; Madhani et al., 1997; R. L. Roberts & Fink, 1994). Ste11p is a substrate of Ste20p, and Ste20p is itself regulated by the small rho-like GTPase Cdc42p and the GTP-binding protein Ras2p (Leberer et al., 1997; Mosch et al., 1996; Peter, Neiman, Park, van Lohuizen, & Herskowitz, 1996). In yeast PKA consists of the regulatory subunit Bcy1p and one of three catalytic subunits Tpk1p, Tpk2p, or Tpk3p; Tpk2p is required for pseudohyphal growth (Pan & Heitman, 1999; Robertson & Fink, 1998). The adenylate cyclase Cyr1p is regulated by Ras2p (Minato et al., 1994); thus, Ras2p acts upstream of both the filamentous growth MAPK and PKA pathways. The serine/threonine kinase Snf1p regulates transcriptional changes associated with glucose derepression, mediates several stress responses, and is required for pseudohyphal growth (Cullen & Sprague, 2000; Vyas, Kuchin, Berkey, & Carlson, 2003). Snf1p, Kss1p, and Tpk2p regulate the activity of *FLO11/MUC1*, which encodes a GPI-anchored cell surface flocculin, which is a key downstream effector of pseudohyphal growth (Guo, Styles, Feng, & Fink, 2000; Karunanithi et al., 2010; Kuchin et al., 2002; W. S. Lo & Dranginis, 1998; Pan & Heitman, 2002; Rupp et al., 1999a).

The genetic basis of the yeast pseudohyphal growth response extends well beyond the core signaling modules outlined above (Granek & Magwene, 2010; Li & Mitchell, 1997; Ma et al., 2007; Ma et al., 2007; Madhani, Galitski, Lander, & Fink, 1999; Mosch & Fink, 1997; Xu et al., 2010). By transposon-mediated gene disruption of 3,627 genes, we have previously identified 309 genes required for pseudohyphal growth in a haploid strain under conditions of butanol induction (Jin et al., 2008). The Boone laboratory has generated genome-wide collections of single gene deletion strains in a filamentous genetic background and has identified 700 genes required for the formation of surface-spread

filaments in a diploid strain under conditions of nitrogen stress (Dowell et al., 2010; Ryan et al., 2012). Thus, loss-of-function studies identify a broad set of genes that contribute to the filamentous growth response; however, even these studies are limited in that: (1) essential genes cannot by easily analyzed other than for haploinsufficiency; (2) some deletion phenotypes may be below a threshold that can be easily observed by standard assays; and (3) many phenotypes may be obscured by compensatory buffering effects in mutational analyses that rely on single gene deletions/disruptions. Obviously, no single genetic approach can be expected to yield comprehensive results, and in this light, gene overexpression-based studies have proven to be an effective complement to loss-of-function analyses (Douglas et al., 2012; Sopko et al., 2006). Upon integration with results from the studies above, the analysis of filamentation phenotypes from gene overexpression should identify more completely the genetic scope of pseudohyphal growth.

We present here the first genome-wide overexpression analysis of yeast pseudohyphal growth. For this study, we systematically overexpressed 4,909 yeast genes and identified 551 genes that enable pseudohyphal growth under conditions of normal vegetative growth. The data set was analyzed computationally to identify enriched pathways and signaling cascades, highlighting networks mediating MAPK signaling and cell cycle progression. Subsequent studies address a function for nuclear localization of the high osmolarity pathway MAPK Hog1p in repressing pseudohyphal growth, relevant to recent reports that the nuclear localization of Hog1p is not required for osmotolerance. Collectively, the work provides a valuable information resource for studies of yeast pseudohyphal growth.

2.2 Materials and Methods

2.2.1 Strains and Growth Conditions

The filamentous strains Y825, Y825/6, and HLY337 used in this study are derived from the Σ1278b genetic background (Gimeno et al., 1992). The genotype of haploid Y825 is *MAT***a** *ura3-52 leu2Δ0*; the genotype of diploid Y825/6 is *ura3-52/ura3-52 leu2Δ0/leu2Δ0*; and the genotype of HLY337 is *MAT**α** ura3-52 trp1-1*. Gene deletion mutants were generated using

PCR-mediated gene disruption with pFA6a-kanMX6 or pUG72 (Gueldener, Heinisch, Koehler, Voss, & Hegemann, 2002; Longtine et al., 1998). In addition to synthetic complete (SC) and SC drop-out media (US Biological), media for specific applications are described below.

2.2.2 The Overexpression Collection and High Throughput Plasmid Transformations

The plasmids utilized for overexpression are high-copy yeast shuttle vectors, with each construct containing a yeast open reading frame (ORF) cloned under transcriptional control of a galactose-inducible promoter. The 3' end of the ORF is fused in-frame with sequence encoding a triple affinity tag of His6, an HA epitope, a protease 3C cleavage site, and the IgG binding domain from protein A. In total, this plasmid collection encompasses 5,854 yeast ORFs, including 4,973 verified protein-coding ORFs as currently annotated in the *Saccharomyces* Genome Database ([www.yeastgenome.org](www.yeastgenome.org)). It should be noted that the affinity tags may perturb protein folding at the carboxy terminus of some of the gene products, but we expect that the majority of genes in this collection (~80-90%) should encode fully functional proteins, extrapolating from large-scale protein localization and affinity purification studies (Bharucha et al., 2008; Gavin et al., 2002; Ghaemmaghami et al., 2003; Y. Ho et al., 2002; Huh et al., 2003; Kumar et al., 2002). To generate overexpression strains for phenotypic analysis of filamentous growth, we introduced the plasmids individually in 96-well format into a diploid strain of the filamentous Σ1278b genetic background by a modified form of lithium acetate-mediated transformation as described (Bharucha et al., 2008; Jin et al., 2008; Kumar, des Etages, Coelho, Roeder, & Snyder, 2000; Kumar, Vidan, & Snyder, 2002; Ma et al., 2007; Ma et al., 2007). All transformants were selected on SC-Ura, and glycerol stock solutions (15% glycerol) were prepared. In total, we performed 6,894 plasmid preparations and yeast transformations to generate a collection of 5,854 strains (~85% efficiency).

2.2.3 Phenotypic Screening

By design of the overexpression vectors, galactose induction was used to regulate transcription of the plasmid-based target genes as follows. Yeast strains were sequentially

17

cultured in a 30° shaking incubator in nitrogen-sufficient minimal liquid media containing glucose, raffinose, and galactose for 2-3 days, overnight, and 6hrs, respectively. Minimal media consisted of 0.67% yeast nitrogen base (YNB) without amino acids and ammonium sulfate (Difco), 2% carbon source (glucose, raffinose, or galactose), 5m$M$ ammonium sulfate (nitrogen sufficiency), and additional amino acids to correct for auxotrophies as necessary. Following galactose induction for 6hrs, yeast cultures were spotted using a multichannel pipette onto agar plates consisting of 2% galactose, 0.67% YNB without amino acids and ammonium sulfate (Difco), 5mM ammonium sulfate, and additional amino acids to correct for auxotrophies. Galactose induction typically drives gene expression to levels 1000-fold of those observed in the presence of glucose (St John & Davis, 1981), and we estimate similar levels of inducible expression here by Western blotting (Supplementary Figure 2.1).

The presence of galactose in the medium significantly diminished the degree of observed surface-spread filamentation for all strains, including wild-type strains under conditions of low nitrogen, consistent with results reported in Lorenz *et al.* (Lorenz et al., 2000). Strong levels of invasive filamentation, however, were still observed, and we used this filamentation phenotype as an indicator of pseudohyphal growth. Invasive growth was assessed by a standard plate-washing assay as follows. Spotted cultures were incubated at 30° for 7 days and photographed before plate washing. Agar plates were rinsed with a gentle stream of water to remove noninvasive cells, and the remaining cells were photographed. Invasive clones were recorded and rescreened with the same protocol in a second pass. The degree of invasive growth was quantified by the pixel intensity ratio of spotted cultures pre- and postwashing.

2.2.4 Quantification of Screen Results

The level of invasiveness for each clone in the second pass was quantitatively measured using the integrated densitometry feature of ImageJ. Images of individual clones pre-and postplate washing were analyzed after background subtraction. Scores indicate the ratios of post- to prewash pixel intensity for each indicated clone.

18

2.2.5 Plasmid Construction

For galactose-independent overexpression, yeast ORFs with 1kb upstream sequence and 300bp downstream sequence were cloned into pRS426 using standard restriction enzyme digestion and ligation techniques (Sikorski & Hieter, 1989).

Plasmids pFA6a-GFP(S65T)-CAAX-kanMX6 and pFA6a-GFP(S65T)-CAAX-HIS3MX6 carrying GFP-CAAX modules were modified from pFA6a-GFP(S65T)-kanMX6 and pFA6a-GFP(S65T)-HIS3MX6 (Longtine et al., 1998). The *Pac1* and *Asc1* restriction sites of these plasmids were used to replace the GFP module with GFP-CAAX module, generated by PCR amplification using a 3' primer encoding the nine carboxy-terminal residues of the budding yeast Ras2p CAAX box (Westfall, Patterson, Chen, & Thorner, 2008). All plasmids available upon request.

2.2.6 Galactose-Independent Overexpression

Y825/6 strains with overexpression vectors (pRS426 carrying yeast ORFs with 1kb upstream sequence and 300 bp downstream sequence) were streaked on synthetic low ammonium dextrose (SLAD) plates (2% glucose, 0.67% YNB without amino acids and ammonium sulfate, 50µM ammonium sulfate, and supplemental leucine to correct for auxotrophy). Plates were incubated 5 days prior to imaging.

2.2.7 Verification of Overexpression by Western Blotting

Selected moveable open reading frame (MORF) strains of the Y825/6 background were cultured in 5ml SC-URA media overnight at 30°, followed by back dilution into nitrogen sufficient minimal media with galactose for 4hrs. Following protein extraction, SDS-PAGE resolution and transfer to nitrocellulose membrane by standard procedures, membranes were incubated with protein A antibody against the tandem affinity purification (TAP) tag in a 1:10,000 dilution. Blots were developed using SuperSignal West Dura Extrended Duration Substrate (Thermo Scientific).

2.2.8 Identifying Network Modules and Signaling Cascades by Computational Analysis

The gene set identified from this overexpression screen was submitted to the functional analysis tool DAVID (Huang da, Sherman, & Lempicki, 2009) to identify enriched Kyoto Encyclopedia of Genes and Genomes (KEGG)-annotated pathways. Since the overexpression screen was genome-wide in scope, the default background set was used. The most enriched pathways, mediating cell cycle progression (sce04111), meiosis (sce04113), and MAPK signaling (sce4011), were selected for further analysis. The KEGG.xml files of these pathway maps were downloaded and parsed using an in-house program that generates nodes and edge lists. The KGML pathway .xml (kgml) file consists of "entry" tags, which can be represented as nodes, and "relation" tags, which can be represented as edges of a network. The entry tags consist of genes, compounds, and complexes, while the relation tags include manually curated molecular interactions, reaction networks, genetic and environmental information processing, and cellular networks (Kanehisa, Goto, Sato, Furumichi, & Tanabe, 2012). Cytoscape (Killcoyne, Carter, Smith, & Boyle, 2009), which constructs a ball-and-stick representation of a network using an edge list, was used to visualize the network. Since the three pathways possess overlapping gene sets, the edge lists were concatenated and visualized as one single network.

2.2.9 Invasive Growth Analysis of Strains with Modified *HOG1* Alleles

Yeast strains of the Y825 genetic background containing integrated *HOG-GFP*, *Hog1p-GFP-CCAAX^{Ras2p}*, and *hog1Δ* alleles were assayed for invasive growth by plating spotted cultures on SLAD plates with 1% (vol/vol) butanol. Plates were sealed in parafilm and incubated for 7 days at 30°. Strains were assayed for invasive growth by rinsing with water and rubbing away nonadherent cells (Cullen & Sprague, 2000). Spotted cultures were photographed pre- and post wash, and invasiveness was measured using the integrated density feature of ImageJ.

2.2.10 *β*-Galactosidase Assays

The *FRE-lacZ* reporter construct (Madhani & Fink, 1997) was used to measure filamentous growth signaling using the Yeast *β*-Galactosidase Assay kit (Thermo Scientific) according to protocols described previously.

2.2.11 Fluorescence Microscopy

Fluorescence images were taken using a DeltaVision-RT Live Cell Imaging system (Applied Precision). Image capture was conducted using Applied Precision's SoftWorx imaging software.

2.3 Results

2.3.1 Generating a Mutant Collection for Genome-Wide Overexpression Analysis

Standard laboratory strains of *S. cerevisiae* (e.g., derivatives of S288c) are nonfilamentous and, consequently, inappropriate for studies of pseudohyphal growth. The Σ1278b strain has emerged as the preferred background for studies of filamentation, since it undergoes a significant and easily controlled transition to filamentous growth (Gimeno et al., 1992; Grenson, 1966); however, no genome-wide mutant collections suitable for this study have been generated previously in the Σ1278b background (Coelho, Kumar, & Snyder, 2000). Here, we sought to construct an extensive reagent base for overexpression studies of pseudohyphal growth, generating a collection of yeast strains in Σ1278b with each mutant carrying a single plasmid enabling galactose-inducible gene overexpression. For this purpose, we utilized the plasmid collection constructed in Gelperin et al. and introduced the plasmids individually by transformation into diploid yeast. Of the 5,854 plasmids encompassed in this overexpression collection, we identified 4,909 clones that: (1) contained an ORF corresponding to an annotated and verified yeast gene and (2) allowed for sufficient cell growth upon galactose induction in the Σ1278b background such that invasive growth assays could be performed.

The design of the phenotypic screen is outlined in Figure 2.1A and detailed in Materials and Methods.  In brief, we drove gene overexpression by growth in galactose under conditions of nitrogen sufficiency; this approach identifies genes that upon overexpression can enable pseudohyphal growth in the absence of stimuli capable of inducing filamentation.  To ensure that gene overexpression was efficient, we analyzed resulting protein levels by Western blotting for a sampling of seven strains in the constructed mutant collection (Supplementary Figure 2.1).  Filamentation was assessed by invasive growth analysis, as surface filamentation is lessened in the presence of galactose (Lorenz et al., 2000).  To confirm that invasive filamentation was indeed an effective indicator of diploid pseudohyphal growth, we cloned five genes along with native promoters into a high-copy yeast shuttle vector such that gene overexpression phenotypes could be measured without effects from galactose induction.  Strains carrying the high-copy number vector clones yielded surface-spread filamentation phenotypes matching the corresponding invasive growth phenotypes observed in the screen.  In addition, a positive control consisting of galactose-induced overexpression of eight genes known to affect pseudohyphal growth yielded exaggerated invasive phenotypes as shown in Figure 2.1B. The phenotypic difference between a wild-type strain and the indicated overexpression mutants is clear and establishes an easily identifiable threshold for positive results.
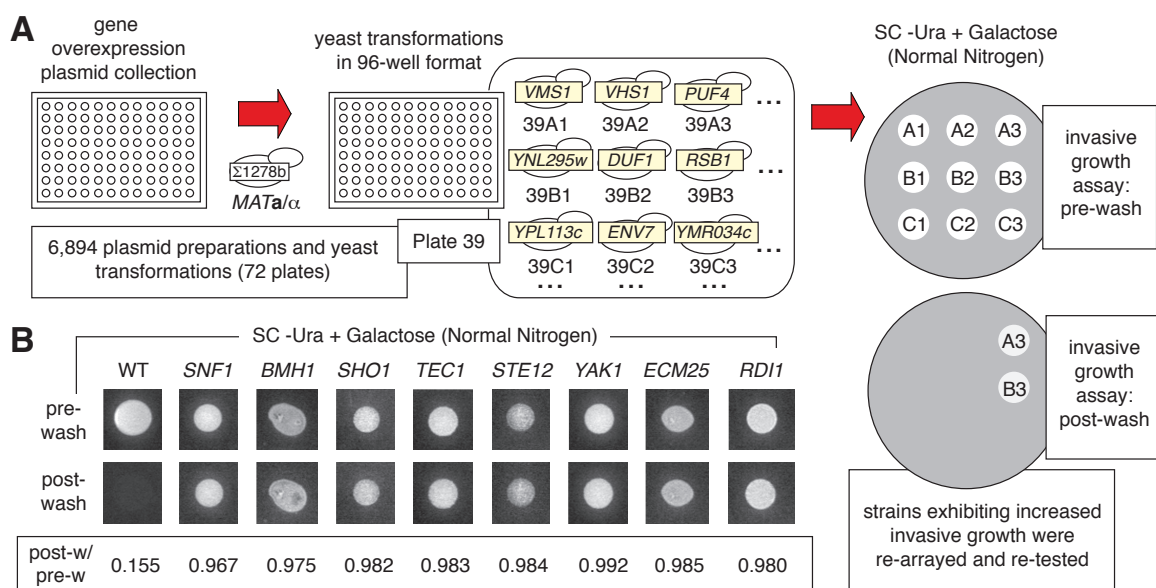
Figure 2.1 Systematic overexpression screen to identify genes capable of inducing filamentous growth. A.) Overview of the experimental design. Sample set of overexpression constructs from plate 39 (of 72 plates in total) is shown. Spotted cultures were assayed for invasive growth in an arrayed pattern with 48 spots per plate. Cultures were rearrayed in an altered pattern during retesting to control for positional effects. B.) Sampling of assay results for the wild-type background strain and eight overexpression mutants yielding invasive growth under conditions of nitrogen sufficiency. The degree of invasive growth was quantified by determining the pixel intensity of the spotted culture postwash relative to its prewash intensity.

## 2.3.2 A Collection of Yeast Genes Capable of Inducing Pseudohyphal Growth

By the systematic genome-wide overexpression analysis described above, we identified 551 genes that resulted in invasive filamentation upon galactose induction under conditions of nitrogen sufficiency (Figure 2.2A); the full gene list is provided in Supplementary Figure 2.2. This gene set is comparable in size to the complement of genes that yield pseudohyphal growth defects upon gene deletion under conditions of butanol induction and nitrogen deprivation (Jin et al., 2008; Ryan et al., 2012). The individual genes, however, vary between these gene sets, and the distinctions between overexpression-based screens vs. loss-of-function screens are presented in Discussion.

By simple Gene Ontology (GO) term analysis, the invasive growth overexpression gene set was not enriched for any molecular functions or protein-associated subcellular

components; however, we did identify several enriched biological process terms (Figure 2B).  Gene annotated as contributing to the regulation of metabolic processes associated with nitrogenous compounds were enriched in the overexpression gene set (P-value of 8.2 x $10^{-7}$).  This is not surprising since nitrogen availability is an important regulator of pseudohyphal growth.  This GO term is broad in scope; among the associated genes are several known pseudohyphal growth regulators, including the *STE12* and *TEC1* genes that collectively encode a transcriptional complex acting downstream of Kss1p to activate gene promoters with filamentation-and-invasion response elements (*FRE*s) (Madhani & Fink, 1997).  Genes involved in the cellular response to nutrient levels were also enriched in the results from our screen, as were overlapping gene sets associated with cytoskeletal organization and spindle pole body organization.  The nutrient-responsive gene set encompasses the *SNF1* kinase gene, which plays an established role in regulating pseudohyphal growth (Kuchin et al., 2002).  Interestingly, a large cohort of 79 functionally uncharacterized genes that lack a standard gene name indicative of function was identified in this screen.  Mutant alleles of these genes lack extensive phenotypic characterization, and, for many of the indicated genes, the overexpression studies presented here offer initial insight into the regulatory consequences of increased transcription, particularly in a filamentous genetic background.

To consider the possibility that genes mediating specific cellular processes may affect pseudohyphal growth to differing degrees, we analyzed our quantified screening results for GO term enrichment within genes grouped by the intensity of observed overexpression-induced invasive growth (Figure 2.2D).  The degree of invasive growth was estimated by the pixel intensity postwash to prewash of each spotted overexpression culture.  The pixel intensities were binned into categories (ranging from 0.94 to 0.99 and above), and the associated genes within each grouping were assessed for enrichment of GO terms.  By this analysis, genes annotated as being associated with M phase of the meiotic cell cycle (GO:0051327) were enriched in the gene set that yielded the strongest level of invasive growth upon overexpression (postwash:prewash pixel intensity greater than 0.99).

**A**  Screening Summary:

Plasmids for gene overexpression:

His₆-HA-ProtA

P_Gal1 — yORF

att    att

Σ1278b

SC -Ura +Gal

4,909 yeast genes screened for overexpression-based invasive growth on normal N

551 genes identified

| 472 | 79 |

Gene "hits" (% screened)

| 472(12.3%) | 3,832 |
| 79(7.3%) | 1,077 |
|  | 100% |

☐ genes with an annotated function (standard name)

☐ functionally uncharacterized genes (sys. name)

**B**  GO biological process terms enriched in the identified gene set:

Regulation of nitrogen compound metabolic processes (GO: 0051171)    $8.2 \times 10^{-7}$

ACT1 ADR1 ARG82 ARP5 ARP8 ATP25 AZF1 BDF1 BRF1 CAF40 CDC28 CEP3 CIN5 CKB2 CKS1 CLB6 CUP2 CYC8 DAL80 DOT6 EDS1 ESA1 ESC1 GAL4 GAL80 GAT2 GAT3 GAT4 GCN5 GLN3 GTS1 GYP1 GYP8 GZF3 HAA1 HAL9 HDA2 HIR2 HMS1 HMS2 HSF1 IOC3 IQG1 IRE1 LEU3 LGE1 LYS14 MDR1 MGA1 MIG1 MIG2 MIG3 MKS1 MOT3 MRS6 MSA1 MSA2 MSN1 NAB2 NDJ1 ORC3 ORC4 PAB1 PCF11 PHO23 PIF1 PKH2 POP2 PUF4 RAS1 RAT1 RDI1 RGD1 RGM1 RGT1 RME1 RNA1 RRD1 RSC2 RTG3 RTT103 RVB2 SET3 SGF73 SIN4 SKP2 SLD7 SMI1 SPP41 SPS18 SPT10 SPT2 SPT21 SSK1 SSN8 STE12 STP2 SUT2 SWC4 TAF1 TBF1 TEC1 TOA1 TOD6 TOP1 TOS8 TYE7 VHR1 WAR1 XBP1 YRB30 YRM1 YRR1

Spindle pole body organization (GO: 0051300)    $1.3 \times 10^{-4}$

CDC28 CDC31 CDH1 CLB2 DSK2 HSF1 KAR1 KIP1 MPS1 MPS2 SFI1 SPC29 SWE1

Cytoskeleton organization and biogenesis (GO: 0007010)    $1.2 \times 10^{-3}$

ABP1 ABP140 ACT1 ARK1 CBK1 CDC28 CDC31 CDH1 CEP3 CLB2 CTF13 DMA1 DSK2 DUO1 ENT3 ENT4 FIN1 HSF1 IQG1 KAR1 KIP1 LAS17 MHP1 MPS1 MPS2 RDI1 RRD1 SFI1 SFK1 SHE1 SLG1 SLK19 SPC29 STU2 SWE1 SYP1 TVP38 VRP1 WSC3

Cellular response to nutrient levels (GO: 0031669)    $4.7 \times 10^{-3}$

ADR1 ARF1 ATG13 ATG14 ATG20 CCZ1 DAL80 DPL1 GAL4 GLN3 GZF3 MIG1 MIG2 PHM8 PRB1 SEC7 SIC1 SIP5 SNF1 SSN8 VAM3

**C**  Functionally uncharacterized genes (79):

YAR070C YBL071C YBL098C YBR090C YBR226C YCL046W YDL221W YDR186C YDR266C YDR282C YDR333C YDR348C YDR387C YDR442W YDR514C YEL030C-A YER064C YER085C YER140W YER184C YFR045W YGL108C YGL177W YGR026W YGR042W YGR064W YGR087C YGR107W YGR125W YGR235C YHR079C-A YHR131W YHR162W YHR177W YIL045C YIL055C YIL077C YIR042C YJL132W YJL222W-B YJR030C YKL027W YKL047W YKL071W YKL156C-A YKR005C YKR051W YKR078W YLL058W YLR057W YLR072W YLR152C YLR177W YLR230W YLR241W YLR253W YLR358C YLR374C YLR428C YML020W YNL022C YNL109W YNL115C YNR021W YOL029C YOL107W YOR022C YOR062C YOR283W YOR387C YPL071C YPL077C YPL109C YPL168W YPR022C YPR077C YPR097W YPR117W YPR148C

**D**

Gene number ↑    Pixel intensity of spotted culture post-wash / pre-wash →

n=50 (0.94)  n=66 (0.95)  n=72 (0.96)  n=81 (0.97)  n=92 (0.98)  n=190 (0.99)

Macroautophagy (GO:0016236) $8.09 \times 10^{-4}$
ATG13 ATG20 ARF1 SEC7 SIC1

Regulation of transcription involved in G1 phase (GO:0000114) $3.9 \times 10^{-3}$
MSA1 MSA2

Osmosensory pathway (GO:0007231) $3.1 \times 10^{-3}$
RGD1 SKS1

M phase of cell cycle (GO:0000087) $4.9 \times 10^{-3}$
CBF5 CDC31 DMA1 DUO1 FIN1 MPS1 MPS2 NUP53

Fungal cell wall organization (GO:0071852) $2.0 \times 10^{-5}$
BCH2 ECM13 ECM25 EMW1 PRS5 SBE2 WSC3

M phase of meiotic cell cycle (GO:0051327) $8.2 \times 10^{-4}$
ADY4 IME2 KAR3 PDS1 RIM4 RME1 SET3 SLK19 SPO23 SWE1

Figure 2.2 Summary of overexpression screen results. A.) Yeast genes were overexpressed by galactose induction using the indicated vector.  Summary of screening results is presented below the vector diagram. The percentage of genes that yielded an overexpression-based filamentous growth phenotypes is shown, with a breakdown separating functionally uncharacterized genes from those with an annotated function and standard name.  Percentages are indicated out of total genes screened per category.  B.) Listing of Gene Ontology (GO) biological process categories enriched in the set of genes yielding filamentous growth phenotypes upon overexpression. Identified genes belonging to each category are indicated; extensively overlapping biological process categories are grouped together for convenience.  C.) Listing of functionally uncharacterized genes identified in the screen. D.) Quantified invasive growth scores were clustered and analyzed for enriched GO biological process terms.  Identified GO terms are indicated along with gene "hits" annotated to each category.  The number of genes (n) within each scoring range is indicated by the bar.

2.3.3 Signaling Pathways That Regulate Pseudohyphal Growth

While the GO term analysis above provides broad indications of cellular processes contributing to pseudohyphal growth, we also sought to identify specific pathways that affect filamentation by searching for KEGG signaling pathways overrepresented in the overexpression screen results.  KEGG is an online database that provides annotated and manually drawn signaling pathway maps for a broad range of eukaryotes (www.genome.jp/kegg/).  For our purposes, KEGG provides the largest set of yeast pathways annotations.

To identify enriched KEGG-annotated signaling pathways in our overexpression data set, we implemented a computational approach utilizing the functional annotational tool DAVID.  By this analysis, we found pathways controlling cell cycle progression (sce04111), meiosis (sce04113), and MAPK signaling (sce04011) to be the most highly enriched in the overexpression data (Figure 2.3A).  As these pathways encompass overlapping gene sets, we constructed network connectivity maps to better visualize the signaling modules (Figure 2.3B).  Genes identified in the overexpression screen were used as core "seeds" along with other annotated components of the three pathways.  The pathways were parsed using an in-house program and subsequently reassembled into a network using Cytoscape (Materials and Methods).  Connections are visualized as ball-and-stick representations in Figure 2.3B.  From this analysis, gene sets exhibiting genetic and/or physical interactions with components of the KEGG-annotated cell cycle and meiosis pathways were densely overlapping; this is not surprising since progression through the cell cycle and meiosis are obviously related processes.  Genes exhibiting connections with MAPK signaling pathways share extensive connectivity with genes associated with meiosis and cell cycle progression.  Interestingly, strictly from connections reported in the KEGG resources, the Kss1p and osmosensing Hog1p MAPK cascades link the MAPK signaling connectivity map with larger gene sets associated with cell cycle progression and meiosis (Figure 2.3B, inset).
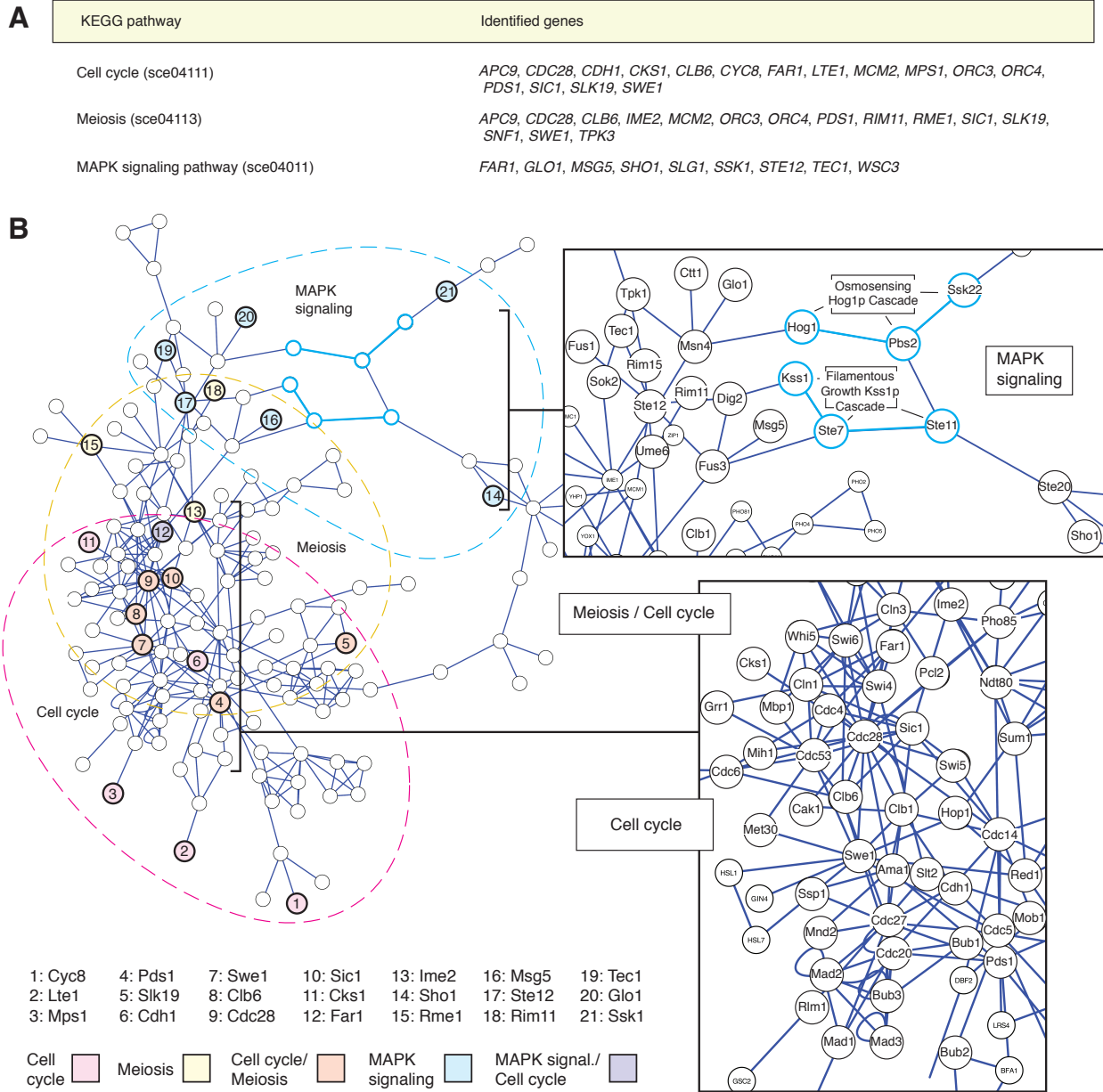
**Figure 2.3 Identification of genetic networks that regulate the induction of filamentous growth. A.)** The overexpression screen data set was analyzed for enrichment of pathways annotated in the Kyoto Encyclopedia of Genes and Genomes (KEGG). Enriched pathways are shown along with gene identified in the screen that are annotated as belonging to the respective pathway. **B.)** Network connectivity map was built for MAPK signaling, meiosis, and cell cycle networks from interactions annotated in KEGG. The numbered circles indicate a subset of the genes identified in the overexpression screen that belong to the respective networks. Blowups of central portions of the cell cycle, meiosis, and MAPK signaling networks are provided, with key network components indicated in larger circles. Components of a given pathway in the map are indicated with a dashed line to highlight the overlap between networks. Two key connections between the MAPK signaling modules and the cell cycle/meiosis networks involving the Kss1p and Hog1p signaling cascades are shown in blue within the inset box.

Thus, from this analysis we identified core networks enriched in the data set mediating MAPK signaling. Consequently, in the following sets of experiments we further investigated the role of nuclear Hog1p in regulating pseudohyphal growth.

2.3.4 Hog1p-Mediated Repression of Pseudohyphal Growth

Genes annotated as contributing to MAPK signaling were enriched in the results of our overexpression screen; in particular, the screen identified several genes known to regulate the activity of Hog1p. The Hog1p kinase is a MAPK best studied for its role in producing glycerol as a compensatory osmolyte in response to increased levels of extracellular osmolarity (Kultz & Burg, 1998; Westfall et al., 2008); however, Hog1p is also known to repress pseudohyphal growth in the absence of filamentation-inducing stimuli (O'Rourke & Herskowitz, 1998; Pitoniak, Birkaya, Dionne, Vadaie, & Cullen, 2009). A simplified representation of the Hog1p pathway is presented in Figure 2.4A. In yeast, high extracellular osmolarity stimulates two putative osmosensors, Sho1p and Sln1p (Posas & Saito, 1997). Sho1p activates the p21-activated kinase family member Ste20p, which in turn activates a cascade of the MAPKKK Ste11p, the MAPKK Pbs2p, and Hog1p (Raitt, Posas, & Saito, 2000). Sln1p, Ypd1p, and Ssk1p are components of a phosphorelay signaling system that activates the partially redundant kinases Ssk1p and Ssk22p upon osmostress; these kinases in turn activate Pbs2p, resulting in activation of Hog1p (Brewster, de Valoir, Dwyer, Winter, & Gustin, 1993; Maeda, Wurgler-Murphy, & Saito, 1994; Posas et al., 1996). Upon activation, Hog1p is rapidly translocated to the nucleus through a process that requires the importin-β family member Nmd5p (Ferrigno, Posas, Koepp, Saito, & Silver, 1998a). Nuclear Hog1p has been identified in complexes at hundreds of promoters and genes, influencing chromatin remodeling and transcription (O'Rourke & Herskowitz, 2004; Pokholok, Zeitlinger, Hannett, Reynolds, & Young, 2006; Zapater, Sohrmann, Peter, Posas, & de Nadal, 2007). Subsequently, Hog1p is largely dephosphorylated by the phosphatases Ptc1p, Ptc2p, Ptc3p, Ptp2p, and Ptp3p (Mattison, Spencer, Kresge, Lee, & Ota, 1999; Robinson, van Zyl, Phizicky, & Broach, 1994; Wurgler-Murphy, Maeda, Witten, & Saito, 1997). Dephosphorylated Hog1p is exported into the cytosol through interaction with the karyopherin Crm1p (Ferrigno et al., 1998a).

Interestingly, three genes involved in the nuclear export of Hog1p (*NBP2*, *PTP2*, and *CRM1*) were identified in the overexpression screen as enabling invasive growth under conditions of nitrogen sufficiency. To further consider the possibility that the nuclear export of Hog1p promotes pseudohyphal growth, we cloned the genes and promoters for *CRM1*, *NBP2*, *PTC3*, *PTP2*, and *PTP3* into a high-copy vector, enabling analysis of overexpression phenotypes without galactose induction. Each of these genes contributes to the dephosphorylation and nuclear export of Hog1p; *NBP2* is not illustrated in Figure 2.4A, but it recruits Ptc1p to the Pbs2p-Hog1p complex (Mapes & Ota, 2004). We introduced these plasmids into a diploid strain of the filamentous Σ1278b genetic background and assayed for surface-spread filamentation under conditions of nitrogen limitation. In each case, the strains exhibited hyperactive surface filamentation relative to a wild-type strain carrying an empty vector control (Figure 2.4B).

Classically, the nuclear form of Hog1p had been thought to mediate osmotolerance; however, Westfall et al. (2008) reported that cells lacking *NMD5* and/or cells with a plasma membrane-tethered form of Hog1p survive hyperosmotic stress. This raises an interesting question regarding the functional contributions of nuclear Hog1p. Considering the overexpression results above, one function of nuclear Hog1p may be to repress pseudohyphal growth in a filamentation-competent strain of *S. cerevisiae*, although it should be noted that other pathways will also be affected by overexpression of genes such as *CRM1* and *NMD5*.

To investigate more directly the effect of spatial compartmentalization of Hog1p function, we constructed a haploid yeast strain in the Σ1278b background wherein endogenous *HOG1* was fused at its 3' end to sequence encoding GFP and the nine C-terminal residues of Ras2p (designated CCAAX[Ras2p]) as in Westfall et al. (2008). By virtue of the S-palmitoylation and S-farnesylation of the cysteine residues in the appended Ras2p carboxy-terminal tail, the translated Hog1p-GFP-CCAAX[Ras2p] chimera should localize at the plasma membrane, and we did observe concentrated fluorescence at the cell periphery in this strain (Figure 2.4C) relative to an otherwise isogenic strain containing an integrated *HOG1-GFP* allele. It should be noted that some Hog1p-GFP-CCAAX[Ras2p] may be present at

the nuclear membrane, although we did not observe any nuclear Hog1p chimera by fluorescence microscopy. Under pseudohyphal growth-inducing conditions of nitrogen stress and butanol treatment, the strain containing the Hog1p-GFP-CCAAX[Ras2p] chimera showed slightly exaggerated invasive growth relative to a strain containing Hog1p-GFP, with invasive growth levels comparable to those observed in a *hog1Δ* strain. Under conditions of nitrogen sufficiency, the mutant strain containing Hog1p-GFP-CCAAX[Ras2p] is hyperfilamentous with respect to a strain containing Hog1p-GFP, although not quite to the level of a *hog1Δ* strain; the degree of filamentous growth activity is measured in Figure 2.4C using a filamentation MAPK Kss1p pathway-specific *FRE-lacZ* reporter.
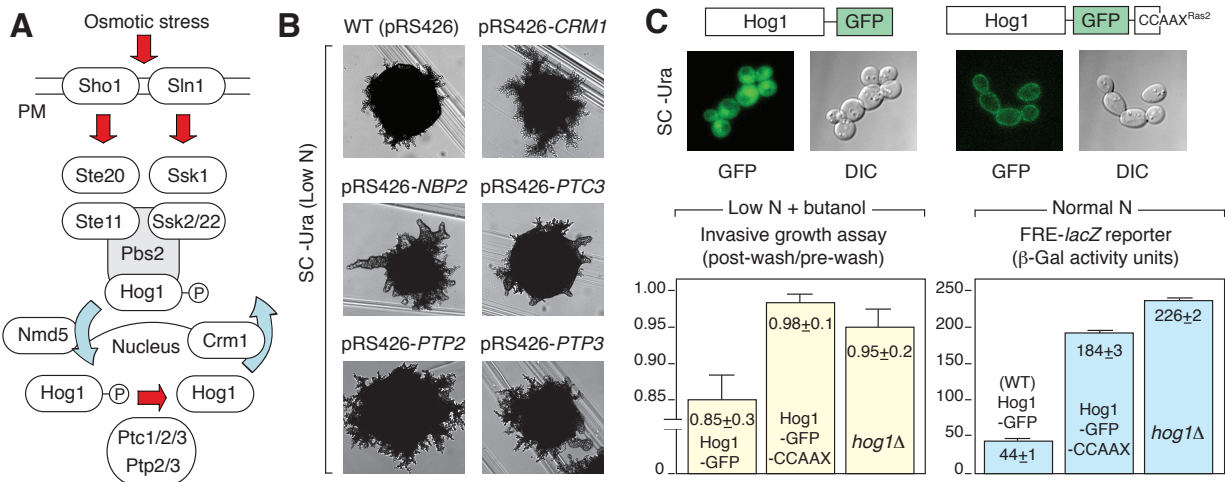


Figure 2.4 Regulated subcellular distribution of Hog1p and resulting filamentous growth phenotypes. A.) Diagram of the Hog1p MAPK osmosensing pathway. Regulated nuclear import and export of Hog1p is indicated. B.) Surface filamentation of genes along with native promoters cloned into a high-copy yeast shuttle vector. The selected genes regulate Hog1p phosphorylation/localization, thereby negatively regulating Hog1p function. C.) Fluorescence images indicate that Hog1p-GFP with the carboxy-terminal Ras palmitoylation/farnesylation tag localizes to the cell periphery. Differential interference contrast (DIC) images are shown along with fluorescence images. Invasive growth assay results are shown for a haploid filamentous strain containing Hog1p-GFP and the plasma membrane-tethered Hog1p-GFP-CCAAX form and a *hog1Δ* strain. The analysis was performed in triplicate, and mean values are shown. Error bars indicate standard deviation. Filamentous growth pathway activity was also assayed in the same three strains using a lacZ reporter driven from a promoter containing filamentation-responsive elements (FREs) recognized by the Ste12p/Tec1p transcription factor complex. Analyses were performed in triplicate, and mean results with standard deviation are indicated.

2.4 Discussion

Here we implemented a systematic and genome-wide analysis of yeast invasive filamentation induced by gene overexpression. Interestingly, as compared against the results from large-scale deletion/disruption screens, systematic overexpression screens typically identify overlapping, but decidedly nonredundant, data sets (Sopko et al., 2006) . We observe similar results here. In this screen, we identified 61 genes that were also reported in the targeted gene deletion screen by Ryan et al. (2012) and 79 genes that yielded pseudohyphal growth defects in a previous transposon-based disruption screen (Jin et al., 2008). Comparisons between these data sets are inexact, however, since: (1) filamentation phenotypes were assayed slightly differently in each screen; (2) the transposon-based study was smaller in scope, encompassing ∼60% of the annotated yeast gene complement; (3) butanol treatment as opposed to nitrogen stress was used to induce filamentation in the transposon mutagenesis study; and (4) a haploid strain was used for transposon mutagenesis while we used diploid cells for this overexpression screen. The partial overlap between loss-of-function and overexpression results stems from the fact that many genes can be required for a given cell process without being sufficient to induce that process upon overexpression. Consequently, we expected to identify a greater number of regulatory genes by this overexpression screen, and we did identify many such genes, including several that regulate cell cycle progression and MAPK signaling. However, we did not observe a statistically significant enrichment for transcription factors, kinases, and/or nutrient sensors in the data set, and the set of gene hits from this overexpression screen that overlapped the genes identified by targeted deletion and transposon-based loss-of-function screening was not significantly enriched for any GO terms. This overlapped gene set does encompass several key pseudohyphal growth genes, including *STE12*, *TEC1*, *SNF1*, and *SHO1*.

In interpreting the results from this study, it is important to bear in mind two caveats. First, 4,909 genes (of 4,973 verified ORFs) were analyzed by overexpression; thus, we do not consider the screen to be comprehensive, although it is the largest overexpression-based screen of pseudohyphal growth to date. Second, the plasmid library

used in this study is a gene fusion library, and for a subset of the genes tested, the carboxy-terminal modification may result in dominant effects that can confound the interpretation of results.  It is difficult to estimate the degree of this effect, but previous studies indicate that ~97% of the cloned gene products do encode full-length proteins (Gelperin et al., 2005), which may mitigate concerns regarding phenotypes from truncated proteins.

The gene set identified in this study appears large at first glance.  However, systematic deletion studies in haploid and diploid strains of the $\Sigma$1278b background have identified comparably large sets of genes yielding pseudohyphal growth phenotypes.  Our previous transposon-based disruption screen of 3,627 genes identified 309 that were required for butanol-induced surface filamentation.  Similarly, our previous small-scale overexpression screen identified 199 genes of 2,043 tested that yielded exaggerated pseudohyphal growth under conditions of butanol induction (Jin et al., 2008). Extrapolating these results to the genome as a whole, we arrive again at comparably sized data sets.  From these systematic disruption and overexpression screens, it is clear that many cellular processes need to occur effectively for surface filaments to appear.  Cell cycle progression, cell budding, polarized growth, cytoskeletal organization, nutrient sensing/responses, and numerous metabolic/biosynthetic processes all contribute to, and are required for, the formation of extensive surface filaments.  The pseudohyphal growth response represents an integrative output, the magnitude of which is modulated by a diverse complement of signaling pathways and genetic networks.  In sum, the complexity and scope of the genetic machinery underlying yeast pseudohyphal growth makes it an ideal subject for genomic analysis.

MAPK signaling pathways are key pseudohyphal growth regulators, and the scope of genes identified in this screen that affect filamentation by impacting a MAPK signaling pathway may be large, as suggested from the network analysis presented here.  In particular, our data encompass the known MAPK regulators/effectors *SHO1*, *MSB2*, *PTP3*, *STE12*, and *TEC1*, and 17 genes identified in this overexpression screen also exhibited increased mRNA transcript abundance upon induction of MAPK pathway activity (C. J. Roberts et al., 2000).

With respect to understanding MAPK cascade activity, considerable research efforts have been expended to consider the mechanisms ensuring MAPK signaling specificity during pseudohyphal growth (Bao, Schwartz, Cantin, Yates, & Madhani, 2004; Hao et al., 2008; Maleri et al., 2004; O'Rourke & Herskowitz, 2004).  In particular, the Hog1p MAPK pathway is known to inhibit pseudohyphal growth in the absence of filamentous growth-inducing stimuli, and *HOG1* deletion mutants exhibit hyperactive surface filamentation under nutrient-rich conditions (O'Rourke & Herskowitz, 1998).  Interestingly, several genes that promote nuclear export of the osmoregulatory MAPK Hog1p, induced invasive growth upon overexpression.  The nuclear-localized form of Hog1p is generally thought to mediate the hyperosmotic response and presumably also represses pseudohyphal growth.  This notion, however, has been called into question, as Westfall et al. (2008) have reported that a yeast strain containing an allele of *HOG1* encoding a plasma membrane-tethered form of the protein is still resistant to hyperosmotic stress.  If nuclear-localized Hog1p is not required for resistance to hyperosmotic stress, the possibility exists that one function of nuclear Hog1p may be to repress pseudohyphal growth.  As presented here, our overexpression screen results are consistent with this possibility, and results using a plasma membrane-tethered form of Hog1p are also consistent with this model.  Identification of the nuclear targets of Hog1p that mediate a repressive effect remains a future goal.  The transcription factor Tec1p is a strong candidate, as Shock et al. (2009) propose that Hog1p prevents Tec1p binding to DNA.

The importance of Hog1p signaling in regulating pseudohyphal growth is not limited to *S. cerevisiae*.  In *C. albicans*, *HOG1* is involved in oxidative stress responses, osmotic stress responses, and in cell wall biosynthesis, and functional Hog1p represses the yeast-to-hyphal transition (Alonso-Monge et al., 1999; Alonso-Monge et al., 2003; Enjalbert et al., 2006; San Jose, Monge, Perez-Diaz, Pla, & Nombela, 1996).  Notably, mutants defective for Hog1p function display reduced virulence in mice and increased susceptibility to phagocytic cells (Cheetham et al., 2011; Gonzalez-Parraga, Alonso-Monge, Pla, & Arguelles, 2010).  The Hog1 MAPK cascade in *C. albicans* encompasses the MAPKK Pbs2 and the MAPKKK Ssk2 (Cheetham et al., 2007), although additional upstream and downstream regulators have not been elucidated as extensively as in *S. cerevisiae*.  As this

*Candida* network becomes more clearly delineated, it will be interesting to determine if the emerging model of Hog1p-mediated regulation of filamentous growth in *S. cerevisiae* is borne out and even further, the degree to which corresponding filamentous growth regulatory networks in baker's yeast contribute to hyphal development and virulence in *C. albicans*.

In sum, we present here the first systematic overexpression screen for genes capable of inducing yeast pseudohyphal growth. Our results provide overexpression phenotypes for a large number of genes with uncharacterized function, and it is tempting to speculate that some of these genes may exhibit functions in the filamentous Σ1278b background but not in nonfilamentous strains. We further identified several signaling networks that modulate pseudohyphal growth levels upon overexpression-based perturbation, and collectively, the work presents a significantly enhanced foundation for the mapping of genetic relationships within the pseudohyphal growth regulatory network.
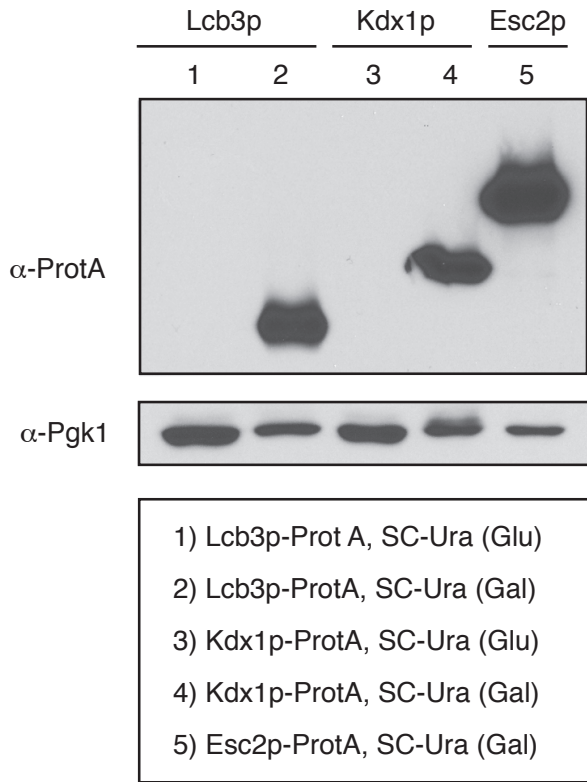
Supplementary Figure 2.1 Western blot indicates galactose overexpression of cloned genes. By virtue of the cloning vector, genes were fused at their 3'-ends to an affinity tag including sequence encoding the IgG binding domain from Protein A. Antibody against Protein A was used to detect the overexpressed gene product in medium with glucose and galactose, respectively, Pgk1p levels were assessed as a loading control. Results for overexpression of three genes are shown here.

Agar invasion score 0.94:

*YAL024C, YAL027W, YBL079W, YBR276C, YCL046W, YCR005C, YDL051W, YDR186C, YDR289C, YDR348C, YGL006W, YGL057C, YGL110C, YGL123W, YGL227W, YGR240C, YHR002W, YIL078W, YKR005C, YKR035C, YKR077W, YLR102C, YLR152C, YLR399C, YLR451W, YML004C, YNL066W, YNL149C, YNL204C, YNL311C, YNR032W, YOL107W, YOL116W, YOR022C, YOR038C, YOR049C, YOR066W, YOR145C, YOR208W, YOR241W, YOR244W, YOR283W, YOR334W, YPL054W, YPL124W, YPL210C, YPL217C, YPR085C, YPR117W, YPR140W*

Agar invasion score 0.95:

*YAR031W, YBL063W, YBL091C-A, YBR021W, YBR152W, YBR226C, YDL113C, YDL192W, YDR034C, YDR162C, YDR170C, YDR295C, YDR514C, YEL005C, YER028C, YER140W, YGL122C, YGL167C, YGL177W, YGL226W, YGR028W, YGR043C, YGR107W, YGR112W, YHR036W, YHR085W, YHR162W, YIL104C, YIL153W, YIR042C, YJL192C, YJL222W-B, YKL051W, YKL135C, YKL156C-A, YKR051W, YLL004W, YLL006W, YLR079W, YLR259C, YLR328W, YLR358C, YLR409C, YLR428C, YMR098C, YMR102C, YMR193W, YMR205C, YNL055C, YNL318C, YOL104C, YOL165C, YOR062C, YOR109W, YOR236W, YOR344C, YOR387C, YPL022W, YPL207W, YPL235W, YPR054W, YPR079W, YPR113W, YPR119W, YPR148C, YPR185W*

Agar invasion score 0.96:

*YAL035W, YBL047C, YBL071C, YBR128C, YBR131W, YBR294W, YDL014W, YDL090C, YDL182W, YDR155C, YDR264C, YDR282C, YDR477W, YER144C, YER151C, YFL039C, YFL050C, YGL055W, YGL064C, YGL096W, YGL099W, YGR002C, YGR052W, YGR064W, YGR094W, YGR119C, YGR125W, YGR243W, YHR104W, YHR109W, YIL158W, YIR028W, YJL127C, YJL134W, YJR045C, YJR117W, YKL071W, YKL143W, YKL144C, YKL166C, YKR034W, YKR053C, YKR097W, YLL024C, YLR057W, YLR084C, YLR230W, YMR115W, YMR168C, YMR235C, YMR276W, YMR283C, YNL059C, YNL127W, YNL288W, YNR052C, YOR034C, YOR039W, YOR048C, YOR070C, YOR205C, YOR237W, YOR245C, YOR384C, YPL040C, YPL077C, YPL242C, YPR004C, YPR008W, YPR021C, YPR077C, YPR162C*

Agar invasion score 0.97:

*YAR007C, YBR024W, YBR260C, YDL028C, YDL089W, YDR085C, YDR130C, YDR173C, YDR212W, YDR266C, YDR333C, YDR376W, YDR387C, YDR464W, YDR517W, YEL030C-A, YEL040W, YER014W, YER025W, YER048C, YER165W, YER176W, YER177W, YFL055W, YFR050C, YGL049C, YGL061C, YGL075C, YGL108C, YGR042W, YGR131W, YGR172C, YGR175C, YGR229C, YGR248W, YGR252W, YHR006W, YHR007C, YHR024C, YHR115C, YIL015W, YIL101C, YIR001C, YIR027C, YJL042W, YJL132W, YJL157C, YJR095W, YJR125C, YKL084W, YKL172W, YKR069W, YLL023C, YLL038C, YLR006C, YLR008C, YLR175W, YLR258W, YML088W, YML130C, YMR003W, YMR006C, YMR063W, YMR153W, YNL025C, YNL135C, YNL175C, YNL189W, YNR021W, YOL029C, YOL054W, YOL100W, YOR060C, YOR090C, YOR168W, YOR172W, YOR188W, YOR194C, YOR257W, YPL168W, YPR022C*

Agar invasion score 0.98:

*YAR070C, YBL009W, YBL031W, YBL043W, YBL096C, YBL103C, YBR033W, YBR083W, YCL044C, YDL135C, YDL140C, YDR068W, YDR120C, YDR142C, YDR216W, YDR294C, YDR351W, YEL060C, YER037W, YER064C, YER088C, YER118C, YFL010C, YFR013W, YFR045W, YGL014W, YGL073W, YGL104C, YGL154C, YGL179C, YGL228W, YGR162W, YGR235C, YGR255C, YHR075C, YHR084W, YHR098C, YHR108W, YHR131W, YIL055C, YIR004W, YJL101C, YJL110C, YJL201W, YJR078W, YJR080C, YKL132C, YKL204W, YKR016W, YKR027W, YKR078W, YLL058W, YLR009W, YLR045C, YLR064W, YLR077W, YLR177W, YLR277C, YLR374C, YML020W, YML038C, YML051W, YMR101C, YMR139W, YMR140W, YMR241W, YMR302C, YNL022C, YNL064C, YNL077W, YNL097C, YNL115C, YNL169C, YNL255C, YNL299W, YNL313C, YNR067C, YOL006C, YOL061W, YOL105C, YOR065W, YOR197W, YOR324C, YOR335C, YOR356W, YOR370C, YPL109C, YPL160C, YPL246C, YPL248C, YPL270W, YPR173C*

Agar invasion score >0.99:

*YBL023C, YBL035C, YBL050W, YBL054W, YBL076C, YBR029C, YBR086C, YBR090C, YBR092C, YBR112C, YBR135W, YBR156C, YBR160W, YBR250W, YBR262C, YBR264C, YBR273C, YCL025C, YCL063W, YCR030C, YCR031C, YCR088W, YDL122W, YDL195W, YDL210W, YDL221W, YDL224C, YDR080W, YDR113C, YDR188W, YDR192C, YDR200C, YDR228C, YDR231C, YDR284C, YDR378C, YDR442W, YER032W, YER040W, YER085C, YER094C, YER105C, YER110C, YER114C, YER161C, YER184C, YFL027C, YFR023W, YGL003C, YGL023C, YGL035C, YGL066W, YGL164C, YGL166W, YGL180W, YGL181W, YGL209W, YGR026W, YGR044C, YGR067C, YGR096W, YGR100W, YGR105W, YGR109C, YGR123C, YGR159C, YGR218W, YGR246C, YGR249W, YGR274C, YHL024W, YHR014W, YHR032W, YHR079C, YHR135C, YHR161C, YHR177W, YIL045C, YIL056W, YIL077C, YIL094C, YIL136W, YIL137C, YIR013C, YJL047C, YJL054W, YJL090C, YJL092W, YJL105W, YJL106W, YJL141C, YJL187C, YJL191W, YJL200C, YJL204C, YJR030C, YJR093C, YJR116W, YJR147W, YKL027W, YKL038W, YKL047W, YKL119C, YKL129C, YKL146W, YKL161C, YKL210W, YKR002W, YKR029C, YKR088C, YLL003W, YLR013W, YLR072W, YLR136C, YLR227C, YLR241W, YLR251W, YLR253W, YLR273C, YLR337C, YLR357W, YLR403W, YLR405W, YML052W, YML057W, YML061C, YML076C, YML081W, YML086C, YMR010W, YMR032W, YMR070W, YMR094W, YMR136W, YMR179W, YMR182C, YMR212C, YMR219W, YMR309C, YNL020C, YNL053W, YNL076W, YNL109W, YNL161W, YNL182C, YNL183C, YNL188W, YNL233W, YNL236W, YNL251C, YNR034W, YNR059W, YOL013C, YOL089C, YOR008C, YOR028C, YOR032C, YOR098C, YOR101W, YOR106W, YOR113W, YOR118W, YOR138C, YOR141C, YOR162C, YOR181W, YOR195W, YOR227W, YOR239W, YOR251C, YOR271W, YOR299W, YOR307C, YOR317W, YOR360C, YPL055W, YPL071C, YPL105C, YPL125W, YPL128C, YPL158C, YPL222W, YPL250C, YPL269W, YPR009W, YPR026W, YPR097W, YPR141C, YPR157W*

Supplementary Figure 2.2 Listing of genes yielding invasion phenotypes upon gene overexpression. Agar invasion scores were generated as the pixel intensity of the spotted culture post-wash relative to its prewash intensity; genes are grouped according to these scores with the genes exhibiting the strongest invasion phenotypes yielding values of 0.99 or greater.

# Chapter 3. Investigation of Filamentous Growth Kinase Signaling Networks

3.1 Introduction

3.1.1 Budding Yeast Filamentous Growth

Filamentation in the budding yeast *Saccharomyces cerevisiae* is a striking morphogenetic change in which cells adopt an elongated cell morphology and remain connected together following cytokinesis to form pseudohyphae. The transition from vegetatively growing cells dividing by simple budding to the filamentous/invasive growth form is a stress response only observed when specific strain backgrounds are deprived of nitrogen or glucose (Cullen & Sprague, 2000; Gimeno et al., 1992). The other hallmarks of the filamentous growth form include an altered budding pattern from axial/bipoloar to distal unipolar, a cell cycle delay at G2/M, and a unique transcriptional profile (Ahn et al., 1999; Gimeno et al., 1992; Ma et al., 2007). The switch to the filamentous hyphal growth form is an established virulence factor for fungal pathogens (H. J. Lo et al., 1997). Importantly, the regulatory machinery governing filamentation in *S. cerevisiae* is largely conserved not only metazoans, but also in pathogenic fungi such as the human opportunistic pathogen *Candida albicans*, making the non-pathogenic filamentous strains of *S. cerevisiae* an ideal model for these pathogens.

3.1.2 Filamentous Growth Regulatory Kinase Signaling Pathways

A number of conserved protein kinases are established regulators of the filamentous growth transition in *S. cerevisiae*. The three most well described protein kinase signaling pathways regulating the filamentous growth transition are the filamentous growth mitogen-activated protein kinase (MAPK) cascade, the cAMP-protein kinase A (PKA)

pathway, and the AMP-activated kinase (AMPK) Snf1p pathway (Kuchin et al., 2002; Madhani et al., 1997; Pan & Heitman, 1999). Ste20p, Ste11p, Ste7p, and Kss1p comprise the MAPK module regulating filamentous growth. In this cascade, the p21-activated kinase Ste20p phosphorylates and activates the MAPKKK Ste11p, which in turn phosphorylates the MAPKK Ste7p, which phosphorylates the MAPK Kss1p. The activated MAPK Kss1p then releases inhibition and activates the transcription factors Ste12p and Tec1p to initiate transcription of downstream target genes (Madhani et al., 1997). Interestingly, Ste20p, Ste11p, and Ste7p likewise function in the mating pheromone responsive MAPK signaling pathway. The Kss1p MAPK is the dedicated filamentous growth MAPK in both haploids and diploids, while the MAPK Fus3p is dedicated to the mating pathway and is not expressed in diploids (H. Liu et al., 1993). In haploids, Fus3p negatively regulates filamentous growth by triggering destruction of transcription factor Tec1p (Chou et al., 2004). The small G protein Ras2p acts both upstream of the Ste20p kinase of the MAPK pathway and also upstream of the cAMP-PKA pathway regulating filamentous growth. Upon activation through Ras2p signaling, the adenylate cyclase Cyr1p generates cAMP, which in turn activates the three paralogues of PKA in budding yeast. The PKA paralogue Tpk2p is thought to play the primarily positive role in regulation of filamentous growth by acting through the transcription factor Flo8p to initiate transcription of downstream target genes (Pan & Heitman, 1999).

Lastly, Snf1p, the homologue of AMPK in budding yeast essential for growth on non-fermentable carbon sources, also plays an essential role in filamentous growth regulation. Snf1p is thought to relieve transcriptional repression by the factors Nrg1p and Nrg2p to allow transcription of effector genes critical for filamentation (Kuchin et al., 2002). The Elm1p protein kinase is one of the three upstream kinases activating Snf1p AMPK in budding yeast (Hong, Leiper, Woods, Carling, & Carlson, 2003). Somewhat counterintuitively, Elm1p negatively regulates filamentation through an incompletely understood regulation of cell morphogenesis involving the cyclin-dependent kinase Cdc28p (Blacketer et al., 1993; Edgington et al., 1999b). The three of these regulatory kinase signaling pathways are thought to converge on the unusually large promoter of the GPI-

anchored cell-surface protein Muc1p, the critical downstream effector for cell-cell adhesion (Rupp, Summers, Lo, Madhani, & Fink, 1999b).

3.1.3 Kinase Signaling Networks

With the advent of more sophisticated mass spectrometry techniques facilitating analysis of the global proteomic landscape, the canonical view of kinase signaling as simple linear pathways is being revisited, with new insights informing a more interconnected network of kinase signaling. Nearly 30% of the budding yeast proteome is predicted to be phosphorylated (Olsen et al., 2006). A kinase and phosphatase interaction map based on affinity purification and mass spectrometric analysis of protein complexes revealed widespread physical interactions between kinases and phosphatases (Breitkreutz et al., 2010). Proteome chip technology has been used to uncover the scope of kinase substrate interactions *in vitro* (Ptacek et al., 2005). More recently, a phosphoproteomic network built through surveying differential phophopeptide abundance in protein kinase and phosphatase deletion mutants was completed. As reported in this study, many kinases and phosphatases have a profound impact on the phosphorylation status of a large fraction of the phosphoproteome, either directly or indirectly, and kinases and phosphatases act in large complex networks in coordinated regulation of disparate cellular processes (Bodenmiller et al., 2010). The specific connections of these kinase signaling networks are expected to be dependent upon environmental context and cellular state, as many kinases are stress activated.

3.1.4 mRNA Decay and Translational Repression

In *S. cerevisiae*, the major pathway of mRNA decay proceeds through deadenylation of the poly(A) tail of the transcript by the Pop2p-Ccr4p-Not1-7p complex, cleavage of the 5' $^{m7}$GpppN cap by the decapping enzymes Dcp1p and Dcp2p, and 5' – 3' exonucleolytic degradation by the exonuclease Xrn1p (Decker & Parker, 1993; Dunckley & Parker, 1999; H. Y. Liu et al., 1998; Tucker et al., 2001). While Dcp1p and Dcp2p catalyze the removal of the 5' cap, a number of accessory factors are thought to activate decapping *in vivo* or

enhance the activity of the decapping enzyme *in vitro*, including Pat1p, Dhh1p, Edc3p, and the LSM1-7p complex (Nissan, Rajyaguru, She, Song, & Parker, 2010).

In the past decade, the formation of mRNA protein (mRNP) granules has been extensively characterized as a stress response in budding yeast correlated with translational repression and mRNA decay.  Processing bodies and stress granules are thought to be two distinct types of mRNP granules induced by a variety of stresses, such as glucose starvation, post-diauxic shift/stationary phase, and heat shock.  Both granules contain non-translating mRNAs; however, processing bodies are composed of mRNAs complexed with mRNA decay protein machinery, while stress granule protein components are generally involved in translation initiation.  During stress, the pool of translating mRNAs dynamically shifts to a non-translating state within these granules, where their fate may be decided, leading to either decay or a return to the translating pool upon stress relief (Brengues, Teixeira, & Parker, 2005; Buchan, Nissan, & Parker, 2010).  Principal components of processing bodies include the decapping enzymes Dcp1p and Dcp2p, the decapping activators Pat1p, Dhh1p, Lsm1-7p, Edc3p, and the exonuclease Xrn1p (Sheth & Parker, 2003).  Pat1p, Dhh1p, and Lsm1-7p comprise a translational repression complex, binding mRNA transcripts at the onset of stress, inhibiting mRNA translation, and then assembling together into the microscopically visible aggregates.  A *dhh1Δ pat1Δ* double null strain is defective in translational repression in response to glucose starvation and the formation of mRNP granules, where this repression takes place (Coller & Parker, 2005).

The relationship between pseudohyphal growth and these steps of mRNA decay, particularly the roles of translational repression, deadenylation, and decapping machinery, is not well understood.  Nevertheless, the cellular processes of mRNA decay and translational regulation represent key regulatory steps in gene expression, and, not surprisingly, have been previously implicated in the regulation of filamentous growth (Kim & Kim, 2002; T. L. Lo et al., 2012; Park, Hur, Ka, & Kim, 2006).  Global translational repression and the formation of p-bodies during filamentous growth has not been tested and a hypothesis is difficult to generate given the seemingly incongruous data present in the literature: Amino acid starvation, butanol stress, and glucose starvation on the twenty and ten minute time-scales respectively result in global translational repression (Ashe, Slaven, De Long, Ibrahimo, & Sachs, 2001; Coller & Parker, 2005; Smirnova et al., 2005),

suggesting a likelihood of p-body formation during filamentous growth; however, nitrogen starvation does not induce p-bodies (Ramachandran, Shah, & Herman, 2011). Signaling pathways regulating the size and number of mRNP granules are likewise not well-described, with only the RAS-PKA pathway thus far shown to play a negative regulatory role (Ramachandran et al., 2011). In addition, the p21-activated protein kinase Ste20p phosphorylates Dcp2p and thereby regulates its incorporation into p-bodies (Yoon, Choi, & Parker, 2010).

The role and importance of p-bodies, the microscopically visible cytosolic aggregates of non-translating mRNAs and mRNA decay machinery in budding yeast, have been questioned, with the finding that ablation of p-bodies in an *edc3Δ* mutant has no obvious effect on translational repression (Decker, Teixeira, & Parker, 2007). Although analogous cytoplasmic granules are found in mammalian cells, they are not required for non-sense mediated decay, which is a proposed function of p-bodies in budding yeast (Sheth & Parker, 2006; Stalder & Muhlemann, 2009). Moreover, mRNAs may not globally associate with p-bodies during stress conditions as has been presumed; in fact, fewer than 400 transcripts can be reactivated for translation upon stress relief (Arribere, Doudna, & Gilbert, 2011).

3.1.5 Inositol Polyphosphate Signaling

Soluble inositol polyphosphates (IPs) are small molecular second messengers in which mono- or pyrophosphate groups are attached to a *myo*-inositol six-carbon ring. In budding yeast and metazoans, the diverse set of soluble IPs in the cell is generated through sequential phosphorylation of $I(1,4,5)P_3$ (hereafter termed $IP_3$), which is produced by the cleavage of $PI(4,5)P_2$ by the phospholipase C homolog Plc1p at the cell and nuclear membranes (Flick & Thorner, 1993). Two *S. cerevisiae* enzymes are known to phosphorylate the remaining hydroxylated carbons of $IP_3$. Upstream in the pathway, Arg82p phosphorylates $IP_3$ twice, to create $I(1,4,5,6)P_4$ and $I(1,3,4,5,6)P_5$, hereafter referred to as $IP_4$ and $IP_5$. Ipk1p phosphorylates the last hydroxylated carbon to produce $IP_6$ (York, Odom, Murphy, Ives, & Wente, 1999). When all six hydroxylated carbons of *myo*-inositol have been phosphorylated, a phosphoryl group can be transferred to one of the six

mono-phosphorylated carbons, to create a pyrophosphoryl moiety. Two kinase enzymes in budding yeast are known to catalyze the generation of soluble inositol pyrophosphate species: Vip1p and Kcs1p. The two kinase enzymes Vip1p and Kcs1p create isomers of $IP_7$ and even $IP_8$, in which phosphates outnumber carbons (Alcazar-Roman & Wente, 2008; Lee, Mulugu, York, & O'Shea, 2007; Mulugu et al., 2007; Saiardi, Erdjument-Bromage, Snowman, Tempst, & Snyder, 1999).

IPs have been implicated in a number of cellular processes in budding yeast *S. cerevisiae* and are thought to regulate protein function through inducing allosteric conformational change upon binding or performing structural roles as cofactors (Alcazar-Roman & Wente, 2008). One of the earliest examples of regulation by an inositol polyphosphate is the regulation of calcium release from the endoplasmic reticulum (ER) in response to $IP_3$, although this mechanism does not occur in budding yeast. Produced through the cleavage of $PIP_2$ at the membrane, $IP_3$ diffuses through the cytoplasm to bind its receptor on the ER, inducing a conformational change in the receptor and allowing calcium release (Berridge, 1993). In budding yeast, $IP_4$ and $IP_5$ are important for nucleosome remodeling of at least one promoter region, as evidenced by lack of chromatin remodeling and recruitment of the SWI/SNF complex to the promoter in an *arg82Δ* strain (Shen, Xiao, Ranallo, Wu, & Wu, 2003; Steger, Haswell, Miller, Wente, & O'Shea, 2003). In budding yeast, $IP_6$ binds to a component of the nuclear pore complex to facilitate mRNA export from the nucleus (Alcazar-Roman, Tran, Guo, & Wente, 2006). Production of $IP_7$ by Vip1p regulates the phosphate starvation response through inhibition of the cyclin-dependent kinase complex Pho80p-Pho85p (Lee et al., 2007; Mulugu et al., 2007).

Inositol polyphosphates have not been directly implicated in the control of filamentous growth in *S. cerevisiae*; however, a *plc1Δ/Δ* mutant and a *vip1Δ/Δ* mutant have been found to display complete loss of filamentation in two separate studies (Ansari, Martin, Farkasovsky, Ehbrecht, & Kuntzel, 1999; Pohlmann & Fleig, 2010). Moreover, although spatial and temporal regulation of inositol kinase gene expression has been studied in a number of systems, possible regulation through post-translational modification has not been explored in budding yeast.

### 3.1.6 Study Overview and Important Findings

The three aforementioned protein kinase pathways, the filamentous growth MAPK pathay, the RAS-cAMP-PKA pathway, and the AMPK Snf1p pathway, are known to regulate transcription of target genes through activation or deactivation of transcription factors in the nucleus; however, the global changes to the phosphoproteome regulated by these protein kinases during the filamentous growth transition is unknown.  As described above, these three kinase signaling pathways are thought to primarily function in the regulation of *MUC1* expression; however, although deletion of the critical cell surface glycoprotein Muc1p abrogates cell-cell adhesion, Muc1p function is not required for cell cycle delay, altered budding pattern, and other properties of the filamentous growth transition (Ahn et al., 1999).  This suggests additional unknown regulatory functions for the control of filamentous growth by the three major protein kinase regulatory pathways.  We reasoned that a more complete understanding of the global phosphorylation changes across the proteomic landscape could give insight into the kinase signaling network regulating the filamentous growth transition.  In turn, further insight into the kinase signaling network governing filamentous growth could allow hypothesis prediction of new phosphorylation events and cellular processes or pathways regulating filamentous growth.

We report here a SILAC mass spectrometry-based analysis of the filamentous growth regulatory kinase signaling network encompassing eight protein kinases: Ste20p, Ste11p, Ste7p, Kss1p, Fus3p, Elm1p, Snf1p, and Tpk2p, each of which is an established positive or negative regulatory of the filamentous growth transition.  We surveyed phosphopeptides mapping to proteins across the phosphoproteome of budding yeast, including novel phosphopeptides not previously observed in any budding yeast genetic background.  Collectively, 752 phosphopeptides were significantly differentially abundant when a protein kinase was rendered catalytically inactive relative to wild type, and these phosphopeptides map to 406 phosphoproteins.  Importantly, of the significantly differentially phosphorylated phosphoproteins, we identify two respective phosphorylation sites on the small G protein Ras2p and the transcription factor Flo8p that are important for the filamentous growth transition, and we note that these are novel

phosphorylation events.  In addition, Gene Ontology analysis of significantly differentially abundant phosphopeptides implicates a role for mRNA decay machinery during filamentous growth.  We find that protein components of the mRNA translational repression/decay complex are essential for filamentous growth regulation through the MAPK filamentation pathway.  Lastly, we uncover differential phosphorylation of enzymes of the soluble inositol polyphosphate pathway, which we find to be a novel mode of filamentous growth regulation.

3.2 Materials and Methods

3.2.1 *S. cerevisiae* Strains and Media

    All strains used throughout this study are derivatives of the filamentous Σ1278b genetic *S. cerevisiae* background.  Haploid strains used were Y825 and HLY337 (H. Liu et al., 1993; Shively et al., 2013).  The genotype of Y825 is *MAT**a** ura3-52 leu2Δ0* and the genotype is HLY337 is *MATα ura3-52 trp1-1*.  All diploids were generated through mating of Y825 to HLY337, with the exception of *plc1Δ/Δ* and *kcs1Δ/Δ*, which were generated through mating type switch and subsequent mating of HLY337 null strains.  Standard protocols and microbiological techniques were used for propagation of budding yeast strains.  Transformations were performed according to a modified lithium acetate and heat shock procedure.

3.2.2 Generation of Gene Disruptions, and N- and C-terminal Genomic Tagging and Genomic Phosphonull Mutations

    Gene deletions and genomic integration tags were generated through one-step PCR-mediated transformation and subsequent PCR-based verification (Baudin, Ozier-Kalogeropoulos, Denouel, Lacroute, & Cullin, 1993).  For gene deletions, dominant drug resistance markers or prototrophic markers were used.  The dominant drug resistance markers conferring resistance to hygromycin B (Invitrogen) or kanamycin (Geneticin G-418, Teknova) were amplified from pAG32 and pFA6a-kanMX6 (Goldstein & McCusker, 1999; Longtine et al., 1998).  *URA3* and *TRP1* prototrophic markers were PCR amplified

from pUG72 and pFA6a-TRP  (Gueldener et al., 2002; Longtine et al., 1998).  N-terminal and C-terminal GFP tagging was performed using plasmid-based modules from Longtine et al. (Longtine et al., 1998).  C-terminal mCherry tagging was performed by PCR amplification of the mCherry- kanamycin or hygromycin cassette of pBS34 or pBS35 (Shaner et al., 2004).

Genomic phosphonull mutations $RAS2^{Y165F,\ T166A}$ and $FLO8^{S587A,S589A,S590A,S593A}$ were generated by *URA* "flip-out" method.  The *URA* cassette of pRS406 (Sikorski & Hieter, 1989) was PCR-amplified and used to disrupt local sequence; a second transformation was then performed to replace the *URA* marker with DNA sequence encoding the desired mutated allele.

3.2.3 Diploid Surface-Spread Filamentation Assay

Surface-spread filamentation (pseudohyphal growth) was assayed in diploids through nitrogen starvation and examination of colony morphology by light microscopy using 10X magnification.  To induce nitrogen starvation, overnight yeast cultures were washed twice with sterile water, then streaked onto synthetic low ammonium dextrose (SLAD) agar plates (0.17% YNB without amino acids and ammonium sulfate (DifCo), 2% glucose, 50μM ammonium sulfate, and necessary amino acids to correct for any auxotrophies) and incubated 3-5 days at 30°.

3.2.4 Haploid Invasive Growth Assays

Haploid invasive growth assays were conducted by spot plating ~6μL of an overnight haploid cell culture onto a rich media YPD agar plate (2% glucose, 2% peptone, and 2% yeast extract), followed by incubation at 30° for 3-5 days.  Following incubation, surface growth was imaged, and the plates were then gently rinsed with a stream of water and imaged, or the surface of the plate was gently rubbed with a gloved finger and running water prior to imaging.  Invasive growth assay methods with and without the use of manual removal of surface growth are acceptable and commonly used in the literature (Cullen & Sprague, 2002; R. L. Roberts & Fink, 1994).  Pre- and post-wash images of

45

positive controls (wild-type haploid) and negative controls are always shown from the same agar plate as experimental strains.

### 3.2.5 *Candida albicans* Strains and Hyphal Growth Assays

*Candida albicans* strains used in this study were derived from CAI4 (*ura3Δ::imm434/ura3Δ::imm434*). *DHH1/dhh1Δ* heterozygote was created by replacement of one endogenous *DHH1* allele with a *URA3* cassette. To induce hyphae formation, strains were spot plated onto YEPD plates (2% glucose, 2% peptone, 1% yeast extract with uridine) containing 1% fetal calf serum (FCS) and 80mg/L uridine (Bharucha et al., 2011; Sudbery, Gow, & Berman, 2004) or carbon-limitation spider medium (10g nutrient broth, 10g mannitol, 2gK2HPO4 per liter media) (H. Liu, Kohler, & Fink, 1994).

### 3.2.6 Cloning of Eight Budding Yeast Protein Kinases

For this study, we created two sets of cloned kinase constructs, followed by site-directed mutagenesis of the invariant lysine to arginine to generate kinase-dead allele clones for each kinase (Hanks, Quinn, & Hunter, 1988; Zheng, Baumann, & Reymond, 2004). For the first set of kinase constructs, each respective protein kinase was Gateway cloned from the filamentous Σ1278b genetic background into a centromeric *LEU* yeast shuttle vector to include a C-terminal HA epitope tag (Advanced Gateway Destination Vectors, Addgene (Alberti, Gitler, & Lindquist, 2007)). To emulate endogenous transcriptional regulation, ~1kb of native DNA sequence upstream of the ATG start codon was included to encompass the approximate promoter region of each protein kinase. In tandem to this set of HA-tagged *LEU* protein kinase constructs, we additionally Gateway cloned our eight protein kinases into a *URA* yeast centromeric vector derived from the Advanced Gateway Destination Vector set and pRS416 (Alberti et al., 2007; Sikorski & Hieter, 1989), with ~1kb upstream of the start ATG codon and ~300bp endogenous sequence downstream (3') of the stop codon for each kinase. For this set of protein kinases carried on *URA* yeast shuttle vectors, we failed to clone *STE20* or *KSS1* with an endogenous 3' UTR. Alternatively, we Gateway cloned KSS1 with ~1kb upstream promoter sequence and an in-frame C-terminal GFP epitope tag carried on a *URA* yeast shuttle vector derived from the Advanced Gateway

Destination Vector set and pRS416 (Alberti et al., 2007; Sikorski & Hieter, 1989). For *STE20*, we used the MOBY construct, which carries *STE20* with native promoter and 3' UTR (C. H. Ho et al., 2009); thus, the *URA* vector carrying *STE20* was the only construct not cloned from the filamentous Σ1278b genetic background. After identifying the invariant lysine for each protein kinase using a kinase domain alignment tool, site-directed mutagenesis was then employed to change the invariant lysine for each protein kinase to arginine in both kinase construct sets, generating kinase-dead allele construct collections.

3.2.7 Preparation of Yeast Strains for Phosphoproteomic Analysis

The biosynthetic genes *ARG4* and *LYS1* were deleted in the haploid Y825 filamentous strain, creating arginine and lysine auxotrophies. The eight protein kinase genes *STE20*, *STE11*, *STE7*, *KSS1*, *ELM1*, *SNF1*, *TPK2*, and *FUS3* were then individually deleted in the filamentous *arg4Δ lys1Δ* auxotrophic haploid Y825 background. These arginine/lysine auxotrophic kinase null strains were then transformed with *LEU* yeast shuttle vectors carrying the respective kinase-dead alleles described above. Stable Isotope Labeling by Amino Acids in Culture (SILAC) methodology was used to differentially label proteins synthesized by kinase-dead allele strains and wild-type (*arg4Δ lys1Δ* Y825). In the SILAC technique, arginine and lysine amino acid residues with different stable isotopes of carbon, nitrogen, and/or hydrogen (deuterium) (light, medium, or heavy) (Cambridge Isotope Laboratories, Inc.) are added to cells actively growing in culture to incorporate light, medium, or heavy isotopically labeled L-arginine and L-lysine residues into all polypeptides synthesized in these cells. Because stable isotopes of carbon (13C), nitrogen (15N), and hydrogen (2H) are available to label L-arginine and L-lysine, SILAC mass spectrometry experiments can be multiplexed to allow comparison of more than one experimental group to a control in each experiment; thus, each mass spectrometry experiment was conducted in triplex, with the light (natural) versions of L-arginine and L-lysine used to label wild-type strain and medium (K4,R6) or heavy (K8,R10) L-arginine and L-lysine labeling two kinase-dead allele strains. It should be noted that the kinase-dead allele strains and wild-type strain not only differed with respect to the kinase-dead substitution mutation, but also with respect to the physical location of wild-type and

kinase-dead alleles: kinase-dead alleles were carried on *LEU* centromeric vectors, while wild-type alleles were at their native locus in the chromatin. (Thus, kinase-dead allele strains were subjected to two additional transformation procedures: knockout of the endogenous wild-type kinase allele and replacement by a vector-borne kinase-dead allele.) This experimental set-up was deemed necessary to allow comparison of two kinase-dead strains to wild-type simultaneously via a triplex experiment. Kinase-dead allele strains paired together in triplex experiments are listed in Table 3.1.

In each triplex experiment, three strains were cultured in parallel during filamentous growth-inducing conditions. Wild-type and two kinase-dead allele strains were cultured overnight in synthetic complete media containing arginine or lysine residues with light, medium, or heavy isotopes overnight at 30°C, to obtain actively growing log-phase cultures. Each culture was then back-diluted to a low starting optical density (OD600 ~0.1) in SILAC media. To induce filamentous growth in these haploid strains, 1% (vol/vol) butanol was added to each culture. These back-diluted cultures were subsequently incubated at 30°C for approximately 5 doublings. This prolonged labeling and culturing step was found to be experimentally necessary to ensure effective metabolic labeling of proteins, as well as to obtain a minimum abundance of labeled protein from each strain.

3.2.8 Peptide Sample Preparation and Phosphopeptide Enrichment

Upon completion of this SILAC labeling step, cells of each strain were pelleted and frozen. Protein was extracted from frozen cell pellets by bead beating and resuspension in lysis buffer (50mM tris buffer [pH 8.2], 8M urea, and protease inhibitors (Roche) and phosphatase inhibitors). Equivalent amounts of protein as measured by Bradford assay from each of the three strains (two experimental and one wild-type) were pooled together, followed by protein enzymatic digestion with trypsin at a trypsin:protein ratio of 1:10 at 37°C overnight. Peptide mixtures were separated by strong cation exchange into 12 fractions, then subjected to phosphopeptide enrichment using $ZrO_2$. The $ZrO_2$ eluate enriched for phosphopeptides and the flow-through of each strong cation exchange fraction were then analyzed by nanoLC-tandem mass spectrometry.

3.2.9 Mass Spectrometric Analysis and SILAC Quantification

Samples were separated using a custom column then introduced via an electrospray device to an LTQ-Orbitrap XL hybrid type mass spectrometer. LC-MS data was quantified using MaxQuant and the Mascot search engine. Yeast open reading frames from the Saccharomyces Genome Database were used for peptide identification. A normalized heavy:light or medium:light ratio with significance score less that 0.05 was considered statistically significant.

3.2.10 Fluorescence Microscopy

Fluorescence images were taken using a DeltaVision-RT Live Cell Imaging system (Applied Precision). Image capture was conducted using Applied Precision's SoftWorx imaging software.

3.2.11 *β*-Galactosidase Assays

The Yeast *β*-Galactosidase Assay kit (Thermo Scientific) was used to measure *β*-galactosidase activity according to the manufacturer's protocol.

3.2.12 Cloning of *IPK1* and *VIP1-GFP*

*IPK1* with ~1kb upstream of the start codon and ~300bp downstream of the stop codon was amplified from the Σ1278b genetic background and Gateway cloned into a centromeric *URA* yeast shuttle vector derived from the Advanced Gateway Destination Vector set and pRS416 (Alberti et al., 2007; Sikorski & Hieter, 1989). *VIP1* with ~1kb upstream of the start codon was amplified from the Σ1278b genetic background and Gateway cloned into a centromeric *URA* vector with an in-frame C-terminal GFP tag derived from the Advanced Gateway Destination Vector set and pRS416 (Alberti et al., 2007; Sikorski & Hieter, 1989).

3.3 Results

3.3.1 Catalytic Activity of Eight Protein Kinases is Required for Wild-type Filamentous Growth

We investigated the contribution of eight protein kinases to the global phosphoproteome during filamentous growth: The MAPKs Ste20p, Ste11p, Ste7p, Fus3p, and Kss1p; AMPK Snf1p; the PKA paralogue Tpk2p, and Elm1p. Importantly, deletion of six of these protein kinases is known to abrogate filamentation, while deletion of the remaining two increases filamentation. We intentionally chose both positive and negative regulatory kinases of the filamentous growth transition in order to investigate the filamentous growth kinase regulatory network in its entirety. In comparison to wild-type, decreased invasive growth is observed in *ste20Δ*, *ste11Δ*, *ste7Δ*, *kss1Δ*, and *tpk2Δ*, and increased invasive growth in *fus3Δ* (Cook et al., 1997; Robertson & Fink, 1998; Rupp et al., 1999a). Deletion of *SNF1* or *ELM1* does not affect invasive growth on rich YPD agar; however, deletion of *SNF1* in haploids is known to cause defective invasive growth on carbon limitation media (Cullen & Sprague, 2000) and *elm1Δ* strains display a hyperfilametous elongated cell shape (Edgington et al., 1999b). Diploids deleted for *STE20*, *STE11*, *STE7*, *TPK2*, and *SNF1* display complete loss of surface-spread pseudohyphal growth, while a striking increase is apparent when *ELM1* is deleted (Kuchin et al., 2002; H. Liu et al., 1993; Pan & Heitman, 2002). Deletion of the terminal MAPKs *KSS1* and *FUS3* shows no differential surface-spread filamentous phenotype in diploids (H. Liu et al., 1993). As the dedicated mating pathway MAPK, Fus3p is not expressed in diploids (H. Liu et al., 1993). *KSS1* is expressed in diploids; however, this kinase possesses both positive and negative regulatory roles in filamentation, which together mask the importance of *KSS1* in diploids (Cook et al., 1997; Madhani et al., 1997).

In addition to the conserved kinase catalytic domain, protein kinases often consist of other functional domains. We sought to determine the specific role of the kinase catalytic activity (transfer of a phosphoryl group to a substrate polypeptide) during filamentous growth for each protein kinase. Protein kinases can be rendered catalytically inactive by mutation of an invariant lysine residue in the ATP-binding pocket of the kinase catalytic

domain to arginine (Hanks et al., 1988).  We individually deleted each of the eight protein kinases in haploid (a) and diploid (a/α) strains of the filamentous Σ1278b background.  Wild-type alleles and kinase-dead alleles of each protein kinase carried on *URA* centromeric shuttle vectors (Materials and Methods) were introduced into the respective kinase diploid knockout strain.  Rescue of nitrogen starvation-induced surface-spread filamentation was observed for *ste20Δ/Δ*, *ste11Δ/Δ, ste7Δ/Δ, tpk2Δ/Δ, snf1Δ/Δ*, and *elm1Δ/Δ* diploid knockouts when wild-type kinase alleles were introduced, yet these six diploid knockouts transformed with kinase-dead allele constructs showed little phenotypic difference from knockouts transformed with empty vector (Figure 3.1A).  The *fus3Δ* haploid strain has a prominent complex colony morphology phenotype with pronounced wrinkling of the colony.  We find that a wild-type appearance can be rescued with *FUS3* allele, yet not with *FUS-KD* (Figure 3.1B).  Similarly, rescue of invasive growth was observed for *kss1Δ* haploid knockouts introduced with the wild-type kinase allele carried on a *URA* centromeric vector, with no appreciable rescue seen in *kss1Δ* carrying kinase-dead alleles on a *URA* centromeric vector (Figure 3.1C).  Importantly, kinase-dead versions of each of these eight protein kinases has been constructed and found to be appropriately expressed (Cairns, Ramer, & Kornberg, 1992; Celenza & Carlson, 1989; Flom, Lemieszek, Fortunato, & Johnson, 2008; Koehler & Myers, 1997; Madhani et al., 1997; Pan & Heitman, 2002; Wu, Whiteway, Thomas, & Leberer, 1995).  Based on the failure of kinase-dead constructs to rescue surface-spread filamentation in *STE20*, *STE11*, *STE7*, *SNF1*, *TPK2*, and *ELM1* diploid kinase knockouts and complex colony morphology/invasive growth in *FUS3* and *KSS1* haploid kinase knockouts, we conclude that the specific catalytic activity of these kinases is critical for filamentous growth, as opposed to any other function or domain of these protein kinases.
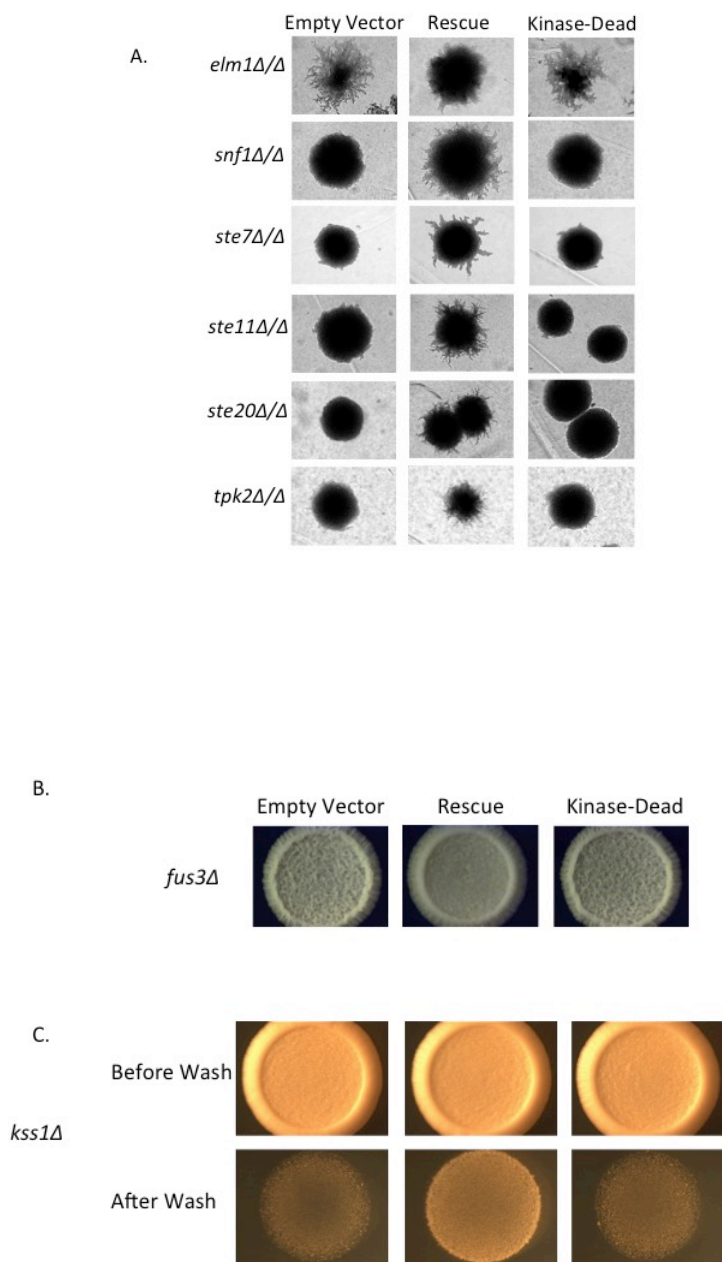
Figure 3.1 Kinase catalytic activity is required for filamentous growth of eight master filamentous growth regulatory protein kinases.  A.) Six indicated diploid kinase null strains were transformed with either empty vector, the wild-type allele, or kinase-dead allele and assayed for surface-spread filamentation on SLAD agar media. B.) Complex colony morphology on solid YPD agar media was imaged pre- and post-wash for *fus3Δ* transformed with empty vector, *FUS3*, or *FUS-KD* alleles.  C.) Invasive growth assay on solid YPD agar media was imaged pre- and post-wash for *kss1Δ* transformed with empty vector, *KSS1*, or *KSS1-KD* alleles.

3.3.2 SILAC Mass Spectrometry-Based Phosphoproteomic Analysis of Eight Kinase-Dead Allele Strains

Because kinase catalytic activity of these eight protein kinases is essential for their contribution to the filamentous growth transition, we reasoned that these protein kinases likely act in complex signaling networks of proteome phosphorylation to regulate filamentous growth.  We analyzed changes in phosphopeptide abundance across the phosphoproteome in eight protein kinase-dead allele haploid strains relative to a wild-type haploid strain using liquid chromatography coupled with tandem mass spectrometry, as described in detail in Materials and Methods.  Briefly, SILAC methodology was used to metabolically label proteins of two respective kinase-dead allele haploid strains and wild-type haploid with light, medium, and heavy arginine and lysine residues during 1% butanol-induced filamentation in a triplex labeling strategy (Table 3.1).  Following protein extraction and trypsin-digestion, phophopeptides were enriched, fractionated by liquid chromatography, and relative abundance of phosphopeptides in kinase-dead strains compared to wild-type haploid was determined by tandem mass spectrometry.

Of the eight kinase-dead allele strains interrogated, we collectively surveyed 670 phosphoproteins.  We identify significant differential abundance of 752 phosphopeptides, mapping to 406 phosphoproteins.  In addition, we identify 692 novel phosphopeptides that have not been previously surveyed in any budding yeast strain.  In an effort to better comprehend this large data set, we have begun to assemble a filamentous growth regulatory kinase signaling network based on statistically significant differential phosphorylation of phosphoproteins in kinase-dead strains (Figure 3.2).  Using Cytoscape (Killcoyne et al., 2009) to construct a node-edge style network, we illustrate interconnectivity among differentially regulated phosphoproteins, with edges connecting selected phosphoproteins to protein kinase-dead allele strains in which they were differentially regulated.  For simplicity, only a small fraction of our phosphoproteomic data is represented: we chose to illustrate only those phosphoproteins likely to play a regulatory or signaling role.  We assembled this list of regulatory phosphoproteins using the Gene Ontology term "signal transduction," augmented with additional phosphoproteins

53

whose molecular functions are likely to be regulatory in nature. As expected, we identify significant differential phosphorylation of known filamentous growth regulators within the network: Ras2p, Flo8p, Hog1p, Sfl1p, Bcy1p, Cyr1p, and Rsr1p. Interestingly, we observe both more abundant and less abundant phosphopeptides in roughly the same ratio for each protein kinase-dead allele strain. We suspect that phosphopeptide abundance changes observed are largely indirect consequences of rendering a protein kinase-dead, which we address in Discussion.

We are also currently comparing the collective set of statistically significant differentially phosphorylated phosphoproteins to previously generated high-throughput data sets to make testable hypotheses. For example, we envision that a small fraction of less abundant phosphopeptides map to phosphoproteins that are direct substrates of filamentous growth regulatory protein kinases. We illustrate a hypothesis prediction of kinase-substrate pairs on the partial regulatory kinase signaling network shown in Figure 3.2. We label connections between potential kinase-substrate pairs by cross-checking high throughput physical interaction data compiled on BioGrid with phosphoproteins found to be significantly decreased in phosphorylation in a given kinase-dead allele strain. Physical interaction data available through BioGrid encompasses several high-throughput methodologies: yeast two-hybrid interactions, proteome-chip interactions, and large-scale affinity purification and mass spectrometric analysis of protein complexes.

Table 3.1. Triplex SILAC Mass Spectrometry Experiments

| Triplex SILAC Labeling | K and R with Light (Natural) Isotopes $^{12}$C and $^{14}$N | "Medium" Label K4 (L-Lysine 4,4,5,5-D4) and R6 (L-Arginine $^{13}$C6) | "Heavy" Label K8 (L-Lysine $^{13}$C6 and $^{15}$N2) and R10 (L-Arginine $^{13}$C6 and $^{15}$N4) |
|---|---|---|---|
| 1 | Y825 *MAT**a** arg4Δ lys1Δ* | Y825 *MAT**a** arg4Δ lys1Δ snf1Δ SNF1-KD* (K84R) | Y825 *MAT**a** arg4Δ lys1Δ tpk2Δ TPK2-KD* (K99R) |
| 2 | Y825 *MAT**a** arg4Δ lys1Δ* | Y825 *MAT**a** arg4Δ lys1Δ tpk2Δ TPK2-KD* (K99R) | Y825 *MAT**a** arg4Δ lys1Δ snf1Δ SNF1-KD* (K84R) |
| 3 | Y825 *MAT**a** arg4Δ lys1Δ* | - | Y825 *MAT**a** arg4Δ lys1Δ ste20Δ STE20-KD* (K649R) |
| 4 | Y825 *MAT**a** arg4Δ lys1Δ* | Y825 *MAT**a** arg4Δ lys1Δ kss1Δ KSS1-KD* (K42R) | - |
| 5 | Y825 *MAT**a** arg4Δ lys1Δ* | Y825 *MAT**a** arg4Δ lys1Δ elm1Δ ELM-KD* (K117R) | Y825 *MAT**a** arg4Δ lys1Δ fus3Δ FUS3-KD* (K42R) |
| 6 | Y825 *MAT**a** arg4Δ lys1Δ* | Y825 *MAT**a** arg4Δ lys1Δ ste7Δ STE7-KD* (K220R) | Y825 *MAT**a** arg4Δ lys1Δ ste11Δ STE11-KD* (K444R) |

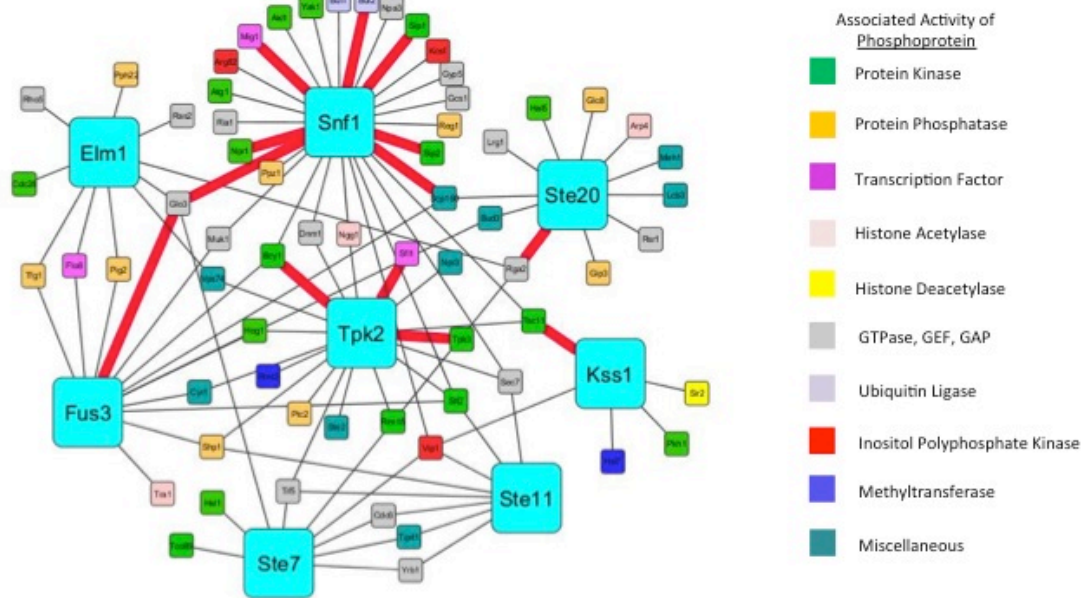Figure 3.2 Partial filamentous growth regulatory kinase signaling network. A node-edge network was created to illustrate regulatory phosphoproteins differentially regulated by a given protein kinase, e.g. a phosphopeptide mapping to the protein kinase was differentially abundant when the kinase was rendered kinase-dead. Bold red edges represent possible kinase-substrate pairs; further details in text.

### 3.3.3 Phosphorylation Events Regulating Filamentous Growth

Among the entire set of significantly differentially phosphorylated phosphoproteins from all eight kinase-dead allele strains, we sought to identify phosphorylation events important for filamentous growth. Here we report three such phosphorylation events. In each case, we replace the wild-type endogenous allele with a phosphonull allele, in which the serine, threonine, or tyrosine predicted to be differentially phosphorylated has been mutated to alanine or phenylalanine, effectively preventing phosphorylation. We then assay filamentous growth of the phosphonull allele strain and compare to wild-type and the deletion mutant. In order to compile a list of candidate phosphorylation events for functional testing, we focused of phosphorylation of proteins known to play roles in the filamentous growth transition. Collectively, our phosphoproteomic analysis identifies differential phosphorylation of a number of such known filamentous growth protein factors. We report regulatory phosphorylation of the HOG1p MAPK, Flo8p transcription factor, and Ras2p small G protein. Conservatively speaking, we find the residues of these phosphoproteins to be important in filamentation.

### 3.3.3.1 Phosphorylation of the MAPK HOG1p

The MAPK Hog1p is critical for adaptive response to osmostress in budding yeast. During osmotic shock, the Hog1p activated through dual phosphorylation at T174 and Y176 by the MAPKK Pbs2p and translocates to the nucleus to initiate target gene expression (Brewster et al., 1993; Ferrigno et al., 1998a). Interestingly, Hog1p actively represses filamentation through the MAPK pathway via an incompletely understood mechanism (Shively et al., 2013; Shock et al., 2009). We identify significant differential abundance of a phosphopeptide mapping to the MAPK Hog1p in which Y176 was phosphorylated. Specifically, the phosphopeptide *IQDPQMTGY(ph)VSTR* was found to be ~9.6 fold more abundant when the PKA paralog Tpk2p was rendered kinase-dead (p~0.00115). Interestingly, this phosphopeptide was also 2.5 fold more abundant when the MAPK Fus3p was inactive (p~0.003081). The predicted phosphorylation occurs at tyrosine 176. We cloned *HOG1* into a centromeric *URA* vector, with ~1kb promoter sequence upstream of the start codon and ~300bp sequence downstream of the stop

57

codon.  Using site-directed mutagenesis, we introduced a substitution mutation encoding phenylalanine for the tyrosine at position 176 found to be phosphorylated by mass spectrometry, thus generating the phosphonull allele *HOG1^Y176F^*.  This phophonull allele fails to rescue a wild-type surface-spread filamentation level in a *hog1Δ/Δ* strain, effectively phenocopying *hog1Δ/Δ* carrying only empty vector (Figure 3.3A).  Since Hog1p is known to repress filamentous growth through inhibition of the filamentous growth MAPK pathway, we employed the MAPK-signaling responsive *FRE(Ty1):: lacZ* reporter construct to assay Y176 phosphorylation function (Madhani & Fink, 1997).  We cloned wild-type *HOG1* and phosphonull *HOG1^Y176F^* alleles into a centromeric *LEU* vector and assayed *β*-galactosidase production in a haploid *hog1Δ* strain complemented with empty vector, vector carrying wild-type *HOG1*, or vector carrying phosphonull *HOG1^Y176F^*.  In parallel to the surface-spread filamentation assay, phosphonull *HOG1^Y176F^* again fails to rescue a wild-type MAPK signaling level (Figure 3.3B).
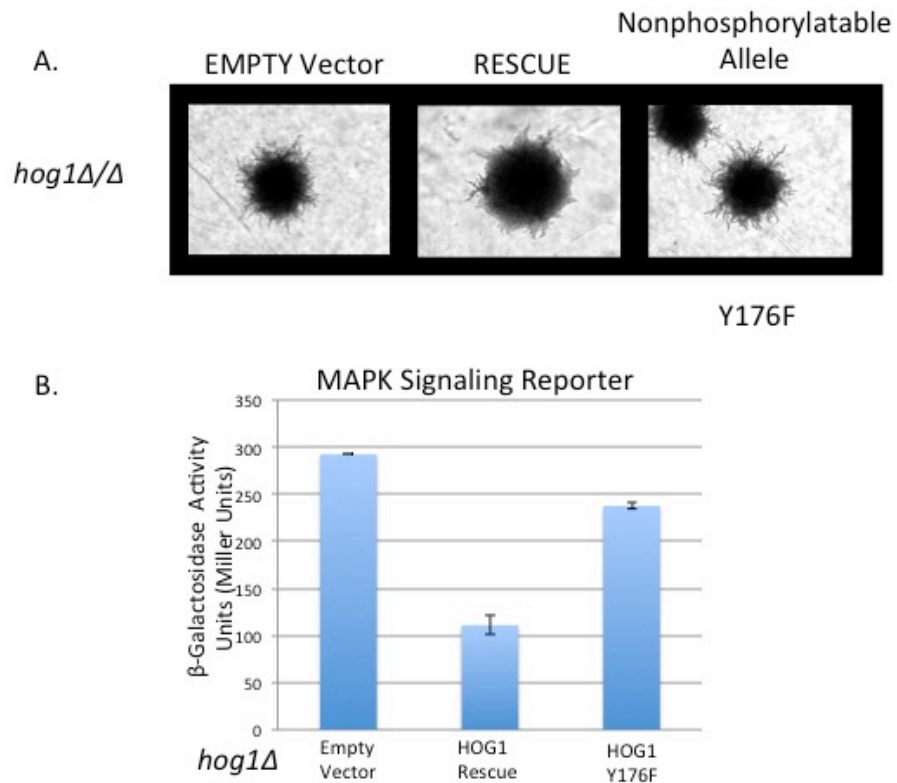
Figure 3.3 Phosphorylation of Hog1p Y176.  A.) Diploid *hog1Δ/Δ* strains carrying either empty vector, *HOG1*, or *HOG1^{Y176F}* were assayed for pseudohyphal growth on SLAD media.  B.) Haploid *hog1Δ* strains carrying empty vector, *HOG1*, or *HOG1^{Y176F}* were assayed for MAPK signaling using a *FRE(Ty1)::lacZ* reporter. Bar height represents mean and error bars represent ±1 standard deviation of three independent trials.

### 3.3.3.2 Phosphorylation of the Small G Protein Ras2p

The G protein Ras2p acts upstream of both the filamentous MAPK pathway and the cAMP-PKA pathway in the regulation of filamentation (Mosch et al., 1996).  We detect differential abundance of a phosphopeptide mapping to the small G protein Ras2p, in which tyrosine 165 and threonine 166 were predicted to both be phosphorylated.  We created a phosphonull *RAS2* strain by mutating Y165 and T166 to phenylalanine and alanine respectively within the genome at the native *RAS2* locus.  We assayed invasive growth of this phosphonull *RAS2^{Y165F, T166A}* haploid strain and observe a defect intermediate between

wild-type haploid and *ras2Δ* strain (Figure 3.4A). We N-terminally tagged wild-type and phosphonull *RAS2^{Y165F,T166A}* with GFP and examined subcellular localization: we observe indistinguishable cell membrane fluorescence in both strains, indicating no localization defect for phophonull *Ras2p^{Y165F,T166A}* (Figure 3.4B). We conclude that phosphorylation of RAS2p at tyrosine 165 and threonine 166 is necessary for optimal molecular function and proper invasive growth.
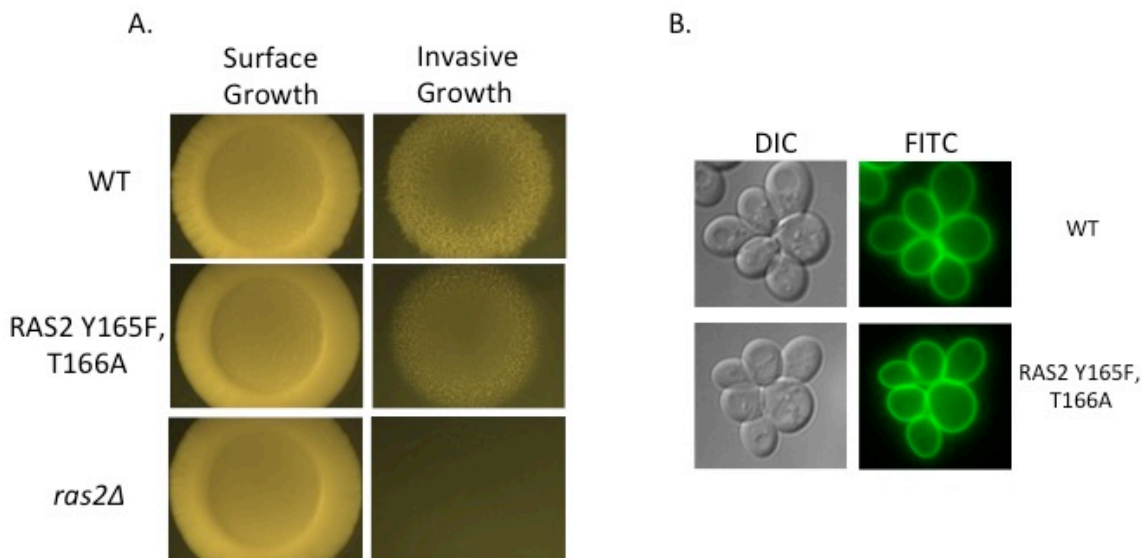


Figure 3.4 Phosphorylation of Ras2p Y165 and T166. A.) Wild-type, phosphonull (*RAS2^{Y165F,T166A}*), and *ras2Δ* haploid strains were assayed for invasive growth on YPD agar media, as described in Materials and Methods. Pre- and post-wash images representing surface and invasive growth are shown. B.) Wild-type *RAS2* and phosphonull *RAS2^{Y165F,T166A}* alleles were N-terminally tagged with GFP. Images were taken during exponential growth phase.

3.3.3.3 Phosphorylation of the Transcription Factor Flo8p

The transcription factor Flo8p is phosphorylated by the PKA paralog Tpk2p to positively regulate the transcription of *MUC1* in the control of filamentous growth; however, the exact site at which Flo8p is phosphorylated by Tpk2p has not been explored (Pan & Heitman, 2002). We uncovered significant differential abundance of a Flo8p phosphopeptide with an amino acid sequence closely resembling the consensus PKA phosphomotif. The phosphopeptide *(ca)VS(ph)AS(ph)S(ph)PLSIATPRSGDAQK* which maps to the transcription factor Flo8p is significantly less phosphorylated in Elm1p-KD and Fus3p-KD kinase-dead allele strains. SKVS(ph) would be a non-conforming phosphosite, given the consensus PKA motif BBXS, where B represents a basic residue arginine or lysine and X represents any amino acid (Shabb, 2001). We mutated each of four serine residues to alanines to create a phosphonull *FLO8$^{S587A,S589A,S590A,S593A}$* allele at the native chromatin locus in a haploid filamentous strain. We chose to additionally mutate S593 although this residue was not predicted to be phosphorylated since Tpk2p may be able to activate Flo8p through phosphorylation of this nearby serine residue. We assayed this phosphonull strain for invasive growth and observe an appreciable defect intermediate between a wild-type haploid strain and *flo8Δ* strain (Figure 3.5A). We further investigated the filamentous growth defect of the phoshonull *FLO8$^{S587A,S589A,S590A,S593A}$* strain using a reporter construct in which FLO8p DNA-binding sites were placed upstream of the reporter gene *lacZ* (Rupp et al., 1999a). We observe defective transcriptional competency for the phosphonull *FLO8$^{S587A,S589A,S590A,S593A}$* allele (Figure 3.5B). Importantly, we observe correct nuclear subcellular localization for phosphonull *FLO8$^{S587A,S589A,S590A,S593A}$* protein when tagged c-terminally with GFP. Wild-type Flo8p and the phosphonull Flo8p both localized to the nucleus in exponentially growing cells, as evidenced by co-localization with the nuclear marker MAD1p-NLS-tdimer (Figure 3.5C). We conclude that phosphorylation of Flo8p is necessary for proper invasive growth and transcriptional activation but is dispensable for nuclear localization.
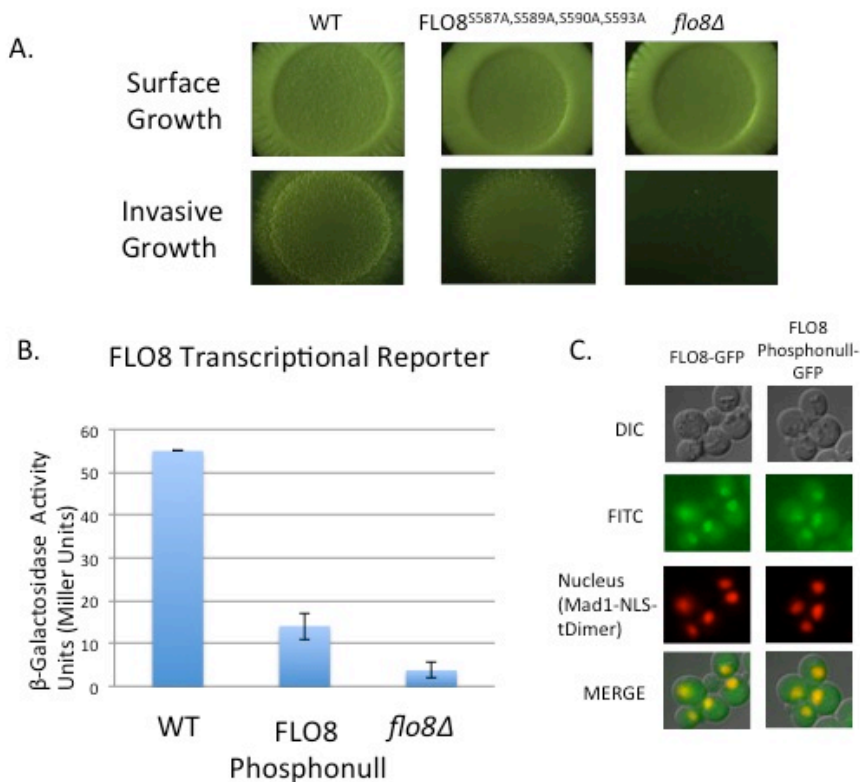
Figure 3.5 Phosphorylation of Flo8p S587, S589, and S590. A.) Haploid strains with wild-type *FLO8*, phosphonull *FLO8[S587A,S589A,S590A,S593A]*, or *flo8Δ* were assayed for invasive growth on solid YPD agar. Pre- and post-wash images representing surface and invasive growth are shown. B.) The transcriptional activation competency of wild-type *FLO8*, phosphonull *FLO8[S587A,S589A,S590A,S593A]*, and *flo8Δ* was assayed using a reporter construct consisting of *FLO8* DNA-binding sites as described in text. Bar height represents mean and error bars represent ±1 standard deviation of three independent trials. C.) *FLO8* and phosphonull *FLO8[S587A,S589A,S590A,S593A]* were C-terminally tagged with GFP, and co-localization with the nuclear marker *MAD1-NLS* was examined during exponential growth.

3.3.4 mRNA Decay Factors Regulating Filamentation

Gene Ontology term enrichment was used to identify over-represented cellular processes among the entire data set of the significantly differentially phosphorylated phosphopeptides (p<.05). Interestingly, mRNP granule assembly and mRNA decay were found to be significantly enriched terms. Table 3.2 presents a partial listing of differentially phosphorylated mRNA decay machinery. Because a significant number of differentially abundant phosphopeptides were annotated to these Gene Ontology terms, we hypothesized that the process of mRNA decay is one unappreciated process regulated within the global kinase signaling network governing filamentous growth.

3.3.4.1 Formation of Stress Granules and P-bodies Is Not Induced During Filamentous Growth

We began an investigation into this possibility by testing whether global mRNA decay is increased during filamentous growth by assaying the presence of enlarged mRNP granules during filamentous growth conditions in the wild-type filamentous yeast strain. Previously, the proper formation of p-bodies has been found to be regulated by the cAMP PKA pathway and the Ste20p kinase in budding yeast (Ramachandran et al., 2011; Yoon et al., 2010) suggesting that p-body formation may be regulated by filamentation or other filamentous growth inducing pathways. However, nitrogen deprivation has been shown not to increase p-body size or number in a non-filamentous *S. cerevisiae* strain (Ramachandran et al., 2011). We analyzed formation of microscopically visible aggregates through genomic tagging of the most commonly used protein markers of stress granules (Pab1p and Pub1p) and p-bodies (Dcp2p, Edc3p, Dhh1p, Pat1p, and Xrn1p) with the fluorescent proteins GFP or mCherry in a haploid filamentous background strain Σ1278b. We observe large foci indicative of p-bodies during high OD stress (~3days incubation) or acute glucose deprivation (~10min), two conditions known to induce p-bodies in the non-filamentous background; however, we do not observe enlarged p-bodies when 1% butanol is added to the liquid culture media proceeded by 5-6hrs incubation to induce filamentous growth (Supplementary Figure 3.1 and data not shown). Filamentous growth is a complex morphogenetic change requiring a prolonged 5-6hr incubation period to be observed using

Table 3.2 mRNA decay factors were significantly differentially phosphorylated across the kinase-dead phosphoproteomic data.

| GENE | Modified Sequence | Ratio | Significance | Kinase-Dead Set |
|---|---|---|---|---|
| DCP2 | _NPISSTVSS(ph)NQQSPK_ | 4.2639 | 0.0077787 | KSS1 |
| DCP2 | _NPISSTVSSNQQS(ph)PK_ | 1.8205 | 0.041805 | FUS3 |
| DCP2 | _RNS(ph)VSKPQNSEENASTSSINDANASELLGMLK_ | 0.43997 | 0.044218 | STE20 |
| DCP2 | _DSGYSSSS(ph)PGQLLDILNSK_ | 2.6493 | 0.041249 | SNF1 |
| DHH1 | _GSINNNFNTNNNS(ph)NTDLDRDWK_ | 0.34361 | 0.047447 | ELM1 |
| PAT1 | _DLS(ph)PEEQR_ | 4.5317 | 0.020682 | STE20 |
| XRN1 | _KGEIKPSSGTNSTECQS(ph)PK_ | 2.8828 | 0.038806 | KSS1 |
| NGR1 | _NGS(ph)HSDLVNLQR_ | 0.17378 | 0.0071177 | SNF1 |
| SBP1 | _FPT(ph)KIDFDNIKENYDTK_ | 5.0655 | 0.013881 | STE20 |
| SBP1 | _FPT(ph)KIDFDNIK_ | 2.7904 | 0.023537 | TPK2 |
| DED1 | _VGS(ph)TSENITQK_ | 4.8823 | 0.015879 | STE20 |
| IGO1 | _EGSISSGPPSSNNGTIGGGSTSSTPVGNHSSS(ph)SSSLYTESPIR_ | 0.031711 | 7.52E-07 | SNF1 |
| IGO1 | _EGSISSGPPSSNNGTIGGGSTSSTPVGNHSSS(ph)SSSLYTESPIR_ | 0.081743 | 7.94E-05 | TPK2 |

1% butanol stress; this time scale difference may account for the previously reported observation that fusel alcohol addition effects a translational inhibition after only 10-20min.  Wild-type yeast cultures grown in parallel under nutrient sufficient, unstressed conditions show mostly diffuse cytosolic fluorescence, with only very small granules occasionally observed.  We conclude that p-bodies do not form during filamentous growth induced by butanol stress.

We also used a genetic strategy to induce filamentous growth and assay formation of p-bodies. We deleted the negative regulator MAPK Hog1p as well as the cyclin Clb2p in the haploid filamentous strain and again observe no difference from wild-type in formation of p-bodies (data not shown). Similarly, we introduced dominant active alleles of the filamentous growth MAPKs Ste11p and Ste7p to the haploid p-body marker strains and again observe little difference from wild-type in p-body formation (data not shown). We conclude that p-bodies are not induced during filamentous growth when filamentation is specifically induced by activation of the filamentous growth MAPK pathway, or by delay of the cell cycle.

We likewise assayed formation of stress granules by genomic fluorescent tagging of the commonly used marker proteins Pab1p and Pub1p. Interestingly, when the commonly used stress granule markers Pab1p and Pub1p are tagged with mCherry, we fail to observe punctate foci under any experimental treatment (data not shown). Stress granules have been observed to form during heat stress, glucose deprivation, and high OD stress in non-filamentous *S. cerevisiae* backgrounds. We suspect that stress granules may be less easily visualized in the filamentous Σ1278b background. Since the formation of p-bodies and stress granules can be used as an indication of global mRNA translational repression and decay, we conclude that the pool of mRNA transcripts in the cell during filamentous growth is not globally shifting to a state of translational repression and decay.

3.3.4.2 The Filamentous Growth Protein Kinases Fus3p, Kss1p, Ste20p, and Tpk2p Co-localize with the P-body/Stress Granule Marker Igo1p During High OD Stress

We reasoned that although mRNA decay may not be globally initiated during filamentous growth, as indicated by the lack of appreciable mRNP granule formation during filamentous growth, the formation of these cytosolic foci during glucose starvation or post-diauxic shift/stationary phase could be utilized as a convenient microscopy assay for the association of our protein kinases with mRNA decay and translational repression machinery by co-localization. We first tested whether protein kinases adopt a punctate localization reminiscent of p-bodies or stress granules during glucose deprivation or high OD stress, two stresses known to induce these mRNP granules. We tagged all eight protein

kinases (Ste20p, Ste11p, Ste7p, Kss1p, Fus3p, Elm1p, Snf1p, and Tpk2p) with GFP in the filamentous Σ1278b strain and examined subcellular localization during nutrient sufficient, glucose deprivation (10min), or "high OD stress" (post-diauxic shift ~3days) conditions. No change in localization was observed for protein kinases during glucose stress conditions when compared to unstressed cells (data not shown).  Strikingly, however, a punctate fluorescence localization pattern was observed for four protein kinases during high OD post-diauxic shift stress at 3 days.  The four protein kinases Tpk2p, Ste20p, Fus3p, and Kss1p all adopt a punctate localization, with typically one focus of fluorescence per cell (Figure 3.6).

The punctate fluorescence pattern of protein kinases during post diauxic shift was reminiscent of p-body aggregates during this stress condition.  We tested co-localization of p-bodies and the Tpk2p, Ste20p, Fus3p, and Kss1p protein kinases by tagging granule components with mCherry and protein kinases with GFP within the genome.  None of the four protein kinases showed strong co-localization with the p-body marker proteins Dcp2p, Edc3p, or Pat1p (Supplemental Figure 3.2 and data not shown).  However, we observe strong co-localization of these four protein kinases with the p-body/stress granule marker Igo1p during post-diauxic shift (Figure 3.6).

We note that Igo1p is not a commonly used marker for p-bodies or stress granules, and that Igo1p is found to have very minimal colocalization with the commonly used markers Dcp2p and Pabp1, with only 4% and 56% colocalization observed 8hrs following glucose exhaustion, respectively (Talarek et al., 2010).  In addition, like the protein kinases Tpk2p, Ste20p, Fus3p, and Kss1p, Igo1p fails to adopt a punctate localization pattern during acute glucose deprivation stress, in which p-bodies are readily seen.  We conclude that Igo1p and the protein kinases Tpk2p, Ste20p, Fus3p, and Kss1p co-localize specifically in a high OD stress-dependent context but may not themselves be constitutive components of p-bodies or stress granules.
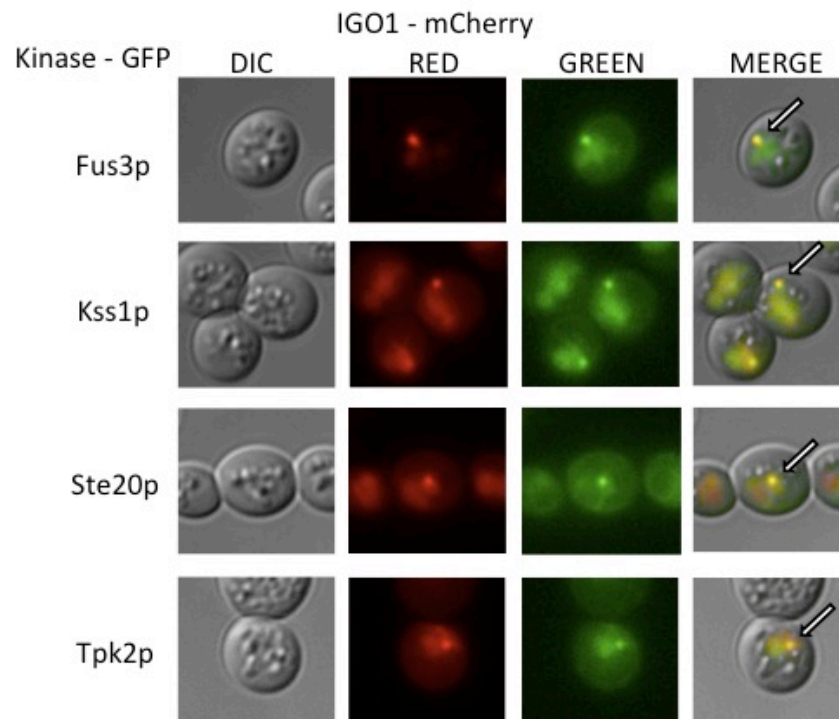
Figure 3.6 Co-localization of protein kinases with the mRNP granule marker Igo1p. *FUS3*, *KSS1*, *STE20*, and *TPK2* were genomically tagged at the C-terminus with GFP in a haploid strain harboring C-terminally mCherry-tagged *IGO1* in the genome. Cells were examined after 3days shaking incubation in liquid culture, corresponding to late post-diauxic shift phase growth. Co-localization of fluorescence foci is indicated with white arrows in the merged image.

3.3.4.3 The mRNA Decay/Translational Repression Factors Lsm1p, Dhh1p, and Pat1p Are Required For Diploid Surface-Spread Filamentation

We next tested a possible role of mRNA decay during filamentous growth by deleting a panel of mRNA decay genes from the haploid and diploid filamentous Σ1278b background and assaying for haploid invasive growth and diploid surface-spread filamentation on SLAD agar media. Dhh1p, Pat1p, and Lsm1p components of the translational repression complex are essential for diploid surface-spread filamentous growth, as indicated by lack of surface-spread filaments in *dhh1Δ/Δ*, *lsm1Δ/Δ*, and *pat1Δ/Δ*

null strains compared to wild-type control strain. In addition, we find that the mRNA-binding proteins Sbp1p and Pbp1p, and the mRNA deadenylation factor Ccr4p are also required for wild-type surface-spread filamentation (Figure 3.7A).

The observed loss of filamentation in *dhh1Δ/Δ*, *lsm1Δ/Δ*, and *pat1Δ/Δ* null mutants is interesting for a number of reasons. First, in agreement with the lack of p-body/stress granule formation during butanol-induced filamentous growth, individual deletion of these factors does not ablate p-body formation, further suggesting that the p-body aggregates themselves are not playing an important role in filamentation and are not responsible for the observed surface-spread filamentation loss. Individual deletion of *DHH1* and *PAT1* results in smaller p-body size, although they remain microscopically detectable; conversely, in an *lsm1Δ* strain, the number of p-body foci increases (Coller & Parker, 2005; Sheth & Parker, 2003). If Dhh1p, Pat1p, and Lsm1p were affecting filamentous growth through p-body function, we would expect similar p-body phenotypes in the respective deletion strains. Second, the only roles of the proteins Pat1p, Dhh1p, and Lsm1p are translational repression and activation of mRNA decapping. Since global translational repression and mRNA decay are not observed during filamentous growth (mRNP granules are not forming), this complex may be specifically degrading the mRNA transcript of a negative regulatory factor of filamentation, of which there are a number described. Third, the regulation of surface-spread filamentation by Dhh1p, Pat1p, and Lsm1p may be through a specific regulatory pathway, since deletion of mRNA decay and translational machinery with similar mechanistic functions do not result in identical abrogated surface-spread filamentation: *sbp1Δ/Δ* displays a strong defect but not total loss, and *scd6Δ/Δ* shows no differential surface-spread filamentation phenotype (Figure 3.7A and data not shown). Sbp1p and Scd6p both regulate global translational repression and mRNA decay through mechanisms similar to Dhh1p, Pat1p, and Lsm1p (Nissan et al., 2010; Segal, Dunckley, & Parker, 2006). Because *sbp1Δ/Δ* and *scd6Δ/Δ* strains do not display the complete pseudohyphal growth loss of the *dhh1Δ/Δ*, *lsm1Δ/Δ*, and *pat1Δ/Δ* strains, the products of these genes must be playing different roles, despite the similar functions of these genes described in the literature.
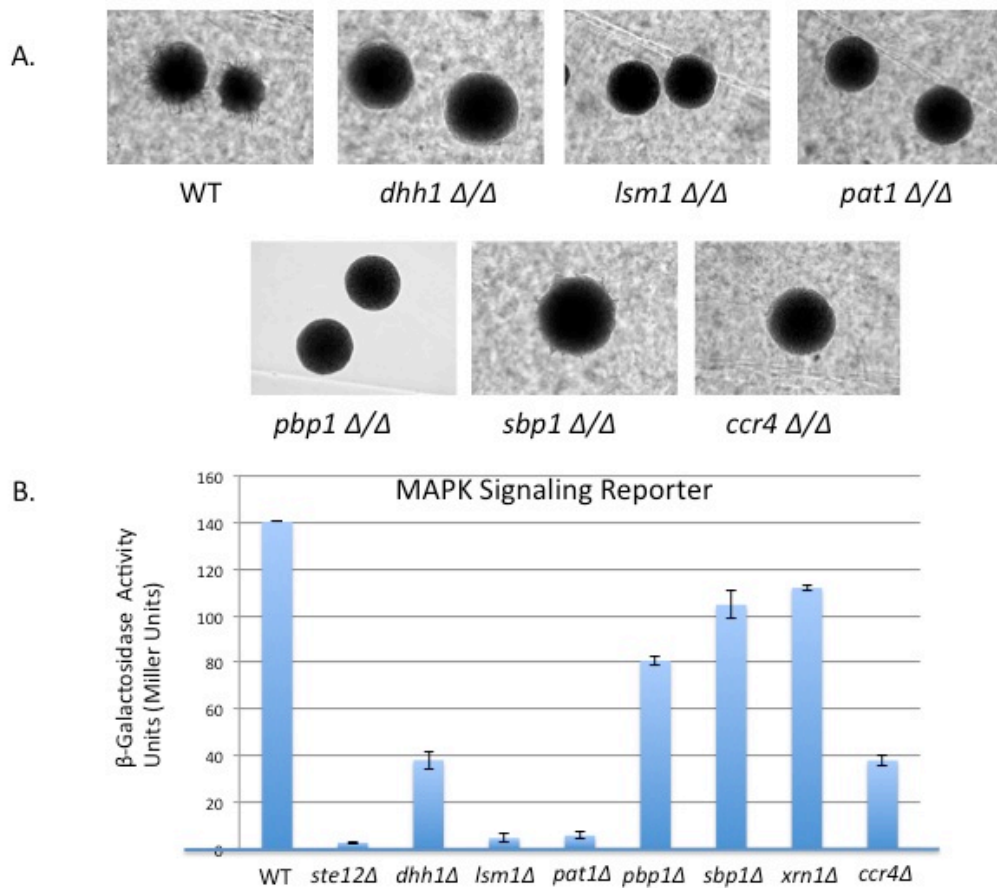
Figure 3.7 Defective filamentous growth in mRNA decay factor null strains. A.) Surface-spread filamentation of wild-type and indicated diploid deletion strains was assayed on SLAD agar media. B.) Filamentous growth MAPK signaling in indicated haploid deletion strains was assayed using the *FRE(Ty1)::lacZ* reporter construct in synthetic complete. Bar height represents mean and error bars represent standard deviation of three independent trials.

## 3.3.4.4 Deletion of mRNA Decay Factors Dhh1p, Lsm1p, and Pat1p Reduces Signaling of the Filamentation-Specific MAPK Pathway

We sought to determine whether the mRNA decay factors important for surface-spread filamentous growth could be regulating filamentous growth through a kinase-signaling pathway. We used the *FRE(Ty1):: lacZ* transcriptional reporter to assay whether MAPK signaling was adversely affected in *dhh1Δ*, *lsm1Δ*, *pat1Δ*, *pbp1Δ*, and *sbp1Δ* haploid mutants. The *FRE(Ty1):: lacZ* reporter construct places consensus DNA binding sequences for the transcription factors Ste12p and Tec1p, which together form a filamentation and

69

invasion response element (*FRE*) upstream of *LACZ*, which encodes the *β*-galactosidase gene product (Madhani & Fink, 1997). This assay effectively measures basal signaling through the MAPK signaling pathway. We introduced the transcriptional reporter into wild-type Σ1278b haploid (positive control), *ste12Δ* mutant (negative control), and each mRNA decay factor null mutant strain and then assayed β-galactosidase production in log phase cultures growing in nutrient replete conditions. As previously described, deletion of *DHH1* decreases MAPK signaling relative to wild-type haploid control. Strikingly, deletion of *LSM1* or *PAT1* has an even more pronounced defect in MAPK signaling, with transcriptional reporter output resembling the low levels of the *ste12Δ* strain. Deletion of *SBP1* and *PBP1* does not have a strong effect on MAPK signaling (Figure 3.7B).

The filamentous growth MAPK signaling pathway hierarchy in yeast is well-described, with cell membrane protein sensors at the cell surface transmitting signal to the Ras2p GTPase, and the MAPKs Ste20p, Ste11p, Ste7p, and Kss1p and terminating in activation of the transcription factors Tec1p and Ste12p in the nucleus (Madhani & Fink, 1997; Madhani et al., 1997; Mosch et al., 1996). We attempted to pinpoint the position at which Lsm1p and Pat1p are acting within the filamentation-specific MAPK pathway through the use of an overactive dominant allele of Ste11p, termed Ste11-4p. *Ste11-4* introduced to the wild-type strain results in a strong increase in basal MAPK signaling relative to wild-type carrying an empty vector (Stevenson, Rhodes, Errede, & Sprague, 1992). However, deletion of Ste7p, which acts downstream of Ste11p, completely abrogates the MAPK signaling even in the presence of the overactive dominant Ste11-4p. We reasoned that if the mRNA decay factors Lsm1p and Pat1p were acting upstream of Ste11p kinase, we should observe a substantial increase in MAPK signaling relative to wild-type when the dominant active *STE11-4* allele was introduced to *lsm1Δ* or *pat1Δ* strains. However, if Lsm1p and Pat1p are acting downstream of Ste11p kinase, we expect MAPK signaling levels to resemble *pat1Δ*, *lsm1Δ*, or *ste7Δ* strains carrying only empty vector. We find that *lsm1Δ* and *pat1Δ* strains carrying overactive dominant *STE11-4* resemble *lsm1Δ* and *pat1Δ* strains carrying only empty vector, suggesting that these factors are playing a role within the MAPK pathway downstream of the MAPKKK Ste11p (Figure 3.8B), at least at the level of transcription. Interestingly, we find that dominant active *STE11-4* likewise

fails to induce filamentation in *lsm1Δ/Δ* and *pat1Δ/Δ* strains at a level comparable to wild-type diploid, when surface-spread filamentation is assayed in the absence of filamentation-inducing conditions (Figure 3.8C).
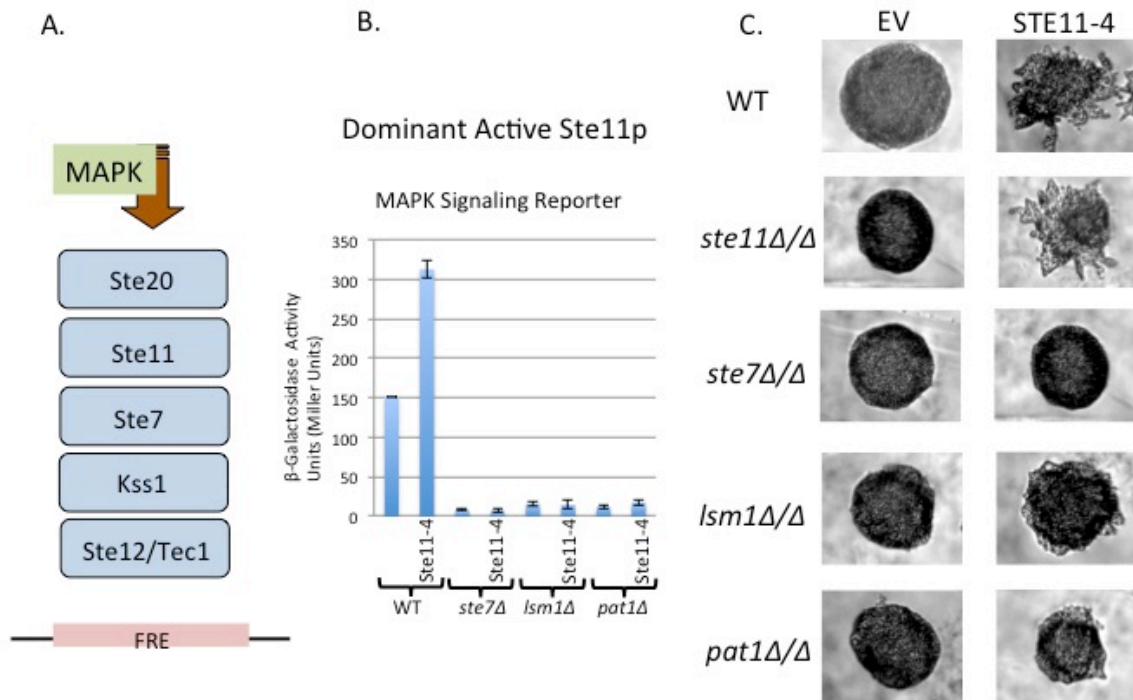


Figure 3.8 *LSM1* and *PAT1* function downstream of *STE11*. A.) Diagram of MAPK signaling cascade. B.) Haploid wild-type, *ste7Δ*, *lsm1Δ*, and *pat1Δ* strains carrying either empty vector or dominant active *STE11-4* allele were assayed for MAPK signaling using the *FRE(Ty1)::lacZ* reporter construct in synthetic complete media. C.) Diploid wild-type, *ste11Δ/Δ*, *ste7Δ/Δ*, *lsm1Δ/Δ*, and *pat1Δ/Δ* strains carrying either empty vector or dominant active *STE11-4* allele were examined for ectopically induced pseudohyphal growth after overnight incubation on synthetic complete agar media.

3.3.4.5 Loss of Surface-Spread Filamentation in *dhh1Δ*, *pat1Δ*, and *lsm1Δ* Strains Is Not Due to Gross Disruption of Global Translational Repression and mRNA Decay

It is possible that the surface-spread filamentation and MAPK signaling defects could be the result of grossly disrupting mRNA decay.  Indeed, the *pat1Δ* strain displays a severe mRNA decapping defect, surpassed only by deletion of the decapping enzymes Dcp1p or Dcp2p (Nissan et al., 2010).  We suspect that Lsm1p and Pat1p are playing a more direct role in filamentous growth.  We were able to test the possibility of filamentous growth reduction through gross disruption of mRNA decay using an *xrn1Δ* mutant, in which the 5'-3' exonucleolytic decay enzyme Xrn1p is deleted.  This mutant is known to display a complete loss of surface-spread filamentation in diploids, as well as loss of invasive growth in haploid null mutants (Kim & Kim, 2002).  However, we find that loss of Xrn1p does not specifically affect MAPK signaling, when we introduce the *FRE(Ty1):: lacZ* reporter construct into the null *xrn1Δ* strain (Figure 3.7B).  We conclude that gross disruption of mRNA decay, by deleting the exonucleolytic decay step of the major route of mRNA decay in budding yeast, does not cause a specific defect in MAPK signaling.  Moreover, while *xrn1Δ* displays a near complete loss in a haploid invasive growth assay, *dhh1Δ*, *pat1Δ*, *lsm1Δ*, *sbp1Δ*, and *pbp1Δ* strains display a subtler defect, again suggesting a difference in mechanism (Supplementary Figure 3.3).

We attempted to generate null mutants of the deadenylation complex and decapping complex machinery for a focused measure of more discrete steps of mRNA decay to filamentation; unfortunately, we were unable to generate *dcp1Δ* or *dcp2Δ* strains in the Σ1278b background and note that *DCP2* is essential for some strain backgrounds (Gaudon, Chambon, & Losson, 1999).  Likewise, the deadenylation factor Pop2p is specifically essential only in the filamentous Σ1278b background (Dowell et al., 2010).  Interestingly, deletion of the deadenylation factor Ccr4p does result in a MAPK signaling response defect comparable to *dhh1Δ*.  Thus, the formal possibility persists that a specific step of the mRNA decay process is essential for filamentous growth MAPK signaling.

### 3.3.4.6 *DHH1* Positively Regulates Hyphal Growth in *Candida albicans*

Lastly, we sought to determine whether orthologous mRNA decay factors in the opportunistic fungal pathogen *Candida albicans* play an analogous role in the regulation of the hyphal growth transition, which has been found to be an important virulence factor. By assaying a heterozygous null mutant *DHH1/dhh1Δ*, loss of one allele of *DHH1* in diploid *C. albicans* results in a substantial loss of hyphal growth. We used carbon limitation as well as pH stress to induce hyphal growth in *C. albicans*, and we observe less surface wrinkling and loss of peripheral hyphae in the *DHH1/dhh1Δ* heterozygote compared to the wild-type strain (Figure 3.9). We therefore posit that a similar mode of regulation may govern hyphal growth in *C. albicans*.

|  | Wild Type | DHH1 / *dhh1Δ* |
|---|---|---|
| YPD (Hyphal Growth Not Induced) | | |
| Serum (Hyphal Growth Induced) | | |
| Carbon Limitation (Hyphal Growth Induced) | | |
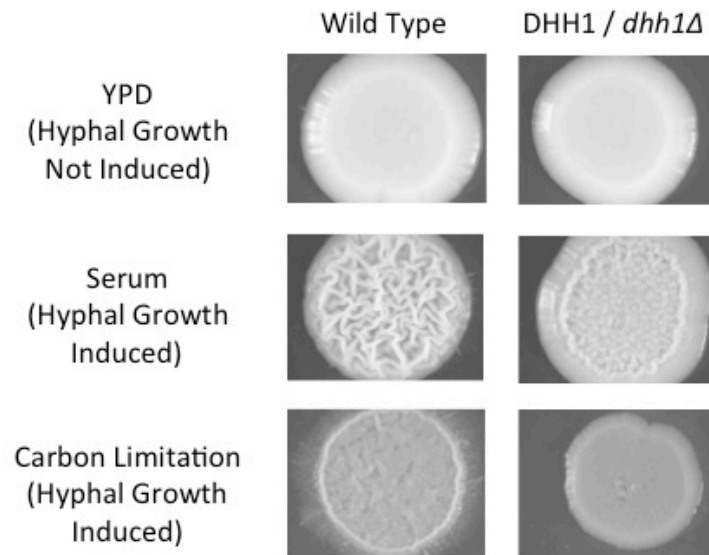
Figure 3.9 A possible role for a homologous *DHH1-PAT1-LSM1-7* complex in *C. albicans* hyphal growth.  A haploinsufficient *DHH1/dhh1Δ* heterozygous *C. albicans* strain is imaged with wild-type grown on three media types: YPD, serum-supplemented YPD, and carbon limitation agar media. Note wrinkling morphology and peripheral hyphal filamentation in wild-type absent in *DHH1/dhh1Δ*.

### 3.3.5 Novel Regulation of Filamentous Growth by Inositol Polyphosphates

Upon completion of our phosphoproteomic analysis, we employed the pathway enrichment tool of yeastmine.yeastgenome.org to identify metabolic and signaling pathways statistically overrepresented in the entire set of significantly differentially phosphorylated phosphosproteins across all eight kinase-dead strains. One significantly statistically enriched cellular pathway identified is "inositol phosphate synthesis" (Pathways Identifier: PWY3O-402, p=0.016928).

Table 3.3 Inositol polyphosphate kinases were differentially phosphorylated phosphoproteins in four kinase-dead allele strains.

| Protein | Modified Sequence | Ratio | Significance | Data Set |
|---------|-------------------|-------|--------------|----------|
| ARG82 | _LSDS(ph)TDNLDSIPVK_ | 2.68 | 0.022 | SNF1 |
| | _LSDS(ph)TDNLDSIPVK_ | 2.30 | 0.032 | SNF1 |
| VIP1 | _EFNNAEKVDPS(ph)KIS(ph)ELYDTM(ox)K_ | 0.22 | 0.015 | SNF1 |
| | _LPPPGIQDDHSEENLT(ph)VHDTLQR_ | 0.053 | $2.56 \times 10^{-5}$ | STE11 |
| | _LPPPGIQDDHS(ph)EENLTVHDTLQR_ | 0.12 | $1.90 \times 10^{-3}$ | STE11 |
| | _LPPPGIQDDHS(ph)EENLTVHDTLQR_ | 0.10 | $4.36 \times 10^{-4}$ | STE7 |
| | _LPPPGIQDDHS(ph)EENLTVHDTLQR_ | 0.22 | 0.011 | KSS1 |
| | _LPPPGIQDDHSEENLT(ph)VHDTLQR_ | 0.24 | 0.015 | KSS1 |
| KCS1 | _ISNALDGSHS(ph)VMDLK_ | 0.24 | 0.021 | SNF1 |

3.3.5.1 Deletion of Inositol Phosphate Kinases Increases Haploid Invasive Growth and Diploid Surface-Spread Filamentation

We identified three of the four inositol kinase enzymes in budding yeast as significantly differentially phosphorylated phosphoproteins in our kinase-dead allele strains (Table 3.3).  We therefore reasoned that production of inositol polyphosphates or inositol pyrophosphates could be an unappreciated filamentous growth regulatory process within the protein kinase signaling network.  A schematic of inositol polyphosphate production by the enzymes of this pathway is presented in Figure 3.10A and reviewed in Introduction.  To test the role of inositol kinases in filamentous growth, we generated deletion mutants of the four inositol kinases Arg82p, Ipk1p, Kcs1p, and Vip1p, as well as Plc1p, which generates IP$_3$.  We then performed an invasive growth assay for these five null haploid strains and compared to the wild-type haploid strain.  As shown in Figure 3.10B, deletion of *PLC1*, *ARG82*, or *KCS1* in haploids does not alter invasive growth.   Intriguingly, deletion of the downstream inositol kinases Vip1p or Ipk1p results in a striking increase in invasive growth.

We further assayed filamentation by testing surface-spread filamentation on SLAD agar media for these five null strains in diploids.  Interestingly, all five null strains displayed an increase in surface-spread filamentation.  However, the *plc1Δ/Δ*, *arg82Δ/Δ*, and *kcs1Δ/Δ* strains displayed a defect in the morphology of peripheral filaments, in which filaments exclusively appear bundled or bunched together.  The *vip1Δ/Δ* and *ipk1Δ/Δ* strains displayed an increase in surface-spread filamentation, without aberrant bundling of peripheral filaments (Figure 3.11).

Deletion of a specific inositol kinase in budding yeast has the interesting consequence of not only lowering the abundance of all IP species downstream of that kinase, but also increasing the abundance of IP species generated upstream of that inositol kinase (York et al., 1999).  Therefore, the observed increase in surface-spread filamentation could be due to increased abundance of a positive regulatory IP species upstream of these inositol kinases or the deletion of a negative regulatory IP species downstream of these inositol kinases.  Because we observe increased surface-spread filamentation in all null

diploid strains, we suspect that a negative regulatory downstream inositol pyrophosphate is no longer being made, which we address further in Discussion.
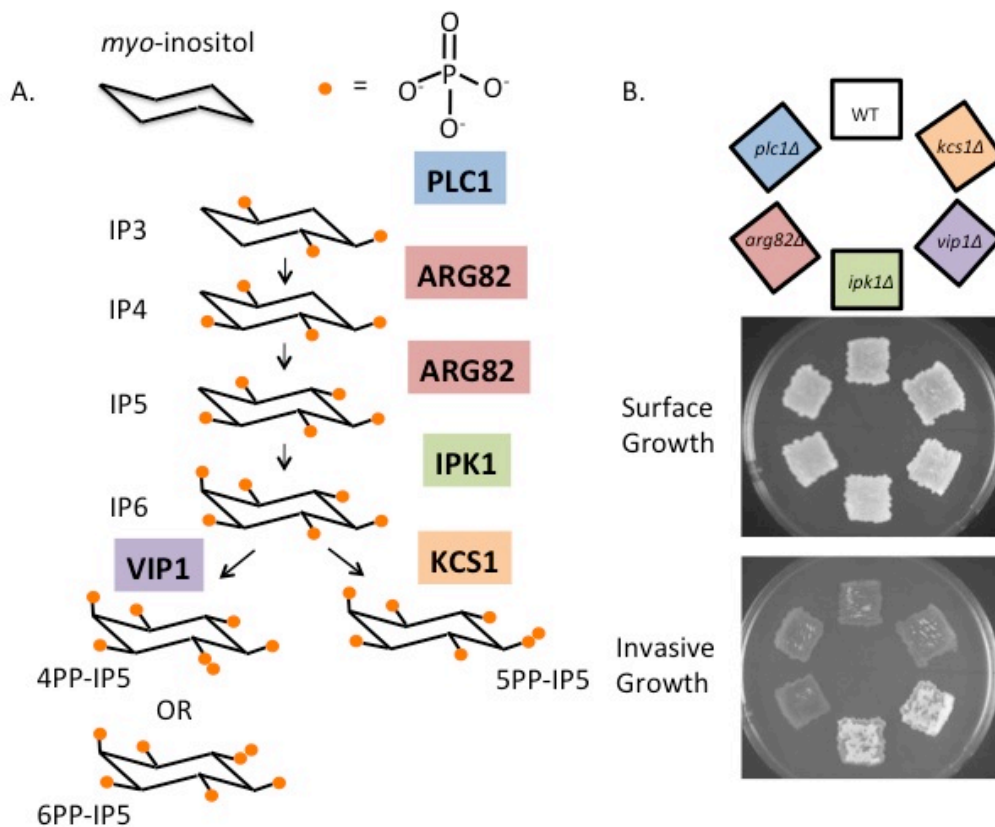


Figure 3.10 The inositol polyphosphate pathway plays a role in filamentous growth. A.) Inositol polyphosphates and pyrophosphates are produced by Plc1p, Arg82p, Ipk1p, Vip1p, and Kcs1p through cleavage of $PIP_2$ and subsequent phosphorylation of $IP_3$. The precise inositol pyrophosphate molecule produced by Vip1p has yet to be determined. The color-coding scheme depicted in the pathway will be used throughout this report. B.) An invasive growth assay was performed for haploid wild-type *plc1Δ*, *arg82Δ*, *ipk1Δ*, *vip1Δ*, and *kcs1Δ* strains by patching strains onto a YPD agar plate. The ordering of patches is shown above the pre- and post-wash images.
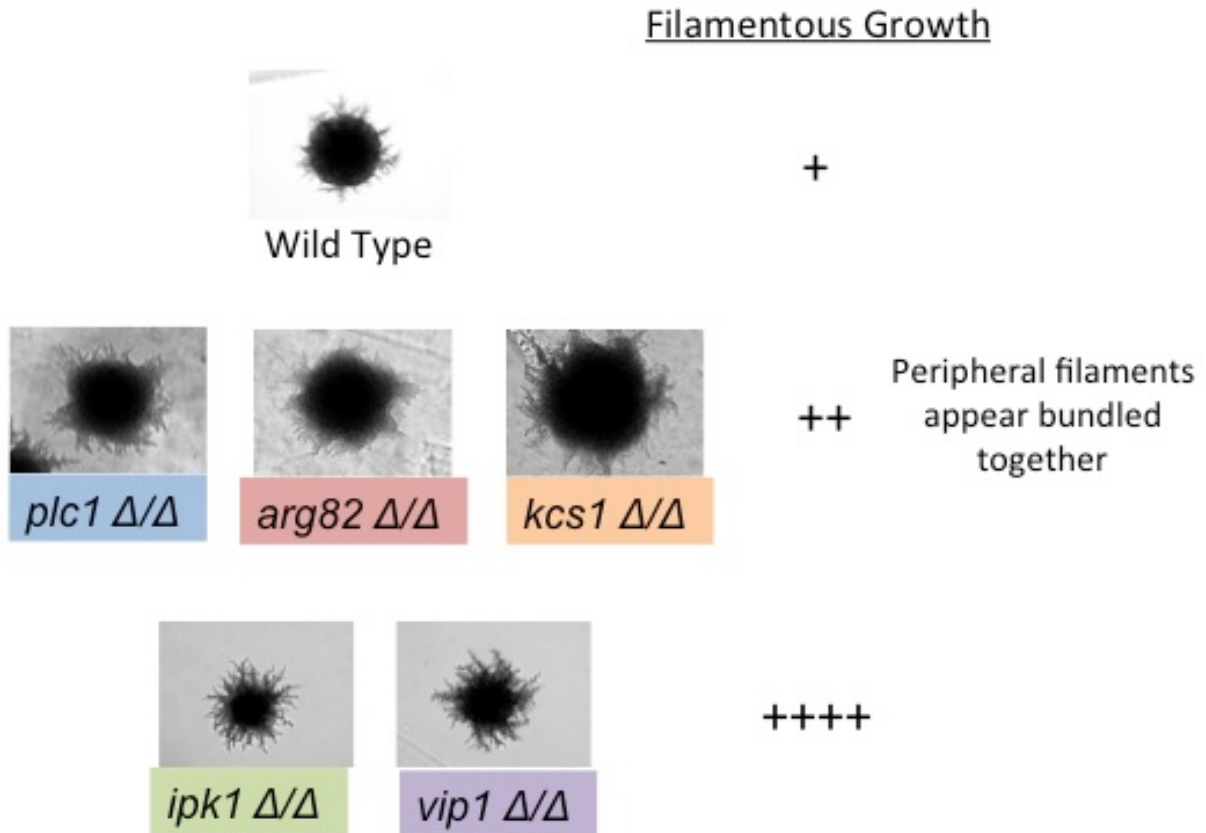
Figure 3.11 Pseudohyphal growth of inositol kinase null diploid strains. Surface-spread filamentation of the indicated strains was assayed on SLAD agar media as described in Materials and Methods, along with a brief qualitative assessment of the filamentous growth phenotype.

## 3.3.5.2 Production of Inositol Polyphosphates Is a Novel Mode of Filamentous Growth Regulation

One possible explanation of the apparent increase in surface-spread filamentation in null diploid strains is simply that deletion of inositol kinases causes an aberrant colony morphology phenotype, in which cells become polarized and fail to completely divide. This could be attributed to misregulation of the cell cycle, cytoskeleton, budding pattern, or cytokinesis, and therefore would not be considered *bona fide* filamentous growth. We suspected that the apparent increased filamentation was not simply an aberrant colony morphology phenotype since it appeared to be exaggerated during nitrogen deprivation. We tested the possibility of simply an aberrant "filamentous-like" phenotype by deleting the inositol kinase enzyme *IPK1* in a non-filamentous background. We examined

microcolonies of inositol kinase knockouts in both the S288c (non-filamentous) and Σ1278b filamentous diploid backgrounds growing on synthetic complete agar media. Strikingly, we observe a minimal level of filamentation when *IPK1* is deleted from the filamentous diploid background, even on nutrient replete conditions.  This minimal filamentation is not observed in the wild-type filamentous diploid strain.  Importantly, this filamentous phenotype is also not observed when *IPK1* was deleted from the non-filamentous diploid background strain (Figure 3.12).  We conclude that deletion of *IPK1* from the diploid filamentous strain results in a filamentation phenotype that does not occur in a non-filamentous background and is therefore reflective of an increase in *bona fide* filamentous growth.
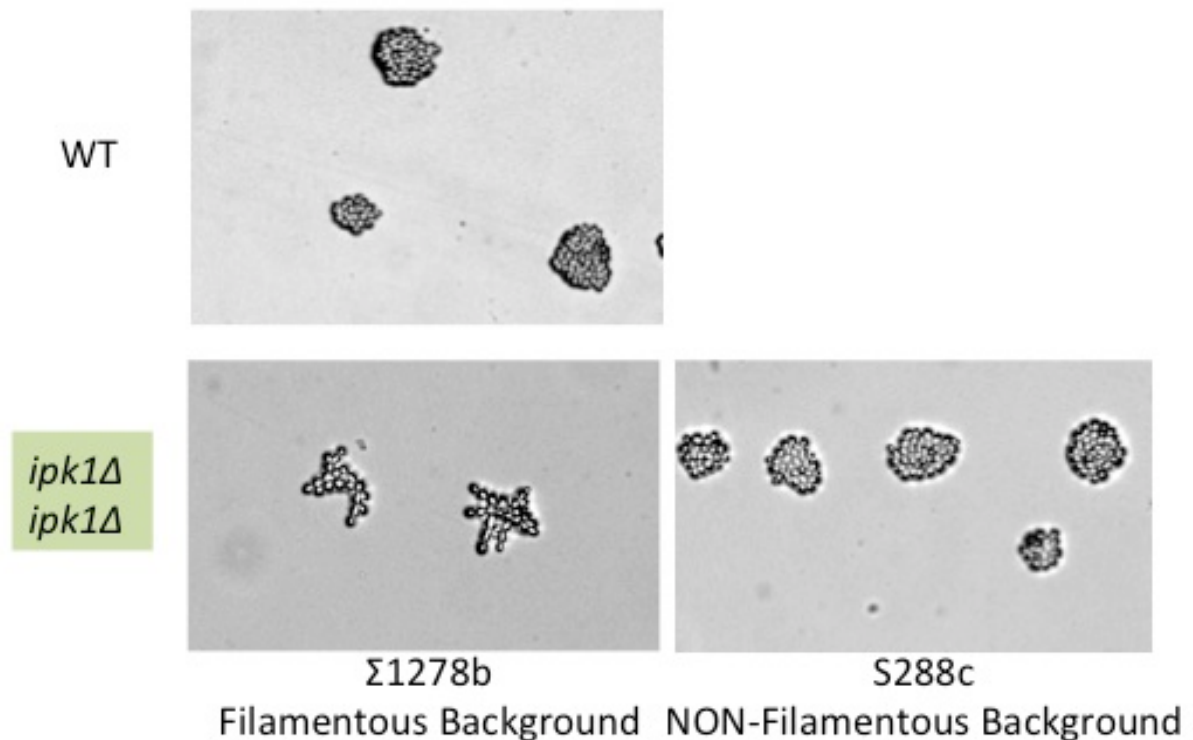


Figure 3.12 Regulation by the inositol polyphosphate pathway constitutes a novel mode of filamentous growth regulation.  Microcolonies of wild-type diploid and *ipk1Δ/Δ* strains in the filamentous Σ1278b and non-filamentous S288c genetic backgrounds are shown after overnight incubation on synthetic complete agar media. Wild-type non-filamentous strain would never be expected to display an aberrant cell or colony morphology and is therefore omitted.

3.3.5.3 Epistasis of Inositol Kinase Genes Suggests Kinase Redundancy

Although deletion of each of the five genes generating inositol polyphosphates and pyrophosphates results in increased filamentation, the colony morphology of *plc1Δ/Δ*, *arg82Δ/Δ*, and *kcs1Δ/Δ* noticeably differs from that of *vip1Δ/Δ* and *ipk1Δ/Δ* null strains. We took advantage of this differential colony morphology to test whether the epistasis of these enzymes in the production of soluble inositol polyphosphates is the same in the context of diploid surface-spread filamentation. We generated the double null strains *ipk1Δ/Δ plc1Δ/Δ*, *ipk1Δ/Δ arg82Δ/Δ*, and *ipk1Δ/Δ kcs1Δ/Δ* and assayed surface spread filamentation in comparison to single null mutant strains. As in the inositol polyphosphate synthesis pathway, we observe that *plc1Δ/Δ* and *arg82Δ/Δ* are both epistatic to *ipk1Δ/Δ* with respect to filamentous growth. When both alleles of both of these genes are deleted from the filamentous background, increased filamentation with bundled peripheral filaments is observed. However, we find that *kcs1Δ/Δ* is also epistatic to *ipk1Δ/Δ* with respect to filamentous growth, as shown in Figure 3.13. Because Kcs1p transfers a phosphate group to a phosphoryl group already present on an inositol polyphosphate, we suspect that Kcs1p may be phosphorylating $IP_4$ or $IP_5$ to generate the substrate of Ipk1p and Vip1p. This intermediate inositol pyrophosphate generated by Kcs1p may also be necessary to prevent the "bundling" filamentation phenomenon observed in *plc1Δ/Δ*, *arg82Δ/Δ*, and *kcs1Δ/Δ* null strains. However, we cannot exclude the possibility that Kcs1p may be acting on two different IP species, with one playing a role in the "bundling" colony morphology and a second further downstream product negatively regulating filamentation.
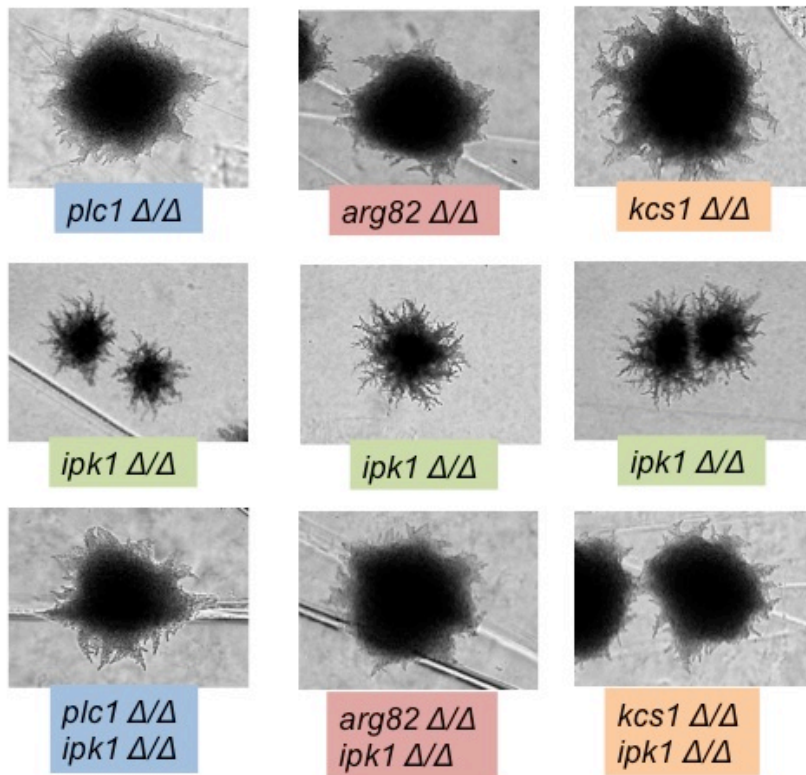
Figure 3.13 Epistasis of inositol kinase genes. Genetic interactions between inositol kinase genes were determined through analysis of diploid surface-spread filamentation on SLAD agar media.

3.3.5.4 Cloned Alleles of *VIP1* and *IPK1* Rescue Wild-Type Filamentous Growth

We successfully cloned both *IPK1* and *VIP1* with 1kb native promoter sequence from the filamentous Σ1278b background into centromeric yeast shuttle vectors. For *IPK1*, we included ~300bp sequence downstream of the stop codon to approximate the 3'UTR, while we cloned *VIP1* in frame with a C-terminal GFP tag (Materials and Methods). In comparison to empty vector controls, we observe rescue of wild-type surface-spread filamentation levels when cloned alleles are introduced into the respective diploid knockout strains and assayed on SLAD agar plates (Figure 3.14A and B).

3.3.5.5 Phosphorylation of the Inositol Kinase Vip1p Is Not Required for Function

We sought to determine the role of the differential phosphorylation of the inositol kinases Arg82p, Kcs1p, and Vip1p detected by mass spectrometry. Because we suspect Vip1p to be the inositol kinase generating the specific inositol pyrophosphate playing a negative regulatory role in filamentous growth, we used site-directed mutagenesis to mutate the four serines and threonines found to be differentially phosphorylated in Vip1p to alanine, to prevent phosphorylation. A phosphonull allele of *VIP1* was created by mutating serine 77, threonine 82, serine 821, and serine 824 to alanine residues. As noted above, wild-type *VIP1–GFP* carried on a vector rescues a wild-type filamentous growth level in the *vip1Δ/Δ* strain. We find that mutation of phosphorylated serines and threonines to alanines does not affect wild-type Vip1p function, since the *VIP1* phosphonull allele (*VIP1$^{S77A,T82A,S821A,S824A}$*) also rescues filamentation in the *vip1Δ/Δ* strain to a wild-type level on SLAD agar media (Figure 3.14B). Interestingly, Vip1p adopts a globular subcellular localization after post-diauxic shift (Narayanaswamy et al., 2009). We assayed the subcellular localization of *VIP1$^{S77A,T82A,S821A,S824A}$* and likewise observe no differential localization phenotype compared to the wild-type *VIP1* allele when phosphorylation is prevented (Figure 3.14C). In parallel to generation of a phosphonull allele, we also constructed a "phosphomimetic" allele by substituting phosphoserines and phosphothreonines with aspartic and glutamic acid residues; we likewise find no affect for a phosphomimetic allele (Figure 3.14B and C). We conclude that the phosphorylation of Vip1p detected by mass spectrometry is dispensable for Vip1p function in filamentation and subcellular localization.

Figure 3.14 Phosphorylation of Vip1p is dispensable for filamentous growth function and subcellular localization.  A.) Wild-type diploid with empty vector, *ipk1Δ/Δ* with empty vector, and *ipk1Δ/Δ* with *IPK1* rescue vector are shown on SLAD agar media.  B.) A diploid *vip1Δ/Δ* strain transformed with either empty vector, *VIP-GFP*, phosphonull *VIP1^S77A,T82A,S821A,S824A-GFP*, or phosphomimetic *VIP1^S77D,T82E,S821D,S824E-GFP* is shown on SLAD agar media.  C.) Subcellular localization of VIP1-GFP, phosphonull *VIP1^S77A,T82A,S821A,S824A-GFP*, or phosphomimetic *VIP1^S77D,T82E,S821D,S824E-GFP* was examined during post-diauxic shift phase.

## 3.4 Discussion

We present here an extensive analysis of kinase signaling activity during the filamentous growth transition stress response in the filamentous haploid Σ1278b *S. cerevisiae* genetic background.  We selected a core set of eight filamentous growth regulatory protein kinases and assayed filamentous growth phenotypes of strains in which each of these regulatory protein kinases were rendered kinase-dead, through substitution mutagenesis of an invariant lysine to arginine within the kinase ATP-binding pocket.

Plasmid-borne kinase-dead alleles failed to effectively rescue filamentation defects in kinase deletion strains (Figure 3.1). The dependence of kinases upon catalytic phosphorylation activity has not been previously shown to be required for filamentous growth for the Snf1p, Elm1p, or Tpk2p kinases (Failure of kinase-dead rescue is reported in (Pan & Heitman, 2002) but data not shown). Because the kinase-dead allele phenocopies the null allele in each instance, we conclude that the kinase catalytic activity and by extension, the kinase's participation in a phosphorylation signaling network are critical for the contribution of these kinases to the filamentous growth transition.

We subsequently surveyed differential phosphorylation across the proteome when these eight kinases were rendered catalytically inactive. Importantly, over 700 phosphopeptides mapping to approximately 400 phosphoproteins were significantly differentially abundant in the collective set of eight kinase-dead allele strains. Moreover, we uncover novel phosphopeptides not previously observed in any yeast background or experimental condition. Similar to a previously described phosphoproteomic study using kinase and phosphatase deletion strains, we identify phosphopeptides both decreased and increased in abundance relative to the wild-type control (Bodenmiller et al., 2010). Although a number of the phophopeptides found to be decreased in abundance in a given kinase-dead allele strain may be direct substrates of the respective kinase, we suspect that indirect changes in phosphopeptide abundance predominate. First, all phosphopeptides significantly increasing in abundance when a kinase is rendered inactive are presumably not substrates of that kinase. Second, our strategy to interrogate kinase signaling networks permanently disabled kinase activity; we note that analysis using a more transient inhibition of kinase activity may be more likely to reveal direct kinase substrates (Holt et al., 2009).

Two important caveats pertaining to the generation of kinase-dead allele haploid strains and the preparation of cultures prior to mass spectrometry analysis should be addressed. First, the eight kinase-dead strains analyzed were generated by deletion of the endogenous allele from the genome and replacement by a kinase-dead allele carried on a centromeric *LEU* vector. However, these kinase-dead allele strains were then compared to

wild-type Σ1278b haploid; thus, each experimental strain differed from the control in two respects: (1) the kinase was rendered catalytically inactive through substitution of an invariant lysine with arginine and (2) the kinase-dead allele was plasmid-borne, whereas the wild-type kinase allele in the control strain was within the genome at its native locus. This plasmid-borne kinase allele strategy was deemed most practical and necessary in order to conduct experiments in triplex and thereby take full advantage of light, medium, and heavy isotopes of the SILAC labeling approach, as well as to minimize handling and repeated transformation of experimental and control strains. Second, 1% butanol treatment was used to induce filamentous growth in kinase-dead and wild-type control strains prior to cell harvesting and phosphoproteomic analysis. Addition of butanol was used as the filamentation inducing stimulus since this induction condition results in little phenotypic heterogeneity among cells in the population: Heitman and colleagues presciently observed in 2000, "Standard pseudohyphal growth is confined to solid medium, and not all cells become elongated or invasive, thus making array experiments extremely difficult. Butanol allows 'filamentous' growth in liquid medium, and virtually all cells show some aspects of this behavior, making the butanol-induced phenomenon amenable to array analysis" (Lorenz et al., 2000). We considered low nitrogen stress in liquid culture to be inappropriate for our haploid strains since nitrogen deprivation is a diploid-specific filamentation induction condition for growth on a solid agar substrate. However, we note that nitrogen deprivation and butanol stress filamentous growth induction conditions utilize overlapping, but not identical upstream regulatory signaling machinery (Lorenz et al., 2000).

3.4.1 Identification of Novel Phosphorylation Events in the Regulation of Filamentation

As global proteomic analyses provided by mass spectrometry continue to give a more complete picture of post-translational modification across the proteome, a crucial next step will involve determining the functional significance of these observed post-translational modification events. We observed significant differential abundance of phosphopeptides mapping to the Hog1p MAPK, the Flo8p transcription factor, and the Ras2p small G protein. The phosphonull alleles $HOG1^{Y176F}$, $RAS2^{Y165F,T166A}$, and

*FLO8^{S587A,S589A,S590A,S593A}* all display filamentation defects intermediate between wild-type and deletion strains, suggesting that the phosphorylation of these proteins uncovered by mass spectrometry is positively regulating the function of these factors. These alleles likely still encode stably expressed proteins, since protein encoded by phosphonull alleles *RAS2^{Y165F,T166A}* and *FLO8^{S587A,S589A,S590A,S593A}* localize appropriately when labeled with GFP, and HOG1^{Y176F} has been reported previously in the literature (Bell & Engelberg, 2003).

An important caveat regarding the use of phosphonull mutants in testing the functional role of protein phosphorylation should be addressed. Not all copies of Hog1p, Ras2p, and Flo8p are phosphorylated; in fact, only a small percentage may be phosphorylated at any given time point. The best *in vivo* mode of testing phosphorylation function is preventing phosphorylation through substitution of the predicted phospho-serine, threonine, or tyrosine with alanine or phenylalanine. However, we cannot rule out the formal possibility that the serine, threonine, or phenylalanine residues of these proteins alone are important in our filamentation assays, making the observed filamentation defect of the phosphonull mutant strains merely an experimental artifact. Only an *in vitro* methodology could more accurately define the specific role of phosphorylation; however, filamentous growth is an inherently *in vivo* phenotype.

The Hog1p MAPK, often referred to as the "stress activated protein kinase" (SAPK) is critical for the cell adaptation and response to osmotic shock. During salt stress, Hog1p becomes phosphorylated by its upstream MAPKK Pbs2p, rapidly activates internal glycerol production to re-establish homeostasis, and translocates to the nucleus to enable gene transcription (Brewster et al., 1993; Westfall et al., 2008). Threonine and tyrosine dual phosphorylation of Hog1p at the MAPK consensus phosphorylation motif TxY, which is T174 and Y176 in the MAPK Hog1p, was initially thought to be essential for Hog1p function; however, Bell and Engelberg find that T174 and Y176 phosphorylation actually have separable functions. Mutation of threonine 174 to alanine caused a hyperactive Hog1p mutant to completely lose catalytic activity; however, the hyperactive Hog1p mutant exhibits activity in a *pbs2Δ* strain, in which the upstream MAPKK has been deleted, preventing phosphorylation of threonine 174. The authors conclude that threonine 174

plays a structural role in the function of Hog1p. Interestingly, mutation of tyrosine 176 to phenylalanine does not prevent Hog1p from rescuing the response to osmotic stress. The authors find that $HOG1^{Y176F}$ is not "maximally activated," yet can still perform the Hog1p role coordinating recovery during osmotic shock (Bell & Engelberg, 2003). Intriguingly, we likewise find an intermediate functional activity for Hog1Y176F; however, this intermediate activity is not sufficient to appropriately repress filamentation, as assayed by either surface-spread filamentation in a diploid strain or MAPK signaling response in a haploid strain (Figure 3.3). Since only tyrosine 176 and not threonine 174 was predicted to be phosphorylated on the detected phosphopepide, phosphorylation of these two residues may also have distinguishable functions in the regulation of filamentation.

We also identify phosphorylation of the transcription factor Flo8p and the small G protein Ras2p and find haploid strains with phosphonull alleles $RAS2^{Y165F,T166A}$ and $FLO8^{S587A,S589A,S590A,S593A}$ to be defective in invasive growth on solid agar media. Importantly, the phosphopeptides mapping to these proteins have not been previously observed; thus, these represent novel phosphorylation events uncovered through our analysis. Genetic data as well as $in\ vitro$ kinase assay evidence suggest that the PKA paralog Tpk2p phosphorylates the transcription factor Flo8p to regulate transcription of $MUC1$. Specifically, this phosphorylation by Tpk2p enables Flo8p binding to the MUC1 promoter region both $in\ vivo$ and $in\ vitro$ (Pan & Heitman, 1999; Pan & Heitman, 2002). We have uncovered a phosphopeptide mapping to Flo8p in which phosphorylated residues closely resemble a consensus PKA phosphomotif; moreover, mutation of the phosphoserines to alanines generating a phosphonull $FLO8^{S587A,S589A,S590A,S593A}$ allele reduces invasive growth and transcriptional competency of Flo8p, consistent with the possibility that S587, S589, S590, and S593 are specific sites of Tpk2p phosphorylation (Figure 3.5). We note that although only one of the three phoshoserines appears to be in an imperfect PKA consensus motif, phosphorylation motifs are not strictly adhered to by protein kinases.

Phosphorylation of the small G protein Ras2p likewise is necessary for proper Ras2p function, albeit dispensable for Ras2p localization (Figure 3.4). The dual phosphorylation of tyrosine 165 and threonine 166 is an unusual phosphorylation pattern.

(Activation of MAPKs by phosphorylation typically proceeds through dual tyrosine and threonine phosphorylation; however a spacer of one amino acid residue separates the tyrosine and threonine.)  We are aware of only one other activating dual phosphorylation of tyrosine directly neighboring a threonine: activation of the cyclin-dependent kinase Cdk1p (Cdc28p).  The upstream kinase for phosphorylation of Cdc28p threonine 169 events is known; however this upstream kinase does not phosphorylate both the threonine and tyrosine (Ross, Kaldis, & Solomon, 2000).  The similar dual phosphorylation of both Ras2p and Cdc28p raises the interesting hypothesis that these two cell cycle factors could be regulated by similar mechanisms.  We consider it possible for the dual phosphorylation to occur via a dual specificity kinase or two distinct upstream kinases.

3.4.2 Protein Components of an mRNA Decay Factor Complex Regulate Filamentation through the MAPK Signaling Pathway

We identify significantly differentially phosphorylated phosphoproteins functioning in mRNA decay and translational repression across our collective phosphoproteomic data set of eight kinase-dead allele strains.  Specifically, we observe statistically significant differential abundance of phosphopeptides mapping to the decapping enzyme Dcp2p; the decapping activators Pat1p, Dhh1p, and Sbp1p; and the exonuclease Xrn1p (Table 3.2).  From these phosphopeptide abundance observations, we hypothesized that mRNA decay may be an unexplored part of the kinase signaling network employed by the eight regulatory kinases in their governance of filamentous growth.

A number of stress conditions induce the formation of enlarged cytoplasmic mRNP granules in budding yeast.  The presence of these mRNP granules indicates a global translational repression, since the mRNP granules are thought to contain mRNA transcripts complexed with translational repression and mRNA decay factors, effectively sequestered away from the translational machinery (Buchan et al., 2010).  We endeavored to use the formation of these mRNP granules as an indicator of global translational repression and mRNA decay during filamentous growth induced through a number of different genetic and chemical means.  The lack of p-body foci formation and enlargement following incubation in 1% butanol liquid media to induce filamentation indicates a lack of sustained p-body

formation and ergo lack of global translational repression (Supplementary Figure 3.1). We likewise fail to observe enlarged p-body foci in constitutively filamentous mutant strains. It would be interesting to test whether p-bodies become appreciably enlarged after only 10-20min exposure to butanol stress; however, filamentous-like projections would not be apparent after such a short induction period, making any connection to filamentation difficult to delineate.

Although p-body foci are not present during filamentation, after readily observing enlarged p-body foci during glucose stress and post-diauxic shift (High OD) stress in the Σ1278b filamentous genetic background, we realized that the formation of these granules could be used as an assay to detect possible association of protein kinases with the translational repression and mRNA decay components of p-bodies. Physical association of protein kinases with these mRNA decay factors could be one possible mechanism explaining the observed differential phosphorylation of these factors when the eight protein kinases were rendered kinase-dead, particularly in the case of less abundant phosphopeptides, and co-localization of protein kinases with p-bodies could indicate a physical association. Protein kinases tagged with GFP do not co-localize with Dcp2p or Edc3p tagged with mCherry; however, the mRNA-binding protein Igo1p does co-localize with four protein kinases Ste20p, Kss1p, Fus3p, and Tpk2p (Figure 3.6 and Supplementary Figure 3.2). Igo1p is a putative p-body and stress granule component, which, together with its paralog Igo2p, is critical for entry into stationary phase. Igo1p and Igo2p are thought to protect mRNA transcripts critical for stationary phase entry and survival by directly binding transcripts and preventing their degradation in a Rim15p kinase-dependent manner (Talarek et al., 2010). Like the protein kinases, a punctate subcellular localization pattern for Igo1p is only observed during post-diauxic shift phase, while neither Igo1p nor the protein kinases adopt a punctate fluorescence pattern during glucose stress, in which p-bodies are readily observed. Two possible conclusions could explain these co-localization data: (1) Igo1p and therefore protein kinases transiently associate with p-bodies and stress granules only in specific cell conditions or (2) Igo1p and protein kinases are components of a cytoplasmic protein granule distinct from p-bodies and stress granules. Either possibility points to an association of filamentous growth regulatory

kinases with proteins regulating mRNA stability.  Interestingly, a phosphopeptide mapping to the C-terminus of Igo1p is significantly less abundant (p~7.94x10$^{-5}$) in the Tpk2p kinase-dead allele strain, raising the possibility of direct phosphorylation of Igo1p by Tpk2p.

We next analyzed surface-spread filamentation phenotypes for mRNA decay diploid null strains and observe stark loss of filamentation in *ccr4Δ/Δ*, *dhh1Δ/Δ*, *pat1Δ/Δ*, *lsm1Δ/Δ*, *pbp1Δ/Δ*, and *sbp1Δ/Δ* strains (Figure 3.7A).  Ccr4p is a component of the deadenylation complex in budding yeast, thought to be the initial step in the major route of mRNA decay (Decker & Parker, 1993).  Dhh1p, Pat1p, and Lsm1-7p form a protein complex that represses translation and activates decapping and subsequent mRNA decay (Coller & Parker, 2005; Nissan et al., 2010).  We further tested the filamentous growth MAPK signaling in these haploid null strains using a *FRE(Ty1):: lacZ* reporter construct and find nearly ablated MAPK signaling in *lsm1Δ* and *pat1Δ* strains, and very minimal signaling in *dhh1Δ* and *ccr4Δ* strains (Figure 3.7B).  Furthermore, the MAPK signaling defect in *lsm1Δ* and *pat1Δ* strains is likely downstream of the MAPKKK Ste11p, as a dominant hyperactive *STE11* allele does not induce the transcriptional filamentation response as strongly in the absence of *LSM1* or *PAT1*.  MAPK signaling assayed via our reporter construct is similar for *lsm1Δ* and *pat1Δ* transformed with *STE11-4* dominant active allele or empty vector, supporting a role for Lsm1p and Pat1p downstream of Ste11p (Figure 3.8B).  However, *lsm1Δ/Δ* and *pat1Δ/Δ* diploids transformed with *STE11-4* dominant active alleles do display a minimal pseudohyphal growth phenotype, albeit less than wild-type carrying the dominant active *STE11-4* (Figure 3.8C).  One possible explanation is that the signaling network regulated by Ste11p encompasses nuclear as well as non-nuclear events.  In other words, Ste11p may regulate facets of the filamentous growth transition other than merely transcription in the nucleus and hyperactivation of these other cellular processes may give rise to the minimal pseudohyphal growth observed in the *lsm1Δ/Δ STE11-4* and *pat1Δ/Δ STE11-4* strains.

Of the Dhh1p-Pat1p-Lsm1-7p complex members, only Dhh1p has been previously implicated in regulation of filamentous growth.  Dhh1p putatively protects the *STE12* mRNA transcript from degradation; thus in the absence of *DHH1*, *STE12* mRNA levels

decrease, resulting in a filamentation decrease (Park et al., 2006). This putative mechanism seems counterintuitive as Dhh1p has a well-described role in repressing translation initiation *in vitro* and activating mRNA decapping *in vivo* (Coller & Parker, 2005; Nissan et al., 2010). We hypothesize that the components of the Dhh1p-Pat1p-Lsm1-7p complex may be specifically degrading the mRNA transcript of a protein negatively regulating the MAPK pathway at or downstream of the Ste11p MAPKKK. Three such negative regulators are described in the literature: Hog1p, Dig1p, and Dig2p (Bardwell, Cook, Zhu-Shimoni, Voora, & Thorner, 1998; Cook et al., 1996; Shock et al., 2009). Future work will focus on assaying mRNA and protein levels of these negative regulators in wild-type, *dhh1Δ*, *pat1Δ*, and *lsm1Δ* strains. Decreased levels of a specific MAPK component would also explain the MAPK signaling defect in *dhh1Δ*, *pat1Δ*, and *lsm1Δ* strains; however, we note that *KSS1* deletion does not give a similar diploid phenotype, and minimal levels of Ste11p, Ste7p, and Ste12p must be present, as *dhh1Δ*, *pat1Δ*, and *lsm1Δ* strains are not sterile.

Although *xrn1Δ* does not have a strong defect in MAPK signaling as assayed by the reporter construct, the formal possibility persists that the abrogated pseudohyphal growth phenotypes of *dhh1Δ/Δ*, *lsm1Δ/Δ*, and *pat1Δ/Δ* are an indirect consequence of an mRNA decay defect. All three of these knockout strains display a general growth defect and pleiotropic effects. A more interesting possibility is that a specific step of the mRNA decay process is somehow monitored as a checkpoint before the filamentous growth transition; unfortunately, we failed to generate haploid or diploid knockouts of the decapping proteins *DCP2* or *DCP1*.

Interestingly, the filamentous growth functions of Dhh1p, Pat1p, and Lsm1p may be conserved in the opportunistic pathogen *C. albicans*, based on the haploinsufficient phenotype of a *DHH1/dhh1Δ* strain (Figure 3.9). We find that a heterozygous *DHH1/dhh1Δ* *C. albicans* strain displays a loss of the typical wrinkling morphology when hyphal growth is induced on a serum-supplemented YEPD agar plate. In agreement with serum-induction result, hyphal growth induction by carbon limitation fails to produce wrinkling or peripheral hyphal filaments in a *DHH1/dhh1Δ* heterozygote. We are interested in also

91

testing the roles of *PAT1* and *LSM1* homologs in *C. albicans*, since the ability to switch among yeast, pseudohyphal, and hyphal growth forms is a key *C. albicans* virulence factor (Sudbery et al., 2004).

3.4.3 Inositol Polyphosphate Synthesis Constitutes a Novel Mode of Filamentous Growth Regulation

This phosphoproteomic analysis also uncovers a role for inositol polyphosphate synthesis in the regulation of filamentous growth. We observed significant differential abundance of phosphopeptides mapping to three of the four inositol kinases of budding yeast (Table 3.3). Intriguingly, the inositol kinase Vip1p was significantly less phosphorylated when the MAPKs Ste11p, Ste7p, Kss1p, and the AMPK Snf1p were rendered catalytically inactive.

We tested the role of inositol polyphosphate production in filamentous growth through gene deletion of the four inositol kinases Arg82p, Ipk1p, Kcs1p, and Vip1p, as well as deletion of Plc1p which generates IP$_3$, the precursor of all soluble phosphorylated inositol species. In an invasive growth assay, *plc1Δ*, *arg82Δ*, and *kcs1Δ* haploid strains confer no differential phenotypes; however *ipk1Δ* and *vip1Δ* strains display a significantly hyperinvasive phenotype (Figure 3.10B). We complemented these invasive growth assays of haploid null strains with analysis of surface-spread filamentous growth in diploid null strains on SLAD agar media. Strikingly, we observe increased filamentation in all five diploid knockouts. However, the colony morphology of *plc1Δ/Δ*, *arg82Δ/Δ*, and *kcs1Δ/Δ* strains has an aberrant appearance in which peripheral pseudohyphal filaments appear bundled or lumped together. This bundling filament phenomenon is not observed in *ipk1Δ/Δ* and *vip1Δ/Δ* strains, which display florid hyperfilamentous growth (Figure 3.11).

We have taken advantage of the differential phenotype of *plc1Δ/Δ*, *arg82Δ/Δ*, and *kcs1Δ/Δ* vs. *ipk1Δ/Δ* and *vip1Δ/Δ* to analyze genetic interactions between these inositol kinase genes. Unexpectedly, we find *KCS1* to be epistatic to *IPK1*, although Kcs1p phosphorylates inositol polyphosphates to form inositol pyrophosphates, a seemingly downstream product (Figure 3.13). We hypothesize that Kcs1p may be phosphorylating

92

IP$_5$, the product of Arg82p, and this product of Kcs1p may then be further phosphorylated by Ipk1p and Vip1.  In other words, our epistasis analysis of filamentous growth phenotypes points to redundancy among the inositol kinases, or perhaps more excitingly, physiological roles for as yet undescribed inositol pyrophosphate species.
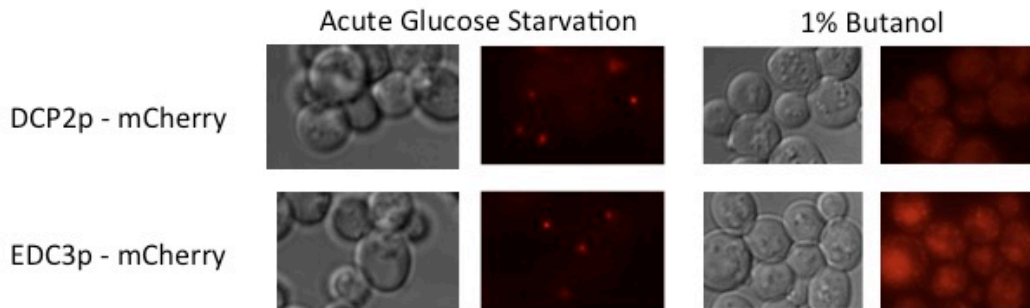
We have developed the following model to explain the hyperfilamentation of inositol kinase deletion mutants and the observed epistatic inositol kinase gene interactions:  We propose that the downstream inositol kinase Vip1p is producing an inositol pyrophosphate species that negatively regulates filamentous growth in both haploids and diploids.  All inositol kinase diploid knockouts display an increased filamentation phenotype to some degree, and this observation would not be expected if a positive regulator IP were accumulating at a particular blocked step in the pathway.  In other words, deletion of any inositol kinase would prevent the formation of the Vip1p product.  In addition, we propose that Kcs1p is generating an inositol pyrophosphate that enables filaments around the periphery of colonies to be separate.  This model would explain the "bundled" filament appearance of *plc1Δ/Δ* and *arg82Δ/Δ*, since these diploid null strains would also lack the inositol pyrophosphate product of Kcs1p.

An exciting future endeavor is to uncover the downstream mechanisms by which the inositol pyrophosphates created by Kcs1p and Vip1p are exerting their effects.  The protein targets for inositol phosphate species produced by Kcs1p are unknown, and we suspect that a number of different cellular processes could result in the observed "bundled" filament phenotype we observe for the *plc1Δ/Δ*, *arg82Δ/Δ*, and *kcs1Δ/Δ* strains.  Intriguingly, the *plc1Δ/Δ*, *arg82Δ/Δ*, and *kcs1Δ/Δ* phenotypes bear a striking resemblance to a *bcy1Δ/Δ tpk2Δ/Δ* strain (Pan & Heitman, 1999).  The resemblance could be entirely correlative, but we note that this colony morphology phenotype is highly unusual, raising the possibility of some relation to the PKA pathway.

The mechanism for the negative regulatory inositol pyrophosphate created by Vip1p is likewise a current research pursuit.  Vip1p is thought to assist Pho81p in the inhibition of the cyclin-cyclin-dependent-kinase complex Pho80p-Pho85p in the response to phosphate starvation.  When phosphate is available, this kinase complex phosphorylates

the transcription factor Pho4p, resulting in its translocation from the nucleus to the cytoplasm.  When this kinase complex is inhibited, the transcription factor Pho4p is no longer phosphorylated and thus remains in the nucleus to activate transcription of phosphate-responsive genes (Lee et al., 2007).  We are currently exploring the possibility that Vip1p function in filamentous growth proceeds through its known target, the cyclin-cyclin-dependent-kinase complex Pho80p-Pho85p.  Neither Pho80p nor Pho85p are known regulators of the filamentous growth transition; however, Pho80p is a general stress-response protein kinase, depending on its cyclin binding partner (Huang, Friesen, & Andrews, 2007).  If Pho80p is not the functional target of the negative regulatory inositol pyrophosphate produced by Vip1p, another candidate protein target is difficult to propose, considering the vast complement of the genome found to contribute to filamentous growth (Jin et al., 2008; Shively et al., 2013).  In addition to regulation through protein binding, IPs can function through regulation of inorganic polyphosphate (poly-p) levels (Lonetti et al., 2011) or through pyrophosphorylation of phosphoproteins (Bhandari et al., 2007).

The function of phosphorylation of the inositol kinases Arg82p, Kcs1p, and Vip1p is unclear at this point.  Our strategy of substituting phosphoserines and phosphothreonines to alanine to generate phosphonull alleles to test phosphorylation function has thus far not been possible for Arg82p and Kcs1p.  We have repeatedly failed to clone *ARG82* and *KCS1*, and genomic mutation of *ARG82* has likewise failed.  Our cloned allele of *VIP1* with a C-terminal GFP tag does, however, rescue a wild-type filamentation level in a *vip1Δ/Δ* strain.  We used site-directed mutagenesis to change all phosphorylated serines and threonines to alanines, generating a phosphonull *VIP1*$^{S77A,T82A,S821A,S824A}$*-GFP* allele, which also effectively rescues a *vip1Δ/Δ* strain (Figure 3.14B).  We conclude that the detected phosphorylation of Vip1p is not required for Vip1p's filamentous growth role.  It is also possible that a plasmid-borne phosphonull allele may mask the effect of preventing phosphorylation, since subtle modulation of protein function could be compensated by slight overexpression from a centromeric vector.  Nonetheless, potential regulation of these inositol kinases through phosphorylation is a fascinating possibility.

|                    | Acute Glucose Starvation | 1% Butanol |
|--------------------|--------------------------|------------|
| DCP2p - mCherry    |                          |            |
| EDC3p - mCherry    |                          |            |

Supplementary Figure 3.1 P-body foci are not readily apparent during butanol-induced filamentation in haploids. Dcp2p and Edc3p were genomically tagged with C-terminal mCherry in two respective haploid Σ1278b strains. Acute glucose starvation (10min) of exponentially growing cells is at left. At right, filamentous growth was induced by incubation in 1% butanol (vol/vol) liquid media for 5hrs.
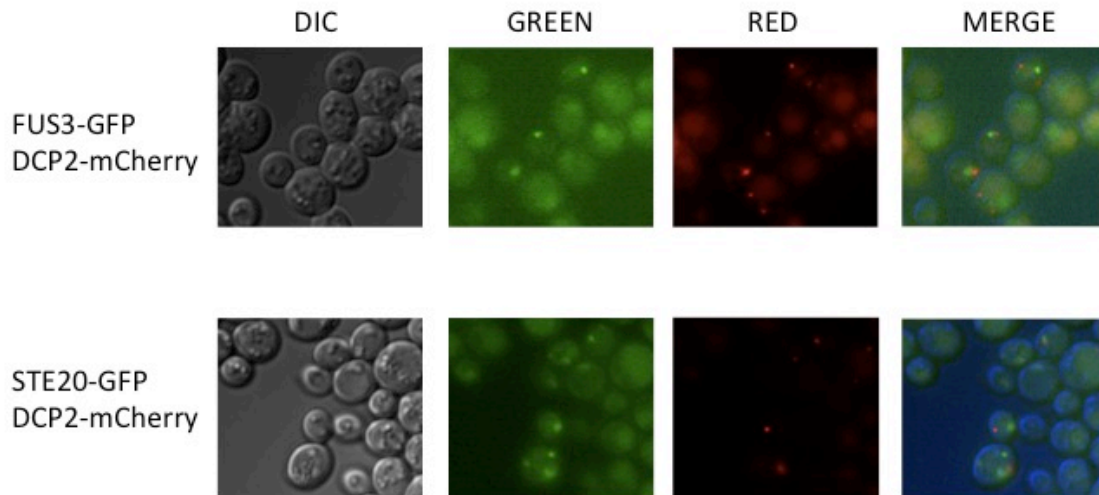
Supplementary Figure 3.2 The Ste20p and Fus3p protein kinases do not co-localize with the p-body marker Dcp2. Fus3p and Ste20p were genomically tagged with C-terminal GFP in haploid strain harboring Dcp2p genomically tagged with mCherry at the C-terminus. Cells were imaged after 3days incubation during post-diauxic shift growth phase.

| | Surface | Invasive | | Surface | Invasive |
|---|---|---|---|---|---|
| WT Haploid | | | pbp1Δ | | |
| flo8Δ | | | sbp1Δ | | |
| dhh1Δ | | | ccr4Δ | | |
| lsm1Δ | | | xrn1Δ | | |
| pat1Δ | | | | | |
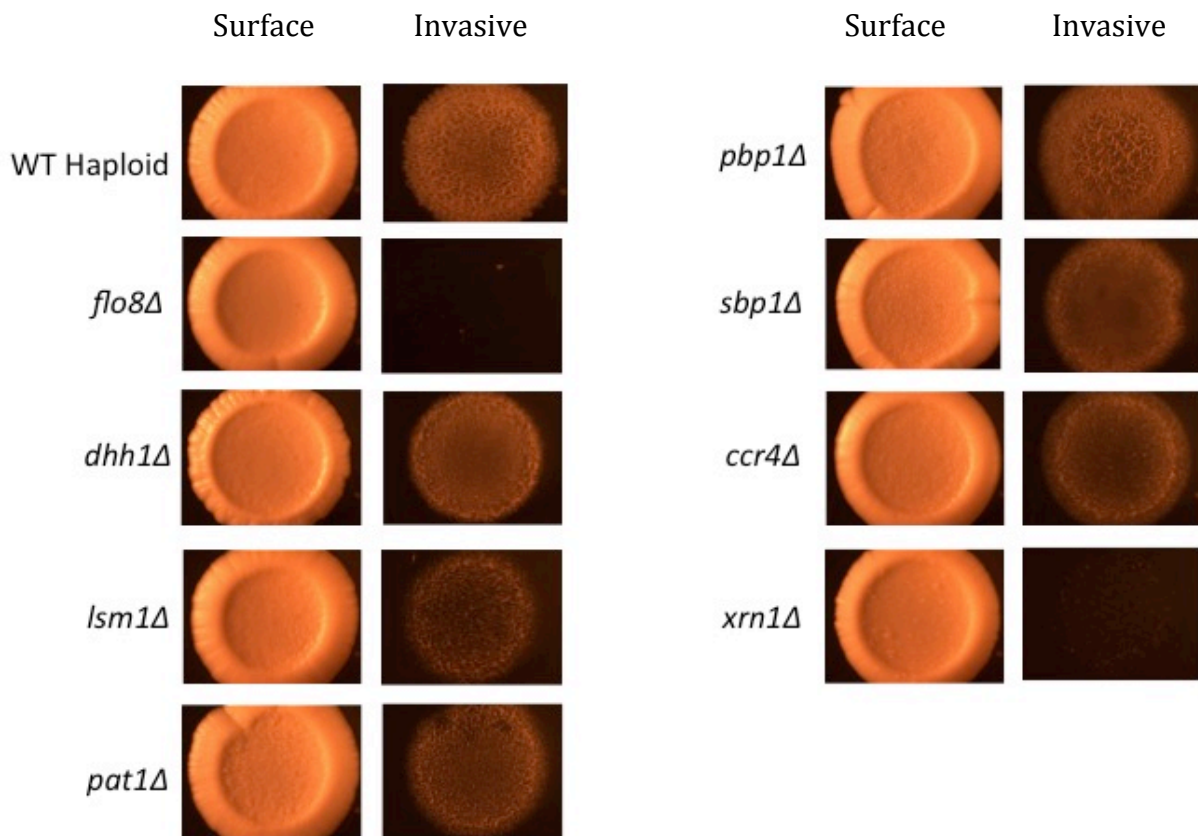
Supplementary Figure 3.3 Invasive growth of haploid mRNA decay factor null mutants. Approximately 7μl of an overnight culture was spot plated onto a rich media YPD plate, incubated 3days, photographed, gently rinsed with water, and re-photographed, as described in Materials and Methods. WT haploid and *flo8Δ* mutant are shown as respective positive and negative controls. The *xrn1Δ* mutant alone shows defective invasion comparable to *flo8Δ*.

# Chapter 4. Conclusions and Future Directions

The transition to a pseudohyphal filamentous growth form is a stress response in *Saccharomyces cerevisiae* that has been under considerable scrutiny greater than two decades. Beginning in 1992, the focus has largely been to uncover the regulatory machinery governing the filamentous growth transition, as the homologs of MAPKs, AMPK, PKA, and small G proteins were all of particular interest since they have clear homologs in humans and play roles in disease (Gimeno et al., 1992; Kuchin et al., 2002; H. Liu et al., 1993; Pan & Heitman, 1999). In the 1990's, interest in filamentous growth of budding yeast was primarily driven by the utility of pseudohyphal growth in *S. cerevisiae* as a model for the hyphal growth switch important for *C. albicans* virulence. However, although *S. cerevisiae* remains a far more tractable model organism that *C. albicans*, molecular biology and genetic techniques in other fungi such as *C. albicans* are rapidly progressing.

Our endeavor throughout this work has been to more thoroughly elucidate the regulatory mechanisms governing this stress response. To that end, we performed a systematic gene overexpression screen aimed to determine the full complement of genes contributing to the filamentous growth phenotype when overexpressed. We identify 551 budding yeast ORFs that enable a filamentous growth phenotype even in conditions of nitrogen sufficiency when overexpressed in the diploid Σ1278b filamentous background. This gene set serves a number of purposes. First, the overexpression gene set serves a complement to filamentous growth regulatory gene sets derived through gene disruption strategies such as transposon mutagenesis or systematic gene deletion. In fact, overexpression identifies overlapping but not identical genes when compared to previously reported gene sets. This may be contributed to differences in assay conditions or strain ploidy, as well as genetic mechanisms.

This gene overexpression set uncovered a possible role for nuclear Hog1p in the repression of filamentous growth via the MAPK signaling pathway.  The Hog1p MAPK is critical for cellular adaptation to hyperosmotic stress.  To coordinate the osmostress response, Hog1p becomes activated through phosphorylation by the MAPKK Pbs2p and translocates to the nucleus.  Hog1p activates the transcription of hundreds of osmo-responsive genes, and this gene expression function of nuclear Hog1p was long considered to be essential for Hog1p regulation of osmotic stress response (Brewster et al., 1993; Ferrigno, Posas, Koepp, Saito, & Silver, 1998b; Posas & Saito, 1997).  Westfall *et al.* (2008) challenged the role of nuclear Hog1p through the use of a *HOG1* allele constitutively tethered to the cell membrane.  Surprisingly, this allele was likewise capable of enabling cell survival through osmotic shock, despite being sequestered from the nucleus, raising a question of what exact role nuclear Hog1p plays.  We find that a nuclear pool of the Hog1p MAPK may play a role in repression of filamentation.  We constructed a Σ1278b strain with genomically integrated *HOG1* tagged with a CAAX box, resulting in tethering to the cell membrane as reported in Westfall *et al.*  We find that this Hog1p-GFP-CCAAX[Ras2p] chimera strain displays defective repression of filamentation, as assayed through invasive growth using SLAD and butanol stress and activation of the *FRE(Ty1)::lacZ* reporter construct measuring MAPK signaling (Madhani & Fink, 1997).  Our finding that a nuclear pool of Hog1p may be important for Hog1p repression of filamentation is consistent with a study by Shock *et al.* (2009), reporting that Hog1p represses filamentation through an incompletely understood mechanism preventing the transcription cofactor Tec1p from appropriately binding DNA in the nucleus.

One possible mechanism to explain the repression of filamentous growth by nuclear Hog1p is Tec1p sumoylation.  Sumoylation has been found to be a modulator of Tec1p function, with increasing sumoylation inhibiting Tec1p activity.  Interestingly, sumoylation can be modulated by Hog1p (Abu Irqeba, Li, Panahi, Zhu, & Wang, 2014; Wang et al., 2009).  This model of regulated sumoylation would provide a potential explanation for Hog1p's filamentation repression function, which may occur by preventing Tec1p from binding upstream of filamentous responsive genes (Shock et al., 2009).

Presented in Chapter 3, the second study is an investigation of the kinase signaling regulatory networks of the filamentous growth transition of *S. cerevisiae*. Filamentous growth is governed by at least three well-studied kinase signaling pathways, including the filamentous growth MAPK pathway, the RAS-cAMP-PKA pathway, and the AMPK Snf1p pathway. Deletion of the components of these pathways confers a dramatically altered filamentous growth phenotype in both haploids and diploids of the Σ1278b genetic background. The canonical view of these kinase signaling pathways holds that they function to regulate the transcriptional activation of *MUC1*, encoding a critical cell-surface glycoprotein essential for pseudohyphal growth. However, a close examination of the literature reveals that abrogation of signaling from these three protein kinase pathways is often much more severe than *muc1Δ*, suggesting that these pathways coordinate other cellular changes in addition to the cell-cell adhesion function of Muc1p (Ahn et al., 1999; Kuchin et al., 2002). Moreover, large-scale mass spectrometry interrogations of the entire yeast phosphoproteome find that even one kinase or phosphatase can have a large impact on the phosphorylation state of the phosphoproteome on the whole, suggesting a more complex network of kinase signaling rather than a simple linear pathway.

We probed the kinase signaling network regulating filamentous growth by generating kinase-dead allele strains of eight master regulatory filamentous growth kinases: *STE20*, *STE11*, *STE7*, *KSS1*, *FUS3*, *ELM1*, *SNF1*, and *TPK2*, which encompass positive and negative regulation of MAPK, RAS-cAMP-PKA, and AMPK Snf1p kinase signaling pathways. We then performed pairwise comparisons of differential phosphopeptide abundance in kinase-dead allele strains versus wild-type using a triplex SILAC labeling and tandem mass spectrometry strategy. From our collective analysis, we find that the kinase signaling network regulating filamentous growth encompasses over a tenth of the proteome on the whole. Specifically, we identify 752 statistically significantly differentially abundant phosphopeptides mapping to 406 phosphoproteins. We also identify many phosphopeptides representing novel phosphorylation events not previously observed in any yeast strain.

We have begun to analyze this collective data set using simple bioinformatics tools such as Gene Ontology term and KEGG pathway enrichment. As expected, we identify significant differential phosphorylation of a number of known filamentous growth factors. In addition, we believe novel kinase-substrate pairs can be predicted based on overlap of our phosphoproteomic data and high-throughput physical interaction data compiled on BioGrid. An interesting future endeavor would be to test these possible kinase substrate pairs and the function of the phosphorylation events through more classical biochemistry approaches.

We uncover novel phosphorylation of the small G protein Ras2p and the transcription factor Flo8p, and importantly, we find that these phosphorylation events are relevant to the function of the proteins in the filamentous growth transition. At least one phosphoserine of the Flo8p phosphopeptide resembles a consensus PKA phosphorylation motif, in alignment with biochemical data suggesting phosphorylation of Flo8p by the PKA paralog Tpk2p in the regulation of *MUC1* transcription (Pan & Heitman, 2002). A remaining question is the kinase(s) responsible for the dual phosphorylation of Ras2p. The predicted phosphopeptide has dual phosphorylation at both tyrosine 165 and threonine 166. Intriguingly, an identical phosphorylation event regulates the activity of the cyclin-dependent kinase Cdc28p (Ross, Kaldis, & Solomon, 2000). Additional work will be required to determine whether Cdc28p and Ras2p share the same upstream kinase. Because *RAS2* has homologs in that are very important in disease, uncovering a potentially novel mode of *RAS2* regulation is very relevant to human health.

In the analysis of our collective phosphoproteomic data set, we identify statistically significant enrichment of Gene Ontology terms pertaining to translational repression and mRNA decay processes. Through analysis of deletion mutants, we find that an mRNA decay factor complex composed of Dhh1p-Pat1p-Lsm1p is critical for surface-spread pseudohyphal growth of diploids, likely by regulating the MAPK pathway. Several questions remain to be addressed. First, expression of MAPK components and negative regulators of the MAPK signaling pathway should be assayed by rt-qPCR and Western blotting to identify a possible mechanism through which *LSM1*, *PAT1*, and *DHH1* could be

regulating MAPK signaling activity.  One would expect that since this pathway is involved in mRNA decay, perhaps the accumulation of a negative MAPK regulator is occurring in *dhh1Δ*, *pat1Δ*, and *lsm1Δ* strains.  Second, although these mRNA decay factors were detected within the kinase signaling regulatory network and clearly play important roles in the filamentous growth transition, what is the function of their phosphorylation? As shown in Table 3.2, phosphorylation of mRNA decay factors Dcp2p, Dhh1p, Pat1p, Pbp1p, Sbp1p, and Xrn1p led to the hypothesis that these factors are part of the signaling network. However, we exhaustively generated phosphonull mutations of DHH1, PAT1, PBP1, and SBP1 and find no differential regulation of surface-spread filamentation in diploids and no failure to transit to mRNP granules during stress conditions (data not shown).  One possibility is that these phosphorylation events very subtly perturb protein function or binding partner interaction to an extent below the level of detection in our assays.  As a final experimental question, we are currently generating a catalytically inactive allele of the decapping activator *DHH1*, found to be essential for diploid surface-spread filamentation. The helicase activity of Dhh1p is necessary for only some of its known functions (Carroll, Munchel, & Weis, 2011), and thereby we expect this catalytically inactive allele to be informative in ascertaining the role of *DHH1* in filamentous growth and the MAPK signaling pathway.

Lastly, we have used this collective phosphoproteomic data to uncover an entirely novel mode of filamentous growth regulation by a set of second messengers in the cell called inositol polyphosphates.  Through assaying invasive growth and surface-spread filamentation of deletion strains, we find that the inositol kinase enzymes are negatively regulating filamentous growth, likely by the production of a negative regulatory inositol pyrophosphate.  In our model, Vip1p, the most downstream inositol kinase, generates a negatively regulatory inositol pyrophosphate; thus deletion of *VIP1* or any upstream inositol polyphosphate-producing gene, including the phospholipase C family member *PLC1*, results in loss of the Vip1p product and a striking increase in filamentation in both haploid and diploid strains.  We also suggest that Kcs1p is producing an inositol pyrophosphate species that when lost, results in aberrant clumping or bundling of peripheral filaments in diploid null strains.  Loss of the product of Kcs1p would explain the

phenotype of *plc1Δ/Δ* and *arg82Δ/Δ* strains, as they would likewise no longer make the Kcs1p product.

We have explored the possible functional relevance of Vip1p phosphorylation by protein kinases, as Vip1p was a phosphoprotein detected within the signaling network encompassing four filamentous growth regulatory kinases (Table 3.3). Post-translational modification of Vip1p has not been explored; however, we find that a phosphonull allele in which Vip1p phosphoserines and phosphothreonines are mutated to alanine displays no differential surface-spread filamentation phenotypes in diploids or differential subcellular localization phenotype. We remain interested in exploring the function of predicted phosphorylation of Arg82p and Kcs1p, which also play important roles in filamentous growth.

A natural outgrowth of our inositol polyphosphate data would be an investigation into the possible downstream mechanism. How is an inositol pyrophosphate generated by Vip1p negatively regulating filamentous growth? Although there are many possibilities, we can effectively rule out any ploidy specific mode of filamentous growth regulation, as the hyperfilamentation phenotype of *vip1Δ* is observed in both haploids and diploids. The mechanism must likewise be the cause of very exaggerated hyperfilamentation, since *ipk1Δ/Δ* is slightly filamentous even without nitrogen starvation. We have also used our *FRE(Ty1):lacZ* reporter construct to assay MAPK signaling in *arg82Δ*, *ipk1Δ*, and *vip1Δ* strains and observe no increased signaling in exponentially growing cells (Data not shown). As Pho85p is the only described downstream target of an inositol pyrophosphate produced by Vip1p (Lee et al., 2007), we are currently testing the possible role of the cyclin-dependent kinase Pho85p in the regulation of filamentous growth by Vip1p. However, we note that the phosphate-responsive pathway in which Pho85p functions has not been previously implicated in the control of filamentous growth.

In sum, the work presented here more completely defines the gene complement contributing to filamentation through overexpression screening and the kinase signaling regulatory network governing filamentation. We also present focused studies of phosphorylation of filamentous growth proteins and two cellular processes which we find

to be critical for filamentous growth regulation: mRNA decay and inositol polyphosphate production.  Taken together, these studies represent an insightful contribution to the field of stress responses in model organisms, with possible implications in human biology.

# REFERENCES

Abu Irqeba, A., Li, Y., Panahi, M., Zhu, M., & Wang, Y. (2014). Regulating global sumoylation by a MAP kinase Hog1 and its potential role in osmo-tolerance in yeast. *PloS One, 9*(2), e87306. doi:10.1371/journal.pone.0087306; 10.1371/journal.pone.0087306

Ahn, S. H., Acurio, A., & Kron, S. J. (1999). Regulation of G2/M progression by the STE mitogen-activated protein kinase pathway in budding yeast filamentous growth. *Molecular Biology of the Cell, 10*(10), 3301-3316.

Alberti, S., Gitler, A. D., & Lindquist, S. (2007). A suite of gateway cloning vectors for high-throughput genetic analysis in saccharomyces cerevisiae. *Yeast (Chichester, England), 24*(10), 913-919. doi:10.1002/yea.1502

Alcazar-Roman, A. R., Tran, E. J., Guo, S., & Wente, S. R. (2006). Inositol hexakisphosphate and Gle1 activate the DEAD-box protein Dbp5 for nuclear mRNA export. *Nature Cell Biology, 8*(7), 711-716. doi:10.1038/ncb1427

Alcazar-Roman, A. R., & Wente, S. R. (2008). Inositol polyphosphates: A new frontier for regulating gene expression. *Chromosoma, 117*(1), 1-13. doi:10.1007/s00412-007-0126-4

Alonso-Monge, R., Navarro-Garcia, F., Molero, G., Diez-Orejas, R., Gustin, M., Pla, J., . . . Nombela, C. (1999). Role of the mitogen-activated protein kinase Hog1p in morphogenesis and virulence of candida albicans. *Journal of Bacteriology, 181*(10), 3058-3068.

Alonso-Monge, R., Navarro-Garcia, F., Roman, E., Negredo, A. I., Eisman, B., Nombela, C., & Pla, J. (2003). The Hog1 mitogen-activated protein kinase is essential in the oxidative stress response and chlamydospore formation in candida albicans. *Eukaryotic Cell, 2*(2), 351-361.

Ansari, K., Martin, S., Farkasovsky, M., Ehbrecht, I. M., & Kuntzel, H. (1999). Phospholipase C binds to the receptor-like GPR1 protein and controls pseudohyphal differentiation in saccharomyces cerevisiae. *The Journal of Biological Chemistry, 274*(42), 30052-30058.

Arribere, J. A., Doudna, J. A., & Gilbert, W. V. (2011). Reconsidering movement of eukaryotic mRNAs between polysomes and P bodies. *Molecular Cell, 44*(5), 745-758. doi:10.1016/j.molcel.2011.09.019; 10.1016/j.molcel.2011.09.019

Ashe, M. P., Slaven, J. W., De Long, S. K., Ibrahimo, S., & Sachs, A. B. (2001). A novel eIF2B-dependent mechanism of translational control in yeast as a response to fusel alcohols. *The EMBO Journal, 20*(22), 6464-6474. doi:10.1093/emboj/20.22.6464

Bao, M. Z., Schwartz, M. A., Cantin, G. T., Yates, J. R.,3rd, & Madhani, H. D. (2004). Pheromone-dependent destruction of the Tec1 transcription factor is required for MAP kinase signaling specificity in yeast. *Cell, 119*(7), 991-1000. doi:10.1016/j.cell.2004.11.052

Bardwell, L., Cook, J. G., Zhu-Shimoni, J. X., Voora, D., & Thorner, J. (1998). Differential

   regulation of transcription: Repression by unactivated mitogen-activated protein

   kinase Kss1 requires the Dig1 and Dig2 proteins. *Proceedings of the National Academy*

   *of Sciences of the United States of America, 95*(26), 15400-15405.

Baudin, A., Ozier-Kalogeropoulos, O., Denouel, A., Lacroute, F., & Cullin, C. (1993). A simple

   and efficient method for direct gene deletion in saccharomyces cerevisiae. *Nucleic*

   *Acids Research, 21*(14), 3329-3330.

Beggs, J. D. (1978). Transformation of yeast by a replicating hybrid plasmid. *Nature,*

   *275*(5676), 104-109.

Bell, M., & Engelberg, D. (2003). Phosphorylation of tyr-176 of the yeast MAPK Hog1/p38 is

   not vital for Hog1 biological activity. *The Journal of Biological Chemistry, 278*(17),

   14603-14606. doi:10.1074/jbc.C300006200

Berman, J., & Sudbery, P. E. (2002). Candida albicans: A molecular revolution built on

   lessons from budding yeast. *Nature Reviews.Genetics, 3*(12), 918-930.

   doi:10.1038/nrg948

Berridge, M. J. (1993). Inositol trisphosphate and calcium signalling. *Nature, 361*(6410),

   315-325. doi:10.1038/361315a0

Bhandari, R., Saiardi, A., Ahmadibeni, Y., Snowman, A. M., Resnick, A. C., Kristiansen, T. Z., . . .

   Snyder, S. H. (2007). Protein pyrophosphorylation by inositol pyrophosphates is a

posttranslational event. *Proceedings of the National Academy of Sciences of the United States of America, 104*(39), 15305-15310. doi:10.1073/pnas.0707338104

Bharucha, N., Chabrier-Rosello, Y., Xu, T., Johnson, C., Sobczynski, S., Song, Q., . . . Krysan, D. J. (2011). A large-scale complex haploinsufficiency-based genetic interaction screen in candida albicans: Analysis of the RAM network during morphogenesis. *PLoS Genetics, 7*(4), e1002058. doi:10.1371/journal.pgen.1002058; 10.1371/journal.pgen.1002058

Bharucha, N., Ma, J., Dobry, C. J., Lawson, S. K., Yang, Z., & Kumar, A. (2008). Analysis of the yeast kinome reveals a network of regulated protein localization during filamentous growth. *Molecular Biology of the Cell, 19*(7), 2708-2717. doi:10.1091/mbc.E07-11-1199; 10.1091/mbc.E07-11-1199

Blacketer, M. J., Koehler, C. M., Coats, S. G., Myers, A. M., & Madaule, P. (1993). Regulation of dimorphism in saccharomyces cerevisiae: Involvement of the novel protein kinase homolog Elm1p and protein phosphatase 2A. *Molecular and Cellular Biology, 13*(9), 5567-5581.

Bodenmiller, B., Wanka, S., Kraft, C., Urban, J., Campbell, D., Pedrioli, P. G., . . . Aebersold, R. (2010). Phosphoproteomic analysis reveals interconnected system-wide responses to perturbations of kinases and phosphatases in yeast. *Science Signaling, 3*(153), rs4. doi:10.1126/scisignal.2001182; 10.1126/scisignal.2001182

Botstein, D., & Fink, G. R. (2011). Yeast: An experimental organism for 21st century biology. *Genetics, 189*(3), 695-704. doi:10.1534/genetics.111.130765; 10.1534/genetics.111.130765

Braun, B. R., & Johnson, A. D. (1997). Control of filament formation in candida albicans by the transcriptional repressor TUP1. *Science (New York, N.Y.), 277*(5322), 105-109.

Braun, B. R., Kadosh, D., & Johnson, A. D. (2001). NRG1, a repressor of filamentous growth in C.albicans, is down-regulated during filament induction. *The EMBO Journal, 20*(17), 4753-4761. doi:10.1093/emboj/20.17.4753

Breitkreutz, A., Choi, H., Sharom, J. R., Boucher, L., Neduva, V., Larsen, B., . . . Tyers, M. (2010). A global protein kinase and phosphatase interaction network in yeast. *Science (New York, N.Y.), 328*(5981), 1043-1046. doi:10.1126/science.1176495; 10.1126/science.1176495

Brengues, M., Teixeira, D., & Parker, R. (2005). Movement of eukaryotic mRNAs between polysomes and cytoplasmic processing bodies. *Science (New York, N.Y.), 310*(5747), 486-489. doi:10.1126/science.1115791

Brewster, J. L., de Valoir, T., Dwyer, N. D., Winter, E., & Gustin, M. C. (1993). An osmosensing signal transduction pathway in yeast. *Science (New York, N.Y.), 259*(5102), 1760-1763.

Buchan, J. R., Nissan, T., & Parker, R. (2010). Analyzing P-bodies and stress granules in saccharomyces cerevisiae. *Methods in Enzymology, 470*, 619-640. doi:10.1016/S0076-6879(10)70025-2; 10.1016/S0076-6879(10)70025-2

Cairns, B. R., Ramer, S. W., & Kornberg, R. D. (1992). Order of action of components in the yeast pheromone response pathway revealed with a dominant allele of the STE11

kinase and the multiple phosphorylation of the STE7 kinase. *Genes & Development,*
*6*(7), 1305-1318.

Carroll, J. S., Munchel, S. E., & Weis, K. (2011). The DExD/H box ATPase Dhh1 functions in
translational repression, mRNA decay, and processing body dynamics. *The Journal of*
*Cell Biology, 194*(4), 527-537. doi:10.1083/jcb.201007151; 10.1083/jcb.201007151

Celenza, J. L., & Carlson, M. (1989). Mutational analysis of the saccharomyces cerevisiae
SNF1 protein kinase and evidence for functional interaction with the SNF4 protein.
*Molecular and Cellular Biology, 9*(11), 5034-5044.

Cheetham, J., MacCallum, D. M., Doris, K. S., da Silva Dantas, A., Scorfield, S., Odds, F., . . .
Quinn, J. (2011). MAPKKK-independent regulation of the Hog1 stress-activated protein
kinase in candida albicans. *The Journal of Biological Chemistry, 286*(49), 42002-42016.
doi:10.1074/jbc.M111.265231; 10.1074/jbc.M111.265231

Cheetham, J., Smith, D. A., da Silva Dantas, A., Doris, K. S., Patterson, M. J., Bruce, C. R., &
Quinn, J. (2007). A single MAPKKK regulates the Hog1 MAPK pathway in the
pathogenic fungus candida albicans. *Molecular Biology of the Cell, 18*(11), 4603-4614.
doi:10.1091/mbc.E07-06-0581

Cherry, J. M., Hong, E. L., Amundsen, C., Balakrishnan, R., Binkley, G., Chan, E. T., . . . Wong, E.
D. (2012). Saccharomyces genome database: The genomics resource of budding yeast.
*Nucleic Acids Research, 40*(Database issue), D700-5. doi:10.1093/nar/gkr1029;
10.1093/nar/gkr1029

Chou, S., Huang, L., & Liu, H. (2004). Fus3-regulated Tec1 degradation through SCFCdc4 determines MAPK signaling specificity during mating in yeast. *Cell, 119*(7), 981-990. doi:10.1016/j.cell.2004.11.053

Coelho, P. S., Kumar, A., & Snyder, M. (2000). Genome-wide mutant collections: Toolboxes for functional genomics. *Current Opinion in Microbiology, 3*(3), 309-315.

Coller, J., & Parker, R. (2005). General translational repression by activators of mRNA decapping. *Cell, 122*(6), 875-886. doi:10.1016/j.cell.2005.07.012

Cook, J. G., Bardwell, L., Kron, S. J., & Thorner, J. (1996). Two novel targets of the MAP kinase Kss1 are negative regulators of invasive growth in the yeast saccharomyces cerevisiae. *Genes & Development, 10*(22), 2831-2848.

Cook, J. G., Bardwell, L., & Thorner, J. (1997). Inhibitory and activating functions for MAPK Kss1 in the S. cerevisiae filamentous-growth signalling pathway. *Nature, 390*(6655), 85-88. doi:10.1038/36355

Cullen, P. J., Sabbagh, W.,Jr, Graham, E., Irick, M. M., van Olden, E. K., Neal, C., . . . Sprague, G. F.,Jr. (2004). A signaling mucin at the head of the Cdc42- and MAPK-dependent filamentous growth pathway in yeast. *Genes & Development, 18*(14), 1695-1708. doi:10.1101/gad.1178604

Cullen, P. J., & Sprague, G. F.,Jr. (2000). Glucose depletion causes haploid invasive growth in yeast. *Proceedings of the National Academy of Sciences of the United States of America, 97*(25), 13619-13624. doi:10.1073/pnas.240345197

Cullen, P. J., & Sprague, G. F.,Jr. (2002). The roles of bud-site-selection proteins during

    haploid invasive growth in yeast. *Molecular Biology of the Cell, 13*(9), 2990-3004.

    doi:10.1091/mbc.E02-03-0151

Cutler, N. S., Pan, X., Heitman, J., & Cardenas, M. E. (2001). The TOR signal transduction

    cascade controls cellular differentiation in response to nutrients. *Molecular Biology of*

    *the Cell, 12*(12), 4103-4113.

Decker, C. J., & Parker, R. (1993). A turnover pathway for both stable and unstable mRNAs

    in yeast: Evidence for a requirement for deadenylation. *Genes & Development, 7*(8),

    1632-1643.

Decker, C. J., Teixeira, D., & Parker, R. (2007). Edc3p and a glutamine/asparagine-rich

    domain of Lsm4p function in processing body assembly in *Saccharomyces cerevisiae.*

    *Journal of Cell Biology*, 179(3), 437-449.

Dickinson, J. R. (1996). 'Fusel' alcohols induce hyphal-like extensions and pseudohyphal

    formation in yeasts. *Microbiology (Reading, England), 142 ( Pt 6)*(Pt 6), 1391-1397.

Douglas, A. C., Smith, A. M., Sharifpoor, S., Yan, Z., Durbic, T., Heisler, L. E., . . . Andrews, B. J.

    (2012). Functional analysis with a barcoder yeast gene overexpression system. *G3*

    *(Bethesda, Md.), 2*(10), 1279-1289. doi:10.1534/g3.112.003400;

    10.1534/g3.112.003400

Dowell, R. D., Ryan, O., Jansen, A., Cheung, D., Agarwala, S., Danford, T., . . . Boone, C. (2010).
Genotype to phenotype: A complex problem. *Science (New York, N.Y.), 328*(5977), 469.
doi:10.1126/science.1189015; 10.1126/science.1189015

Dunckley, T., & Parker, R. (1999). The DCP2 protein is required for mRNA decapping in
saccharomyces cerevisiae and contains a functional MutT motif. *The EMBO Journal,
18*(19), 5411-5422. doi:10.1093/emboj/18.19.5411

Edgington, N. P., Blacketer, M. J., Bierwagen, T. A., & Myers, A. M. (1999a). Control of
saccharomyces cerevisiae filamentous growth by cyclin-dependent kinase Cdc28.
*Molecular and Cellular Biology, 19*(2), 1369-1380.

Edgington, N. P., Blacketer, M. J., Bierwagen, T. A., & Myers, A. M. (1999b). Control of
saccharomyces cerevisiae filamentous growth by cyclin-dependent kinase Cdc28.
*Molecular and Cellular Biology, 19*(2), 1369-1380.

Enjalbert, B., Smith, D. A., Cornell, M. J., Alam, I., Nicholls, S., Brown, A. J., & Quinn, J. (2006).
Role of the Hog1 stress-activated protein kinase in the global transcriptional response
to stress in the fungal pathogen candida albicans. *Molecular Biology of the Cell, 17*(2),
1018-1032. doi:10.1091/mbc.E05-06-0501

Ferrigno, P., Posas, F., Koepp, D., Saito, H., & Silver, P. A. (1998a). Regulated
nucleo/cytoplasmic exchange of HOG1 MAPK requires the importin beta homologs
NMD5 and XPO1. *The EMBO Journal, 17*(19), 5606-5614.
doi:10.1093/emboj/17.19.5606

Ferrigno, P., Posas, F., Koepp, D., Saito, H., & Silver, P. A. (1998b). Regulated

    nucleo/cytoplasmic exchange of HOG1 MAPK requires the importin beta homologs

    NMD5 and XPO1. *The EMBO Journal, 17*(19), 5606-5614.

    doi:10.1093/emboj/17.19.5606

Flick, J. S., & Thorner, J. (1993). Genetic and biochemical characterization of a

    phosphatidylinositol-specific phospholipase C in saccharomyces cerevisiae. *Molecular*

    *and Cellular Biology, 13*(9), 5861-5876.

Flom, G. A., Lemieszek, M., Fortunato, E. A., & Johnson, J. L. (2008). Farnesylation of Ydj1 is

    required for in vivo interaction with Hsp90 client proteins. *Molecular Biology of the*

    *Cell, 19*(12), 5249-5258. doi:10.1091/mbc.E08-04-0435; 10.1091/mbc.E08-04-0435

Gancedo, J. M. (2001). Control of pseudohyphae formation in saccharomyces cerevisiae.

    *FEMS Microbiology Reviews, 25*(1), 107-123.

Gaudon, C., Chambon, P., & Losson, R. (1999). Role of the essential yeast protein PSU1 in

    p6anscriptional enhancement by the ligand-dependent activation function AF-2 of

    nuclear receptors. *The EMBO Journal, 18*(8), 2229-2240. doi:10.1093/emboj/18.8.2229

Gavin, A. C., Bosche, M., Krause, R., Grandi, P., Marzioch, M., Bauer, A., . . . Superti-Furga, G.

    (2002). Functional organization of the yeast proteome by systematic analysis of

    protein complexes. *Nature, 415*(6868), 141-147. doi:10.1038/415141a

Gelperin, D. M., White, M. A., Wilkinson, M. L., Kon, Y., Kung, L. A., Wise, K. J., . . . Grayhack, E. J. (2005). Biochemical and genetic analysis of the yeast proteome with a movable ORF collection. *Genes & Development, 19*(23), 2816-2826. doi:10.1101/gad.1362105

Ghaemmaghami, S., Huh, W. K., Bower, K., Howson, R. W., Belle, A., Dephoure, N., . . . Weissman, J. S. (2003). Global analysis of protein expression in yeast. *Nature, 425*(6959), 737-741. doi:10.1038/nature02046

Giaever, G., Chu, A. M., Ni, L., Connelly, C., Riles, L., Veronneau, S., . . . Johnston, M. (2002). Functional profiling of the saccharomyces cerevisiae genome. *Nature, 418*(6896), 387-391. doi:10.1038/nature00935

Gimeno, C. J., Ljungdahl, P. O., Styles, C. A., & Fink, G. R. (1992). Unipolar cell divisions in the yeast S. cerevisiae lead to filamentous growth: Regulation by starvation and RAS. *Cell, 68*(6), 1077-1090.

Goehring, A. S., Rivers, D. M., & Sprague, G. F.,Jr. (2003). Urmylation: A ubiquitin-like pathway that functions during invasive growth and budding in yeast. *Molecular Biology of the Cell, 14*(11), 4329-4341. doi:10.1091/mbc.E03-02-0079

Goffeau, A., Barrell, B. G., Bussey, H., Davis, R. W., Dujon, B., Feldmann, H., . . . Oliver, S. G. (1996). Life with 6000 genes. *Science (New York, N.Y.), 274*(5287), 546, 563-7.

Goldstein, A. L., & McCusker, J. H. (1999). Three new dominant drug resistance cassettes for gene disruption in saccharomyces cerevisiae. *Yeast (Chichester, England), 15*(14), 1541-1553. doi:2-K

Gonzalez-Parraga, P., Alonso-Monge, R., Pla, J., & Arguelles, J. C. (2010). Adaptive tolerance
to oxidative stress and the induction of antioxidant enzymatic activities in candida
albicans are independent of the Hog1 and Cap1-mediated pathways. *FEMS Yeast
Research, 10*(6), 747-756. doi:10.1111/j.1567-1364.2010.00654.x; 10.1111/j.1567-
1364.2010.00654.x

Gow, N. A., van de Veerdonk, F. L., Brown, A. J., & Netea, M. G. (2011). Candida albicans
morphogenesis and host defence: Discriminating invasion from colonization. *Nature
Reviews.Microbiology, 10*(2), 112-122. doi:10.1038/nrmicro2711;
10.1038/nrmicro2711

Granek, J. A., & Magwene, P. M. (2010). Environmental and genetic determinants of colony
morphology in yeast. *PLoS Genetics, 6*(1), e1000823.
doi:10.1371/journal.pgen.1000823; 10.1371/journal.pgen.1000823

Grenson, M. (1966). Multiplicity of the amino acid permeases in saccharomyces cerevisiae.
II. evidence for a specific lysine-transporting system. *Biochimica Et Biophysica Acta,
127*(2), 339-346.

Gueldener, U., Heinisch, J., Koehler, G. J., Voss, D., & Hegemann, J. H. (2002). A second set of
loxP marker cassettes for cre-mediated multiple gene knockouts in budding yeast.
*Nucleic Acids Research, 30*(6), e23.

Guo, B., Styles, C. A., Feng, Q., & Fink, G. R. (2000). A saccharomyces gene family involved in
invasive growth, cell-cell adhesion, and mating. *Proceedings of the National Academy of*

*Sciences of the United States of America, 97*(22), 12158-12163.

doi:10.1073/pnas.220420397

Hanks, S. K., Quinn, A. M., & Hunter, T. (1988). The protein kinase family: Conserved

features and deduced phylogeny of the catalytic domains. *Science (New York, N.Y.),*

*241*(4861), 42-52.

Hao, N., Nayak, S., Behar, M., Shanks, R. H., Nagiec, M. J., Errede, B., . . . Dohlman, H. G. (2008).

Regulation of cell signaling dynamics by the protein kinase-scaffold Ste5. *Molecular*

*Cell, 30*(5), 649-656. doi:10.1016/j.molcel.2008.04.016; 10.1016/j.molcel.2008.04.016

Hinnen, A., Hicks, J. B., & Fink, G. R. (1978). Transformation of yeast. *Proceedings of the*

*National Academy of Sciences of the United States of America, 75*(4), 1929-1933.

Ho, C. H., Magtanong, L., Barker, S. L., Gresham, D., Nishimura, S., Natarajan, P., . . . Boone, C.

(2009). A molecular barcoded yeast ORF library enables mode-of-action analysis of

bioactive compounds. *Nature Biotechnology, 27*(4), 369-377. doi:10.1038/nbt.1534;

10.1038/nbt.1534

Ho, J., & Bretscher, A. (2001). Ras regulates the polarity of the yeast actin cytoskeleton

through the stress response pathway. *Molecular Biology of the Cell, 12*(6), 1541-1555.

Ho, Y., Gruhler, A., Heilbut, A., Bader, G. D., Moore, L., Adams, S. L., . . . Tyers, M. (2002).

Systematic identification of protein complexes in saccharomyces cerevisiae by mass

spectrometry. *Nature, 415*(6868), 180-183. doi:10.1038/415180a

Holt, L. J., Tuch, B. B., Villen, J., Johnson, A. D., Gygi, S. P., & Morgan, D. O. (2009). Global analysis of Cdk1 substrate phosphorylation sites provides insights into evolution. *Science (New York, N.Y.), 325*(5948), 1682-1686. doi:10.1126/science.1172867; 10.1126/science.1172867

Hong, S. P., Leiper, F. C., Woods, A., Carling, D., & Carlson, M. (2003). Activation of yeast Snf1 and mammalian AMP-activated protein kinase by upstream kinases. *Proceedings of the National Academy of Sciences of the United States of America, 100*(15), 8839-8843. doi:10.1073/pnas.1533136100

Huang da, W., Sherman, B. T., & Lempicki, R. A. (2009). Systematic and integrative analysis of large gene lists using DAVID bioinformatics resources. *Nature Protocols, 4*(1), 44-57. doi:10.1038/nprot.2008.211; 10.1038/nprot.2008.211

Huang, D., Friesen, H., & Andrews, B. (2007). Pho85, a multifunctional cyclin-dependent protein kinase in budding yeast. *Molecular Microbiology, 66*(2), 303-314. doi:10.1111/j.1365-2958.2007.05914.x

Huh, W. K., Falvo, J. V., Gerke, L. C., Carroll, A. S., Howson, R. W., Weissman, J. S., & O'Shea, E. K. (2003). Global analysis of protein localization in budding yeast. *Nature, 425*(6959), 686-691. doi:10.1038/nature02026

Jayatilake, J. A., Samaranayake, Y. H., Cheung, L. K., & Samaranayake, L. P. (2006). Quantitative evaluation of tissue invasion by wild type, hyphal and SAP mutants of candida albicans, and non-albicans candida species in reconstituted human oral epithelium. *Journal of Oral Pathology & Medicine : Official Publication of the*

*International Association of Oral Pathologists and the American Academy of Oral Pathology, 35*(8), 484-491. doi:10.1111/j.1600-0714.2006.00435.x

Jin, R., Dobry, C. J., McCown, P. J., & Kumar, A. (2008). Large-scale analysis of yeast filamentous growth by systematic gene disruption and overexpression. *Molecular Biology of the Cell, 19*(1), 284-296. doi:10.1091/mbc.E07-05-0519

Kanehisa, M., Goto, S., Sato, Y., Furumichi, M., & Tanabe, M. (2012). KEGG for integration and interpretation of large-scale molecular data sets. *Nucleic Acids Research, 40*(Database issue), D109-14. doi:10.1093/nar/gkr988; 10.1093/nar/gkr988

Karunanithi, S., Vadaie, N., Chavel, C. A., Birkaya, B., Joshi, J., Grell, L., & Cullen, P. J. (2010). Shedding of the mucin-like flocculin Flo11p reveals a new aspect of fungal adhesion regulation. *Current Biology : CB, 20*(15), 1389-1395. doi:10.1016/j.cub.2010.06.033; 10.1016/j.cub.2010.06.033

Killcoyne, S., Carter, G. W., Smith, J., & Boyle, J. (2009). Cytoscape: A community-based framework for network modeling. *Methods in Molecular Biology (Clifton, N.J.), 563*, 219-239. doi:10.1007/978-1-60761-175-2_12; 10.1007/978-1-60761-175-2_12

Kim, J., & Kim, J. (2002). KEM1 is involved in filamentous growth of saccharomyces cerevisiae. *FEMS Microbiology Letters, 216*(1), 33-38.

Koehler, C. M., & Myers, A. M. (1997). Serine-threonine protein kinase activity of Elm1p, a regulator of morphologic differentiation in saccharomyces cerevisiae. *FEBS Letters, 408*(1), 109-114.

Kron, S. J., Styles, C. A., & Fink, G. R. (1994). Symmetric cell division in pseudohyphae of the

yeast saccharomyces cerevisiae. *Molecular Biology of the Cell, 5*(9), 1003-1022.

Kuchin, S., Vyas, V. K., & Carlson, M. (2002). Snf1 protein kinase and the repressors Nrg1

and Nrg2 regulate FLO11, haploid invasive growth, and diploid pseudohyphal

differentiation. *Molecular and Cellular Biology, 22*(12), 3994-4000.

Kultz, D., & Burg, M. (1998). Evolution of osmotic stress signaling via MAP kinase cascades.

*The Journal of Experimental Biology, 201*(Pt 22), 3015-3021.

Kumar, A., Agarwal, S., Heyman, J. A., Matson, S., Heidtman, M., Piccirillo, S., . . . Snyder, M.

(2002). Subcellular localization of the yeast proteome. *Genes & Development, 16*(6),

707-719. doi:10.1101/gad.970902

Kumar, A., des Etages, S. A., Coelho, P. S., Roeder, G. S., & Snyder, M. (2000). High-

throughput methods for the large-scale analysis of gene function by transposon

tagging. *Methods in Enzymology, 328*, 550-574.

Kumar, A., Vidan, S., & Snyder, M. (2002). Insertional mutagenesis: Transposon-insertion

libraries as mutagens in yeast. *Methods in Enzymology, 350*, 219-229.

Leberer, E., Wu, C., Leeuw, T., Fourest-Lieuvin, A., Segall, J. E., & Thomas, D. Y. (1997).

Functional characterization of the Cdc42p binding domain of yeast Ste20p protein

kinase. *The EMBO Journal, 16*(1), 83-97. doi:10.1093/emboj/16.1.83

Lee, Y. S., Mulugu, S., York, J. D., & O'Shea, E. K. (2007). Regulation of a cyclin-CDK-CDK

inhibitor complex by inositol pyrophosphates. *Science (New York, N.Y.), 316*(5821),

109-112. doi:10.1126/science.1139080

Li, W., & Mitchell, A. P. (1997). Proteolytic activation of Rim1p, a positive regulator of yeast

sporulation and invasive growth. *Genetics, 145*(1), 63-73.

Liu, H., Kohler, J., & Fink, G. R. (1994). Suppression of hyphal formation in candida albicans

by mutation of a STE12 homolog. *Science (New York, N.Y.), 266*(5191), 1723-1726.

Liu, H., Styles, C. A., & Fink, G. R. (1993). Elements of the yeast pheromone response

pathway required for filamentous growth of diploids. *Science (New York, N.Y.),

262*(5140), 1741-1744.

Liu, H., Styles, C. A., & Fink, G. R. (1996). Saccharomyces cerevisiae S288C has a mutation in

FLO8, a gene required for filamentous growth. *Genetics, 144*(3), 967-978.

Liu, H. Y., Badarinarayana, V., Audino, D. C., Rappsilber, J., Mann, M., & Denis, C. L. (1998).

The NOT proteins are part of the CCR4 transcriptional complex and affect gene

expression both positively and negatively. *The EMBO Journal, 17*(4), 1096-1106.

doi:10.1093/emboj/17.4.1096

Lo, H. J., Kohler, J. R., DiDomenico, B., Loebenberg, D., Cacciapuoti, A., & Fink, G. R. (1997).

Nonfilamentous C. albicans mutants are avirulent. *Cell, 90*(5), 939-949.

Lo, T. L., Qu, Y., Uwamahoro, N., Quenault, T., Beilharz, T. H., & Traven, A. (2012). The mRNA

decay pathway regulates the expression of the Flo11 adhesin and biofilm formation in

saccharomyces cerevisiae. *Genetics, 191*(4), 1387-1391.

doi:10.1534/genetics.112.141432; 10.1534/genetics.112.141432

Lo, W. S., & Dranginis, A. M. (1998). The cell surface flocculin Flo11 is required for

pseudohyphae formation and invasion by saccharomyces cerevisiae. *Molecular Biology

of the Cell, 9*(1), 161-171.

Lonetti, A., Szijgyarto, Z., Bosch, D., Loss, O., Azevedo, C., & Saiardi, A. (2011). Identification

of an evolutionarily conserved family of inorganic polyphosphate

endopolyphosphatases. *The Journal of Biological Chemistry, 286*(37), 31966-31974.

doi:10.1074/jbc.M111.266320; 10.1074/jbc.M111.266320

Longtine, M. S., McKenzie, A.,3rd, Demarini, D. J., Shah, N. G., Wach, A., Brachat, A., . . .

Pringle, J. R. (1998). Additional modules for versatile and economical PCR-based gene

deletion and modification in saccharomyces cerevisiae. *Yeast (Chichester, England),

14*(10), 953-961. doi:2-U

Lorenz, M. C., Cutler, N. S., & Heitman, J. (2000). Characterization of alcohol-induced

filamentous growth in saccharomyces cerevisiae. *Molecular Biology of the Cell, 11*(1),

183-199.

Lorenz, M. C., & Heitman, J. (1997). Yeast pseudohyphal growth is regulated by GPA2, a G

protein alpha homolog. *The EMBO Journal, 16*(23), 7008-7018.

doi:10.1093/emboj/16.23.7008

Lorenz, M. C., & Heitman, J. (1998). The MEP2 ammonium permease regulates

    pseudohyphal differentiation in saccharomyces cerevisiae. *The EMBO Journal, 17*(5),

    1236-1247. doi:10.1093/emboj/17.5.1236

Lorenz, M. C., Pan, X., Harashima, T., Cardenas, M. E., Xue, Y., Hirsch, J. P., & Heitman, J.

    (2000). The G protein-coupled receptor gpr1 is a nutrient sensor that regulates

    pseudohyphal differentiation in saccharomyces cerevisiae. *Genetics, 154*(2), 609-622.

Ma, J., Jin, R., Dobry, C. J., Lawson, S. K., & Kumar, A. (2007). Overexpression of autophagy-

    related genes inhibits yeast filamentous growth. *Autophagy, 3*(6), 604-609.

Ma, J., Jin, R., Jia, X., Dobry, C. J., Wang, L., Reggiori, F., . . . Kumar, A. (2007). An

    interrelationship between autophagy and filamentous growth in budding yeast.

    *Genetics, 177*(1), 205-214. doi:10.1534/genetics.107.076596

Madhani, H. D., & Fink, G. R. (1997). Combinatorial control required for the specificity of

    yeast MAPK signaling. *Science (New York, N.Y.), 275*(5304), 1314-1317.

Madhani, H. D., & Fink, G. R. (1998). The control of filamentous differentiation and

    virulence in fungi. *Trends in Cell Biology, 8*(9), 348-353.

Madhani, H. D., Galitski, T., Lander, E. S., & Fink, G. R. (1999). Effectors of a developmental

    mitogen-activated protein kinase cascade revealed by expression signatures of

    signaling mutants. *Proceedings of the National Academy of Sciences of the United States

    of America, 96*(22), 12530-12535.

Madhani, H. D., Styles, C. A., & Fink, G. R. (1997). MAP kinases with distinct inhibitory

    functions impart signaling specificity during yeast differentiation. *Cell, 91*(5), 673-684.

Maeda, T., Wurgler-Murphy, S. M., & Saito, H. (1994). A two-component system that

    regulates an osmosensing MAP kinase cascade in yeast. *Nature, 369*(6477), 242-245.

    doi:10.1038/369242a0

Malcher, M., Schladebeck, S., & Mosch, H. U. (2011). The Yak1 protein kinase lies at the

    center of a regulatory cascade affecting adhesive growth and stress resistance in

    saccharomyces cerevisiae. *Genetics, 187*(3), 717-730.

    doi:10.1534/genetics.110.125708; 10.1534/genetics.110.125708

Maleri, S., Ge, Q., Hackett, E. A., Wang, Y., Dohlman, H. G., & Errede, B. (2004). Persistent

    activation by constitutive Ste7 promotes Kss1-mediated invasive growth but fails to

    support Fus3-dependent mating in yeast. *Molecular and Cellular Biology, 24*(20), 9221-

    9238. doi:10.1128/MCB.24.20.9221-9238.2004

Mapes, J., & Ota, I. M. (2004). Nbp2 targets the Ptc1-type 2C ser/thr phosphatase to the

    HOG MAPK pathway. *The EMBO Journal, 23*(2), 302-311.

    doi:10.1038/sj.emboj.7600036

Mattison, C. P., Spencer, S. S., Kresge, K. A., Lee, J., & Ota, I. M. (1999). Differential regulation

    of the cell wall integrity mitogen-activated protein kinase pathway in budding yeast by

    the protein tyrosine phosphatases Ptp2 and Ptp3. *Molecular and Cellular Biology,*

    *19*(11), 7651-7660.

Miled, C., Mann, C., & Faye, G. (2001). Xbp1-mediated repression of CLB gene expression contributes to the modifications of yeast cell morphology and cell cycle seen during nitrogen-limited growth. *Molecular and Cellular Biology, 21*(11), 3714-3724. doi:10.1128/MCB.21.11.3714-3724.2001

Minato, T., Wang, J., Akasaka, K., Okada, T., Suzuki, N., & Kataoka, T. (1994). Quantitative analysis of mutually competitive binding of human raf-1 and yeast adenylyl cyclase to ras proteins. *The Journal of Biological Chemistry, 269*(33), 20845-20851.

Mosch, H. U., & Fink, G. R. (1997). Dissection of filamentous growth by transposon mutagenesis in saccharomyces cerevisiae. *Genetics, 145*(3), 671-684.

Mosch, H. U., Roberts, R. L., & Fink, G. R. (1996). Ras2 signals via the Cdc42/Ste20/mitogen-activated protein kinase module to induce filamentous growth in saccharomyces cerevisiae. *Proceedings of the National Academy of Sciences of the United States of America, 93*(11), 5352-5356.

Mulugu, S., Bai, W., Fridy, P. C., Bastidas, R. J., Otto, J. C., Dollins, D. E., . . . York, J. D. (2007). A conserved family of enzymes that phosphorylate inositol hexakisphosphate. *Science (New York, N.Y.), 316*(5821), 106-109. doi:10.1126/science.1139099

Narayanaswamy, R., Levy, M., Tsechansky, M., Stovall, G. M., O'Connell, J. D., Mirrielees, J., . . . Marcotte, E. M. (2009). Widespread reorganization of metabolic enzymes into reversible assemblies upon nutrient starvation. *Proceedings of the National Academy of Sciences of the United States of America, 106*(25), 10147-10152. doi:10.1073/pnas.0812771106; 10.1073/pnas.0812771106

Nissan, T., Rajyaguru, P., She, M., Song, H., & Parker, R. (2010). Decapping activators in saccharomyces cerevisiae act by multiple mechanisms. *Molecular Cell, 39*(5), 773-783. doi:10.1016/j.molcel.2010.08.025; 10.1016/j.molcel.2010.08.025

Olsen, J. V., Blagoev, B., Gnad, F., Macek, B., Kumar, C., Mortensen, P., & Mann, M. (2006). Global, in vivo, and site-specific phosphorylation dynamics in signaling networks. *Cell, 127*(3), 635-648. doi:10.1016/j.cell.2006.09.026

Orlova, M., Kanter, E., Krakovich, D., & Kuchin, S. (2006). Nitrogen availability and TOR regulate the Snf1 protein kinase in saccharomyces cerevisiae. *Eukaryotic Cell, 5*(11), 1831-1837. doi:10.1128/EC.00110-06

Orlova, M., Ozcetin, H., Barrett, L., & Kuchin, S. (2010). Roles of the Snf1-activating kinases during nitrogen limitation and pseudohyphal differentiation in saccharomyces cerevisiae. *Eukaryotic Cell, 9*(1), 208-214. doi:10.1128/EC.00216-09; 10.1128/EC.00216-09

O'Rourke, S. M., & Herskowitz, I. (1998). The Hog1 MAPK prevents cross talk between the HOG and pheromone response MAPK pathways in saccharomyces cerevisiae. *Genes & Development, 12*(18), 2874-2886.

O'Rourke, S. M., & Herskowitz, I. (2004). Unique and redundant roles for HOG MAPK pathway components as revealed by whole-genome expression analysis. *Molecular Biology of the Cell, 15*(2), 532-542. doi:10.1091/mbc.E03-07-0521

Pan, X., & Heitman, J. (1999). Cyclic AMP-dependent protein kinase regulates pseudohyphal differentiation in saccharomyces cerevisiae. *Molecular and Cellular Biology, 19*(7), 4874-4887.

Pan, X., & Heitman, J. (2002). Protein kinase A operates a molecular switch that governs yeast pseudohyphal differentiation. *Molecular and Cellular Biology, 22*(12), 3981-3993.

Park, Y. U., Hur, H., Ka, M., & Kim, J. (2006). Identification of translational regulation target genes during filamentous growth in saccharomyces cerevisiae: Regulatory role of Caf20 and Dhh1. *Eukaryotic Cell, 5*(12), 2120-2127. doi:10.1128/EC.00121-06

Peter, M., Neiman, A. M., Park, H. O., van Lohuizen, M., & Herskowitz, I. (1996). Functional analysis of the interaction between the small GTP binding protein Cdc42 and the Ste20 protein kinase in yeast. *The EMBO Journal, 15*(24), 7046-7059.

Petter, R., Chang, Y. C., & Kwon-Chung, K. J. (1997). A gene homologous to saccharomyces cerevisiae SNF1 appears to be essential for the viability of candida albicans. *Infection and Immunity, 65*(12), 4909-4917.

Pitoniak, A., Birkaya, B., Dionne, H. M., Vadaie, N., & Cullen, P. J. (2009). The signaling mucins Msb2 and Hkr1 differentially regulate the filamentation mitogen-activated protein kinase pathway and contribute to a multimodal response. *Molecular Biology of the Cell, 20*(13), 3101-3114. doi:10.1091/mbc.E08-07-0760; 10.1091/mbc.E08-07-0760

Pohlmann, J., & Fleig, U. (2010). Asp1, a conserved 1/3 inositol polyphosphate kinase,

    regulates the dimorphic switch in schizosaccharomyces pombe. *Molecular and Cellular*

    *Biology, 30*(18), 4535-4547. doi:10.1128/MCB.00472-10; 10.1128/MCB.00472-10

Pokholok, D. K., Zeitlinger, J., Hannett, N. M., Reynolds, D. B., & Young, R. A. (2006).

    Activated signal transduction kinases frequently occupy target genes. *Science (New*

    *York, N.Y.), 313*(5786), 533-536. doi:10.1126/science.1127677

Posas, F., & Saito, H. (1997). Osmotic activation of the HOG MAPK pathway via Ste11p

    MAPKKK: Scaffold role of Pbs2p MAPKK. *Science (New York, N.Y.), 276*(5319), 1702-

    1705.

Posas, F., Wurgler-Murphy, S. M., Maeda, T., Witten, E. A., Thai, T. C., & Saito, H. (1996).

    Yeast HOG1 MAP kinase cascade is regulated by a multistep phosphorelay mechanism

    in the SLN1-YPD1-SSK1 "two-component" osmosensor. *Cell, 86*(6), 865-875.

Ptacek, J., Devgan, G., Michaud, G., Zhu, H., Zhu, X., Fasolo, J., . . . Snyder, M. (2005). Global

    analysis of protein phosphorylation in yeast. *Nature, 438*(7068), 679-684.

    doi:10.1038/nature04187

Raitt, D. C., Posas, F., & Saito, H. (2000). Yeast Cdc42 GTPase and Ste20 PAK-like kinase

    regulate Sho1-dependent activation of the Hog1 MAPK pathway. *The EMBO Journal,*

    *19*(17), 4623-4631. doi:10.1093/emboj/19.17.4623

Ramachandran, V., Shah, K. H., & Herman, P. K. (2011). The cAMP-dependent protein kinase

   signaling pathway is a key regulator of P body foci formation. *Molecular Cell, 43*(6),

   973-981. doi:10.1016/j.molcel.2011.06.032; 10.1016/j.molcel.2011.06.032

Roberts, C. J., Nelson, B., Marton, M. J., Stoughton, R., Meyer, M. R., Bennett, H. A., . . . Friend,

   S. H. (2000). Signaling and circuitry of multiple MAPK pathways revealed by a matrix of

   global gene expression profiles. *Science (New York, N.Y.), 287*(5454), 873-880.

Roberts, R. L., & Fink, G. R. (1994). Elements of a single MAP kinase cascade in

   saccharomyces cerevisiae mediate two developmental programs in the same cell type:

   Mating and invasive growth. *Genes & Development, 8*(24), 2974-2985.

Robertson, L. S., & Fink, G. R. (1998). The three yeast A kinases have specific signaling

   functions in pseudohyphal growth. *Proceedings of the National Academy of Sciences of

   the United States of America, 95*(23), 13783-13787.

Robinson, M. K., van Zyl, W. H., Phizicky, E. M., & Broach, J. R. (1994). TPD1 of

   saccharomyces cerevisiae encodes a protein phosphatase 2C-like activity implicated in

   tRNA splicing and cell separation. *Molecular and Cellular Biology, 14*(6), 3634-3645.

Ross, K. E., Kaldis, P., & Solomon, M. J. (2000). Activating phosphorylation of the

   saccharomyces cerevisiae cyclin-dependent kinase, cdc28p, precedes cyclin binding.

   *Molecular Biology of the Cell, 11*(5), 1597-1609.

Rua, D., Tobe, B. T., & Kron, S. J. (2001). Cell cycle control of yeast filamentous growth.

   *Current Opinion in Microbiology, 4*(6), 720-727.

Rupp, S., Summers, E., Lo, H. J., Madhani, H., & Fink, G. (1999a). MAP kinase and cAMP

filamentation signaling pathways converge on the unusually large promoter of the

yeast FLO11 gene. *The EMBO Journal, 18*(5), 1257-1269. doi:10.1093/emboj/18.5.1257

Rupp, S., Summers, E., Lo, H. J., Madhani, H., & Fink, G. (1999b). MAP kinase and cAMP

filamentation signaling pathways converge on the unusually large promoter of the

yeast FLO11 gene. *The EMBO Journal, 18*(5), 1257-1269. doi:10.1093/emboj/18.5.1257

Ryan, O., Shapiro, R. S., Kurat, C. F., Mayhew, D., Baryshnikova, A., Chin, B., . . . Boone, C.

(2012). Global gene deletion analysis exploring yeast filamentous growth. *Science (New

York, N.Y.), 337*(6100), 1353-1356. doi:10.1126/science.1224339;

10.1126/science.1224339

Saiardi, A., Erdjument-Bromage, H., Snowman, A. M., Tempst, P., & Snyder, S. H. (1999).

Synthesis of diphosphoinositol pentakisphosphate by a newly identified family of

higher inositol polyphosphate kinases. *Current Biology : CB, 9*(22), 1323-1326.

San Jose, C., Monge, R. A., Perez-Diaz, R., Pla, J., & Nombela, C. (1996). The mitogen-activated

protein kinase homolog HOG1 gene controls glycerol accumulation in the pathogenic

fungus candida albicans. *Journal of Bacteriology, 178*(19), 5850-5852.

Scherens, B., & Goffeau, A. (2004). The uses of genome-wide yeast mutant collections.

*Genome Biology, 5*(7), 229. doi:10.1186/gb-2004-5-7-229

Segal, S. P., Dunckley, T., & Parker, R. (2006). Sbp1p affects translational repression and decapping in saccharomyces cerevisiae. *Molecular and Cellular Biology, 26*(13), 5120-5130. doi:10.1128/MCB.01913-05

Shabb, J. B. (2001). Physiological substrates of cAMP-dependent protein kinase. *Chemical Reviews, 101*(8), 2381-2411.

Shaner, N. C., Campbell, R. E., Steinbach, P. A., Giepmans, B. N., Palmer, A. E., & Tsien, R. Y. (2004). Improved monomeric red, orange and yellow fluorescent proteins derived from discosoma sp. red fluorescent protein. *Nature Biotechnology, 22*(12), 1567-1572. doi:10.1038/nbt1037

Shen, X., Xiao, H., Ranallo, R., Wu, W. H., & Wu, C. (2003). Modulation of ATP-dependent chromatin-remodeling complexes by inositol polyphosphates. *Science (New York, N.Y.), 299*(5603), 112-114. doi:10.1126/science.1078068

Sheth, U., & Parker, R. (2003). Decapping and decay of messenger RNA occur in cytoplasmic processing bodies. *Science (New York, N.Y.), 300*(5620), 805-808. doi:10.1126/science.1082320

Sheth, U., & Parker, R. (2006). Targeting of aberrant mRNAs to cytoplasmic processing bodies. *Cell, 125*(6), 1095-1109. doi:10.1016/j.cell.2006.04.037

Shively, C. A., Eckwahl, M. J., Dobry, C. J., Mellacheruvu, D., Nesvizhskii, A., & Kumar, A. (2013). Genetic networks inducing invasive growth in saccharomyces cerevisiae

identified through systematic genome-wide overexpression. *Genetics, 193*(4), 1297-1310. doi:10.1534/genetics.112.147876; 10.1534/genetics.112.147876

Shock, T. R., Thompson, J., Yates, J. R.,3rd, & Madhani, H. D. (2009). Hog1 mitogen-activated protein kinase (MAPK) interrupts signal transduction between the Kss1 MAPK and the Tec1 transcription factor to maintain pathway specificity. *Eukaryotic Cell, 8*(4), 606-616. doi:10.1128/EC.00005-09; 10.1128/EC.00005-09

Sikorski, R. S., & Hieter, P. (1989). A system of shuttle vectors and yeast host strains designed for efficient manipulation of DNA in saccharomyces cerevisiae. *Genetics, 122*(1), 19-27.

Smirnova, J. B., Selley, J. N., Sanchez-Cabo, F., Carroll, K., Eddy, A. A., McCarthy, J. E., . . . Ashe, M. P. (2005). Global gene expression profiling reveals widespread yet distinctive translational responses to different eukaryotic translation initiation factor 2B-targeting stress pathways. *Molecular and Cellular Biology, 25*(21), 9340-9349. doi:10.1128/MCB.25.21.9340-9349.2005

Sopko, R., Huang, D., Preston, N., Chua, G., Papp, B., Kafadar, K., . . . Andrews, B. (2006). Mapping pathways and phenotypes by systematic gene overexpression. *Molecular Cell, 21*(3), 319-330. doi:10.1016/j.molcel.2005.12.011

St John, T. P., & Davis, R. W. (1981). The organization and transcription of the galactose gene cluster of saccharomyces. *Journal of Molecular Biology, 152*(2), 285-315.

Stalder, L., & Muhlemann, O. (2009). Processing bodies are not required for mammalian

    nonsense-mediated mRNA decay. *RNA (New York, N.Y.), 15*(7), 1265-1273.

    doi:10.1261/rna.1672509; 10.1261/rna.1672509

Steger, D. J., Haswell, E. S., Miller, A. L., Wente, S. R., & O'Shea, E. K. (2003). Regulation of

    chromatin remodeling by inositol polyphosphates. *Science (New York, N.Y.), 299*(5603),

    114-116. doi:10.1126/science.1078062

Stevenson, B. J., Rhodes, N., Errede, B., & Sprague, G. F.,Jr. (1992). Constitutive mutants of

    the protein kinase STE11 activate the yeast pheromone response pathway in the

    absence of the G protein. *Genes & Development, 6*(7), 1293-1304.

Sudbery, P., Gow, N., & Berman, J. (2004). The distinct morphogenic states of candida

    albicans. *Trends in Microbiology, 12*(7), 317-324. doi:10.1016/j.tim.2004.05.008

Talarek, N., Cameroni, E., Jaquenoud, M., Luo, X., Bontron, S., Lippman, S., . . . De Virgilio, C.

    (2010). Initiation of the TORC1-regulated G0 program requires Igo1/2, which license

    specific mRNAs to evade degradation via the 5'-3' mRNA decay pathway. *Molecular*

    *Cell, 38*(3), 345-355. doi:10.1016/j.molcel.2010.02.039; 10.1016/j.molcel.2010.02.039

Tucker, M., Valencia-Sanchez, M. A., Staples, R. R., Chen, J., Denis, C. L., & Parker, R. (2001).

    The transcription factor associated Ccr4 and Caf1 proteins are components of the

    major cytoplasmic mRNA deadenylase in saccharomyces cerevisiae. *Cell, 104*(3), 377-

    386.

Uetz, P., Giot, L., Cagney, G., Mansfield, T. A., Judson, R. S., Knight, J. R., . . . Rothberg, J. M.

    (2000). A comprehensive analysis of protein-protein interactions in saccharomyces

    cerevisiae. *Nature, 403*(6770), 623-627. doi:10.1038/35001009

Vyas, V. K., Kuchin, S., Berkey, C. D., & Carlson, M. (2003). Snf1 kinases with different beta-

    subunit isoforms play distinct roles in regulating haploid invasive growth. *Molecular*

    *and Cellular Biology, 23*(4), 1341-1348.

Wach, A., Brachat, A., Pohlmann, R., & Philippsen, P. (1994). New heterologous modules for

    classical or PCR-based gene disruptions in saccharomyces cerevisiae. *Yeast (Chichester,*

    *England), 10*(13), 1793-1808.

Wang, Y., Abu Irqeba, A., Ayalew, M., & Suntay, K. (2009). Sumoylation of transcription

    factor Tec1 regulates signaling of mitogen-activated protein kinase pathways in yeast.

    *PloS One, 4*(10), e7456. doi:10.1371/journal.pone.0007456;

    10.1371/journal.pone.0007456

Westfall, P. J., Patterson, J. C., Chen, R. E., & Thorner, J. (2008). Stress resistance and signal

    fidelity independent of nuclear MAPK function. *Proceedings of the National Academy of*

    *Sciences of the United States of America, 105*(34), 12212-12217.

    doi:10.1073/pnas.0805797105; 10.1073/pnas.0805797105

Winzeler, E. A., Shoemaker, D. D., Astromoff, A., Liang, H., Anderson, K., Andre, B., . . . Davis,

    R. W. (1999). Functional characterization of the S. cerevisiae genome by gene deletion

    and parallel analysis. *Science (New York, N.Y.), 285*(5429), 901-906.

Wu, C., Whiteway, M., Thomas, D. Y., & Leberer, E. (1995). Molecular characterization of Ste20p, a potential mitogen-activated protein or extracellular signal-regulated kinase kinase (MEK) kinase kinase from saccharomyces cerevisiae. *The Journal of Biological Chemistry, 270*(27), 15984-15992.

Wurgler-Murphy, S. M., Maeda, T., Witten, E. A., & Saito, H. (1997). Regulation of the saccharomyces cerevisiae HOG1 mitogen-activated protein kinase by the PTP2 and PTP3 protein tyrosine phosphatases. *Molecular and Cellular Biology, 17*(3), 1289-1297.

Xu, T., Shively, C. A., Jin, R., Eckwahl, M. J., Dobry, C. J., Song, Q., & Kumar, A. (2010). A profile of differentially abundant proteins at the yeast cell periphery during pseudohyphal growth. *The Journal of Biological Chemistry, 285*(20), 15476-15488. doi:10.1074/jbc.M110.114926; 10.1074/jbc.M110.114926

Yang, H. Y., Tatebayashi, K., Yamamoto, K., & Saito, H. (2009). Glycosylation defects activate filamentous growth Kss1 MAPK and inhibit osmoregulatory Hog1 MAPK. *The EMBO Journal, 28*(10), 1380-1391. doi:10.1038/emboj.2009.104; 10.1038/emboj.2009.104

Yoon, J. H., Choi, E. J., & Parker, R. (2010). Dcp2 phosphorylation by Ste20 modulates stress granule assembly and mRNA decay in saccharomyces cerevisiae. *The Journal of Cell Biology, 189*(5), 813-827. doi:10.1083/jcb.200912019; 10.1083/jcb.200912019

York, J. D., Odom, A. R., Murphy, R., Ives, E. B., & Wente, S. R. (1999). A phospholipase C-dependent inositol polyphosphate kinase pathway required for efficient messenger RNA export. *Science (New York, N.Y.), 285*(5424), 96-100.

Zapater, M., Sohrmann, M., Peter, M., Posas, F., & de Nadal, E. (2007). Selective requirement

    for SAGA in Hog1-mediated gene expression depending on the severity of the external

    osmostress conditions. *Molecular and Cellular Biology, 27*(11), 3900-3910.

    doi:10.1128/MCB.00089-07

Zheng, L., Baumann, U., & Reymond, J. L. (2004). An efficient one-step site-directed and site-

    saturation mutagenesis protocol. *Nucleic Acids Research, 32*(14), e115.

    doi:10.1093/nar/gnh110

Zhu, H., Bilgin, M., Bangham, R., Hall, D., Casamayor, A., Bertone, P., . . . Snyder, M. (2001).

    Global analysis of protein activities using proteome chips. *Science (New York, N.Y.),*

    *293*(5537), 2101-2105. doi:10.1126/science.1062191